

Nicholas Giourmas Master's Thesis

**The potential therapeutic
effect of spermidine
supplementation on the mdx
mouse phenotype**

Supervisors: Dr. Craig Goodman and Prof. Alan Hayes

Acknowledgements

Firstly, I would like to express my deepest gratitude to my supervisors Craig Goodman and Alan Hayes. Both supervisors have not only contributed greatly to the conception of this project, but their constant guidance and deliberation throughout has allowed the scope of this project to be broadened with seemingly endless opportunities. Without them I would have not been able to complete such a lengthy time course on a large number of mice, which has allowed for the generation of such interesting and significant data. Besides this project, having both Craig and Alan as my mentors from honours onwards has allowed for me to grow as a researcher in ways that would not have been possible without their feedback and direction.

Secondly, I would like to thank Dean Campelj, Danielle Debruin and Cara Timpani for their generosity in teaching me certain techniques that I used throughout this project, whilst also providing great advice during troubleshooting periods. Having them within the lab space was important, as the best of advice was only a conversation away.

Thirdly, I would like to thank Hannah Lalunio for her generosity with helping throughout the treatment of my mice with both animal weighing and supplementing. The sheer number of mice, as well as a staggered program resulting in daily treatments, would have been extremely difficult for just one person for the amount of time that it ran for. It is doubtful that the volume of data generated would have been possible without her help throughout the treatments.

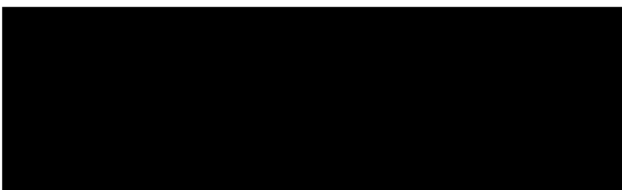
Lastly, I would like to extend an overwhelming thank you to Anne Luxford for being responsible for the breeding program at WCHRE, which allowed me to have the mice that I used for this project. Not only that, but without her I would not have been able to have finished my animal study due to Covid-19 lockdowns, meaning my data would have been severely compromised.

Declaration

“I, Nicholas Giourmas, declare that the Master of Applied Research thesis entitled the potential therapeutic effect of spermidine supplementation on the *mdx* mouse phenotype, is no more than 50,000 words in length including quotes and exclusive of tables, figures, appendices, bibliography, references and footnotes. This thesis contains no material that has been submitted previously, in whole or in part, for the award of any other academic degree or diploma. Except where otherwise indicated, this thesis is my own work”.

“I have conducted my research in alignment with the Australian Code for the Responsible Conduct of Research and Victoria University’s Higher Degree by Research Policy and Procedures”.

“All research procedures reported in the thesis were approved by the Victoria University Animal Ethics Committee (AEC 19-002)”



Nicholas Giourmas 27/9/2021

Table of Contents

Acknowledgements	2
Declaration	3
1. Abstract	7
2. Aims of the Project.....	7
3. Contribution to Knowledge	8
4. Literature Review	8
4.1 Skeletal Muscle.....	8
4.2 Duchenne Muscular Dystrophy	9
4.3 Current treatments for DMD.....	11
4.4 C57Bl/10mdx Mouse Model.....	13
4.4 Dystrophic Muscle Mechanisms.....	14
4.5 Autophagy.....	17
4.6 Rapamycin/mTOR/Autophagy Pathway.....	21
4.7 Spermidine and the Polyamine Pathway	21
4.8 Potential mechanisms for spermidine-induced autophagy	23
5. Methodology and Conceptual Framework	25
5.1 Spermidine supplementation from 3 to 16 weeks of age	25
5.2 7-day Autophagy Flux Assay	28
5.3 Contractile Function	30
5.4 Histology – Haematoxylin and Eosin (H and E) Stain.....	31
5.5 Western Blotting.....	31
6. Statistical Analysis	33
Results	34
7. Genotypic differences in the expression of polyamine pathway proteins and the effect of 13 weeks of spermidine supplementation	34
7.1 Fast-twitch EDL muscle	34
7.2 Slow-twitch SOL muscle.....	36
8. The effect of spermidine supplementation on body weight, muscle mass, force output and fatigue	38
8.1 Body Weight	38
8.2 EDL – Muscle Mass, absolute/specific forces and fatiguability	41
8.3 SOL – Muscle Mass, absolute/specific forces and fatiguability.....	45
9. The effect of spermidine supplementation on muscle structure	49
9.1 EDL – Haematoxylin and Eosin (H&E) Stain for muscle fibre size and muscle health	49

9.2 SOL – Haematoxylin and Eosin (H&E) Stain for muscle fibre size and muscle health	52
10. The effect of spermidine supplementation on autophagy-related proteins.....	55
10.1 Fast-twitch EDL muscle.....	56
10.2 Slow-twitch SOL muscle.....	63
11. The effect of spermidine supplementation on the autophagy flux assay	70
11.1 Fast-twitch EDL muscle.....	70
11.2 Slow-twitch SOL muscle.....	73
Discussion	77
12. Expression of polyamine pathway enzymes in wild type vs <i>mdx</i> skeletal muscle	77
13. The effect of spermidine supplementation on body weight, muscle force output and fatigue	80
14. The effect of spermidine supplementation on muscle morphology	83
15. The effect of spermidine supplementation on key autophagy-related proteins and autophagy-regulating signalling pathways	86
16. The effect of spermidine supplementation on autophagy flux in WT and <i>mdx</i> skeletal muscle.....	91
17. Limitations.....	94
18. Future Directions	95
19. Conclusion	96
20. References	96

List of Figures

Figure 1. Dystrophin extracellular matrix/cytoskeleton complex.	9
Figure 2. <i>mdx</i> mouse postnatal age to muscle necrosis relation.	13
Figure 3. Autophagic Pathway - Elongation and maturation.	18
Figure 4. Polyamine Pathway.....	22
Figure 5. Spermidine/AMPK/Autophagy Pathway..	24
Figure 6. 3–16 week spermidine supplementation animal study.....	27
Figure 7. 7-day spermidine supplemented autophagy flux animal experiment.....	29
Figure 8. The genotype and spermidine supplementation effect on polyamine pathway proteins within the EDL.	35
Figure 9. The genotype and spermidine supplementation effect on polyamine pathway proteins within the SOL.	37
Figure 10. The effect of spermidine supplementation on absolute body weights.	39
Figure 11. The effect of spermidine supplementation on body weight percentage change. .	40
Figure 12. Volume of water ingested throughout 3–16-week animal study.	41
Figure 13. The genotype and spermidine supplementation effects on EDL muscle mass. ..	42
Figure 14. Optimal length of EDL from functional studies.....	43
Figure 15. The effect of spermidine supplementation on EDL functionality.....	44
Figure 16. Spermidine supplementations impact on EDL fatigue.	45

Figure 17. The genotype and spermidine supplementation effects on SOL muscle mass. . .	46
Figure 18. Optimal length of SOL from functional studies.....	47
Figure 19. The effect of spermidine supplementation on SOL functionality.	48
Figure 20. Spermidine supplementations impact on SOL fatigue.	49
Figure 21. The effect of spermidine supplementation on muscle fibre health in WT and mdx EDL muscles.....	50
Figure 22. The effect of spermidine supplementation on muscle tissue health in WT and mdx EDL muscles.....	51
Figure 23. The effect of spermidine supplementation on muscle fibre size in WT and mdx EDL muscles.....	52
Figure 24. The effect of spermidine supplementation on muscle fibre health in WT and mdx SOL muscles.	53
Figure 25. The effect of spermidine supplementation on muscle tissue health in WT and mdx SOL muscles.	54
Figure 26. The effect of spermidine supplementation on muscle fibre size in WT and mdx SOL muscles.	55
Figure 27. The effect of spermidine supplementation on MAP1S in EDL muscles.....	57
Figure 28. The effect of spermidine supplementation on phosphorylated and total AMPK in EDL muscles.....	58
Figure 29. The effect of spermidine supplementation on phosphorylated and total p70 ^{S6K1} in EDL muscles.	60
Figure 30. The effect of spermidine supplementation on phosphorylated and total 4EBP1 in EDL muscles.....	61
Figure 32. The effect of spermidine supplementation on MAP1S in SOL muscles.	63
Figure 33. The effect of spermidine supplementation on phosphorylated and total AMPK in SOL muscles.	65
Figure 34. The effect of spermidine supplementation on phosphorylated and total p70 ^{S6K1} in SOL muscles.	66
Figure 35. The effect of spermidine supplementation on phosphorylated and total 4EBP1 in SOL muscles.	68
Figure 36. The effect of spermidine supplementation on LC3B and p62 in SOL muscles. . .	69
Figure 37. The effect of spermidine supplementation on p62 in 7-day autophagy flux EDL muscles.	71
Figure 38. The effect of spermidine supplementation on LC3B in 7-day autophagy flux EDL muscles.....	73
Figure 39. The effect of spermidine supplementation on p62 in 7-day autophagy flux SOL muscles.....	74
Figure 40. The effect of spermidine supplementation on LC3B in 7-day autophagy flux SOL muscles.....	76

List of Tables

Table 1. Western blotting antibodies and dilutions	32
Table 2. Homogenisation buffer composition	33

1. Abstract

Duchenne Muscular Dystrophy (DMD) is one of the most severe forms of inheritable muscular dystrophies that affects 1 in every 5,000 boys. DMD is caused by a genetic mutation on the X chromosome, which results in the loss of the full-length protein, dystrophin. Dystrophin plays a stabilising role by connecting the cytoskeleton of muscle fibres to the extracellular matrix, with the absence of dystrophin directly correlating with the severity of DMD. It has been previously shown that the drug, rapamycin, improves dystrophic muscle function, in part, through the upregulation of the process known as autophagy. This autophagic process plays a role in degrading/removing damaged molecules, including lipids and proteins. Long term use of rapamycin, however, may result in toxic side effects that makes its use as a DMD treatment limited. Because of this, finding a non-toxic inducer of autophagy may be beneficial in treating DMD. One molecule that is known to activate autophagy in a range of tissues, including skeletal muscle, is the polyamine spermidine. To date, however, the effect of spermidine-induced autophagy has not been investigated regarding its potential to improve the DMD muscle phenotype, as well as the differences between polyamine pathway enzyme levels between dystrophic skeletal muscle and WT.

2. Aims of the Project

- Determine whether there are any genotypic differences within the polyamine pathway enzymes
- Determine whether polyamine pathway protein expression is altered with spermidine supplementation
- Determine whether spermidine supplementation improves the dystrophic phenotype of *mdx* mice i.e. muscle structure and function
- Determine whether any beneficial effect of spermidine is associated with increased autophagic activity

3. Contribution to Knowledge

The current gap in knowledge is that no studies have investigated whether spermidine has an impact on the regulation of autophagy in a model of DMD. Literature has indicated spermidine's ability to induce autophagy in many different models, including skeletal muscle. Increased autophagy has also been shown to improve skeletal muscle in many models of dystrophy, including DMD, however to date, no studies have examined whether spermidine supplementation improves dystrophic skeletal muscle function and histopathology in a model of DMD, and whether this would be associated with increased autophagy. Furthermore, no studies examined potential differences in the expression of key enzymes within the polyamine pathway in DMD muscle compared to healthy muscle.

4. Literature Review

4.1 Skeletal Muscle

Skeletal muscle is the largest of the three types of muscle tissues, making up roughly 40% of the total human body (1). The importance of skeletal muscle is exemplified in its roles in bodily movement and posture, maintaining body temperature, whole body metabolism, disease prevention and sustaining a person's overall quality of life (2, 3). Thus, the overall maintenance of muscle mass and function is essential in maintaining/increasing overall health status. Those who exhibit dysfunctional skeletal muscle have shown a decrease in muscle function and an increase in morbidity, resulting in an increased burden on family and caregivers, the patients decreased independence, lifespan and quality of life (4-6). Some diseases that are associated with dysfunctional muscle include aging (7), immobilisation (8), diabetes (9), obesity (10), Human Immunodeficiency Virus (HIV) (11), Amyotrophic Lateral Sclerosis (ALS) (12), and Duchenne Muscular Dystrophy (DMD) (13).

4.2 Duchenne Muscular Dystrophy

DMD is a progressive neuromuscular disease caused by genetic recessive mutations within the dystrophin gene (*DMD* gene) on the X chromosome, resulting in premature stop codons and the loss of expression of the full-length 427 kDa cytoplasmic protein, dystrophin (14, 15). DMD affects 1 in every 5,000 newborn males which results in mechanistic changes that lead to muscle weakness and damage, usually noticed at ages 2-5 and continuing throughout the remainder of their shortened lifespan (16).

The dystrophin protein is comprised of four main functional domains: an n-terminal domain which allows for actin binding (ABD1), a central rod domain that is comprised of 24 spectrin protein repeats which is interspaced with proline-rich hinges providing flexibility, a cysteine-rich domain for β -dystroglycan binding, and a carboxyl-terminus for the binding of scaffolding proteins such as syntrophins and dystrobrevin (17).

Dystrophin is found primarily in muscle cells and plays an essential role in muscle membrane stability through establishing a connection between the extracellular matrix and cytoskeletal actin (Fig. 1) (18).

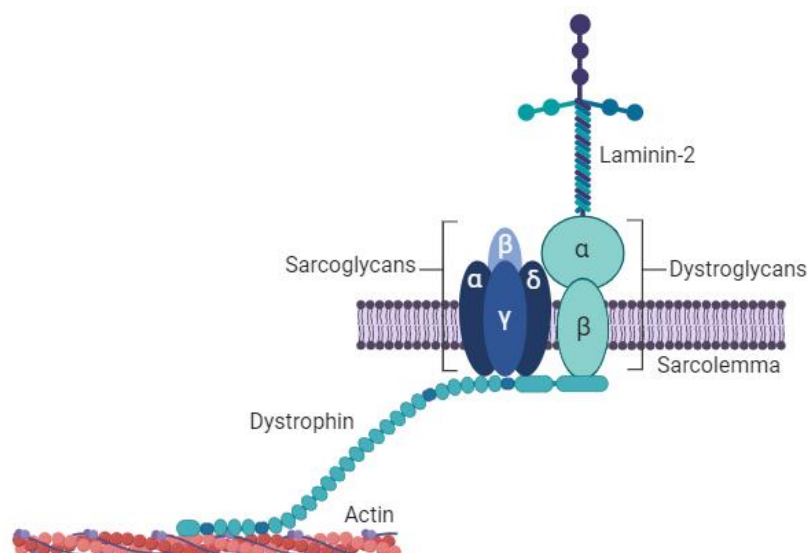


Figure 1. Dystrophin extracellular matrix/cytoskeleton complex. Dystrophin is a rod-shaped protein that forms a connection between the extracellular matrix and the γ -actin of the subsarcolemmal cytoskeleton of muscle fibres. This is done via dystrophin's ability to interact with the α/β dystroglycan and laminin-2 complex, which is then bound to the sarcoglycan subcomplex (consisting of α , β , γ and δ sarcoglycan), allowing for stability of the muscle fibres through muscle contractions. Created with BioRender.

More specifically, dystrophin connects the γ -actin of the subsarcolemmal cytoskeleton of muscle fibres to proteins on the extracellular matrix, forming part of the dystrophin protein complex (DPC) (18, 19). Dystrophin, through its functionality as a flexible cytoplasmic protein, interacts directly with β -dystroglycan, a transmembrane protein, and allows for the DPC's connection to α -dystroglycan, an extracellular protein, via its cysteine-rich C-terminal region (20). α -dystroglycan is heavily glycosylated, permitting it to function as a receptor to Laminin-2, an extracellular ligand responsible for the migration and organization of cells into muscle tissue (21).

This α/β -dystroglycan complex is tightly bound to the transmembrane sarcoglycan subcomplex that is present within the plasma membrane of a muscle cell known as the sarcolemma (17). Within skeletal muscle, this sarcoglycan subcomplex is created through 4 individual transmembrane proteins; α -sarcoglycan, β -sarcoglycan, γ -sarcoglycan and δ -sarcoglycan (17). This sarcoglycan subcomplex aids in the stability of the sarcolemma, with the loss of any of the sarcoglycan subunits directly effecting the stability of the DPC (17).

This connection of the γ -actin of the subsarcolemmal cytoskeleton to the sarcolemmal dystroglycan/sarcoglycan complex via dystrophin, results in muscle stability through low to high force contractions. Specifically, the force of a contraction is decreased on the sarcolemma, through dystrophin's central rod domain allowing for the absorption and mitigation of forces produced, decreasing the susceptibility of sarcolemmal damage (22). In DMD however, the DPC is compromised in both structure and function due to the loss of full-length dystrophin (17, 23). More precisely, this loss of full-length dystrophin results in the sarcolemma taking the vast majority of forces produced during muscle contractions, largely due to the compromised connection between the γ -actin of the subsarcolemmal cytoskeleton and the extracellular matrix (24, 25). Repeated contractions of even relatively low forces, such as during walking, can lead to significant muscle fibre damage.

Because of this, DMD muscles are continuously undergoing cycles of damage and repair/regeneration, that eventually leads to muscle wasting, fibrosis and fatty tissue infiltration

(26-28). Consequently, DMD muscles become very weak and those afflicted are typically left wheelchair bound early in life and die within their 20-30's primarily due to respiratory failure (29-31). Because of DMD's negative effects on those affected both physically and mentally, sustainable long-term treatments are desperately needed to help improve the quality of life for those suffering from DMD.

4.3 Current treatments for DMD

The only approved treatments currently being used for those with DMD are the synthetic glucocorticoid corticosteroids prednisone and deflazacort. Studies have shown that both treatment of both prednisone and deflazacort, to differing degrees, have resulted in improved muscle strength, reduced risk of scoliosis, and improved pulmonary and motor function. This is hypothesised to be due to a stabilizing effect on the sarcolemma throughout low force repeated contractions via reduced inflammation (32-37). Despite these promising results, both prednisone and deflazacort come with continuous side effects throughout usage that effect the patient's quality of life, due to their immunosuppressant nature. These side effects consist of weight gain, stunted growth, delayed puberty, gastrointestinal symptoms, osteoporosis and behavioural changes (32-37). These side effects, although potentially intolerable, are still favourable compared to the alternative of leaving DMD untreated. Nonetheless, because of this, there is an urgent need to identify other potential treatments with less severe side effects.

The most promising, yet limited, current treatment being studied is the insertion of a micro-dystrophin gene via an adeno-associated (AAV) viral vector. This micro gene insertion has shown improvements to both skeletal muscle structure and function in a canine model of DMD (38). Despite these improvements, however, this technique is limited as AAVs have a limited packing size and therefore cannot be used to package the full length dystrophin gene, which is the largest gene in the genome (39). As such, this would not result in the 'restoration' of a full-length functional dystrophin protein, further highlighting the necessity for an affordable and practical treatment for DMD.

Potential treatments utilizing different gene therapy techniques, such as exon skipping and nonsense suppression, are currently being explored. Exon skipping aims to silence specific mutated exons within the dystrophin gene through the introduction of mRNA sections that cause the exon containing the mutated codon to be skipped during translation, resulting in the production of a smaller, yet more functional dystrophin protein (40). Nonsense suppression therapy uses aminoglycosides to partially restore dystrophin's function, through the suppression of a premature translation-termination codon (41, 42). The primary issue that gene therapy techniques face in the context of DMD, is that due to the size of the gene, mutations within it are vastly different, and occur at random sections of the gene (43).

DMD in ~65% of patients are due to substantial deletions within the DMD gene, with ~7-10% occurring through duplications of a single or multiple exons within the DMD gene (44, 45). Additionally, ~25-30% of those with DMD have splicing and point mutations, as well as small deletions and insertions within the DMD gene (44, 45). Because of these varying mutations and their location along the DMD gene, both exon skipping and nonsense suppression have a low success rate in the majority of DMD cases. The most successful exon skipping, skipping exon 51, only works for 13% of DMD patients. Moreover, only 13-15% of those with DMD contain a mutation where nonsense suppression is a viable treatment (45-48). Furthermore, the success of these treatments drops significantly for those with multiple mutations of the DMD gene (45). Coupled with low success rate of these techniques, and the reality that each technique is specified to one person and can't be applied to the majority of DMD patients, are the extensive costs that most can't afford (~\$300,000-\$1,000,000) per patient (49).

Due to the issues outlined with current DMD treatments, and limitation with gene therapy techniques, there is an urgency for new immediate treatment options that not only prolong lifespan, but also improve the patient's quality of life. For this to occur, however, a deeper understanding of the mechanistic changes that occur through the loss of dystrophin is essential. Because of the need for identifying the molecular consequences of the loss of dystrophin, and testing of novel therapeutic agents in DMD boys would be unethical, several

animal models have been used for mechanistic preclinical testing with the most common being the C57Bl/10mdx (*mdx* mouse) mouse model (14, 15).

4.4 C57Bl/10mdx Mouse Model

The *mdx* mouse model is the most commonly used model of DMD, due to the presence of a genetic mutation on exon 23 of the X chromosome that causes a premature stop codon within the dystrophin gene (14, 15). Specifically, this mutation changes the amino acid that codes for glutamine, to a stop codon (14). This stop codon results in the loss of full-length dystrophin, ultimately resulting in a model that closely mimics that of human DMD (14, 15).

The *mdx* mouse model results in aggressive cycles of muscle damage and repair, that peaks at 3 weeks of age, followed by stabilised but still elevated levels chronic muscle damage from 6 weeks onwards (Fig. 2) (50).

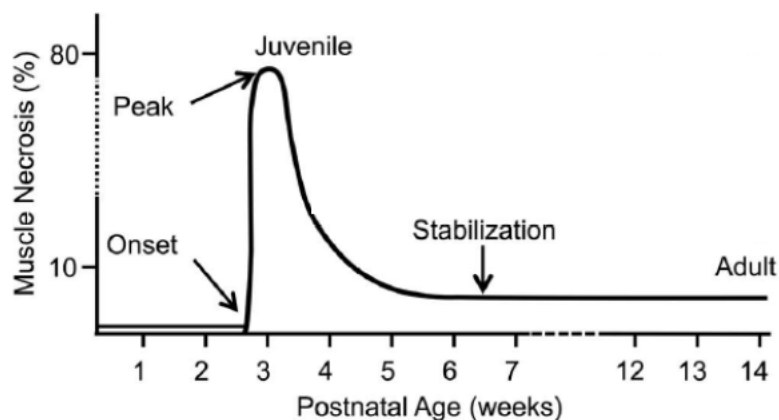


Figure 2. mdx mouse postnatal age to muscle necrosis relation. The mutation on exon 21 of the DMD gene occurs at 3 weeks of age. Subsequently, aggressive muscle damage and necrosis initiates and is consistent until 6 weeks. From 6 weeks onwards, the *mdx* mice then have a stabilized, yet still elevated, level of muscle necrosis until cull date. (48)

Insights gained from using the *mdx* mouse model have shown that the loss of dystrophin results in at least three major mechanistic changes that play key roles in DMD-induced muscle wasting and dysfunction. The three mechanisms are increased levels of reactive oxygen

species (ROS) (51, 52), abnormal intracellular calcium homeostasis (53-55), and prolonged chronic inflammation (56-59).

4.4 Dystrophic Muscle Mechanisms

4.4.1 Reactive Oxygen Species

Reactive oxygen species (ROS) are naturally created by-products from oxygen molecules during oxidative cellular metabolism (60). They are highly reactive molecules that primarily consist of having an unpaired electron, enabling them to steal electrons from other proteins they come into contact with. ROS signalling is neutralized through interacting with antioxidants, which donate their spare electron to neutralise its reactivity with other proteins and providing redox homeostasis (61). Varying ROS levels are responsible for the regulation of cell signalling and differentiation, cell survival and death, and within DMD primarily upregulated in inflammation factor production (52).

ROS are produced at rest, with an upregulation in their production during muscular contractions (62). Normal levels of ROS play important roles in cell signalling through their modification of cell signalling proteins that change their functionality (62). When ROS production is markedly elevated for extended periods of time, they outnumber antioxidants synthesised, resulting in ROS remaining unbalanced and subsequent oxidative stress (52). The consequences are a negative impact on cellular function through the unmitigated and excessive electron theft, and thus damage and instability of DNA, proteins and lipids (63).

Within DMD muscle, oxidative stress occurs when the production of ROS is greater than the production of antioxidants, resulting in macromolecule oxidation which, in turn, contributes to an increased muscular damage and dysfunction (52). Enhanced protein oxidation, and subsequent oxidative stress, has been documented in both the *mdx* mouse model (64, 65) and human DMD muscle biopsies (66). Furthermore, *mdx* mouse myotubes have shown an increased vulnerability to oxidative stress compared to control myotubes (67).

Specifically, this damage is caused through the increase of malfunctional or unstable proteins through ROS interaction, further exacerbating the dystrophic phenotype (26). In order to neutralise ROS, the upregulation of certain antioxidant pathways, such as Nuclear factor-erythroid factor 2 (NRF2), have been documented to potentially help mitigate oxidative stress within muscle (52). The data suggests that although oxidative stress results in the exacerbation of DMD, their neutralization or removal could prove beneficial to improving muscle structure and function (62).

Another potential consequence of elevated ROS in DMD muscles, that is believed to play a role in dystrophic muscle damage, is elevated resting levels of intracellular calcium.

4.4.2 Abnormal Calcium Homeostasis

During the initiation of a normal muscle contraction, calcium is released from the sarcoplasmic reticulum (SR) leading to an increase in cytosolic calcium concentration within the muscle, which then decreases back to resting levels when calcium is 'pumped' back into the SR when the contraction is completed (68). This relation between both an increase and decrease in cytosolic calcium is recurrent, highlighting the importance for the maintenance of this calcium homeostasis (55). Conversely, in models of muscle disease and ageing, there is an increase in basal levels of intracellular calcium compared to healthy muscle (69, 70). Further, the loss of dystrophin within DMD skeletal muscle makes the sarcolemma susceptible to damage, and combined with increased activation of stretch-activated calcium channels, there is a highly negative impact on calcium homeostasis within the muscle (51, 71, 72).

Data gathered from the *mdx* mouse has shown that muscle contractions result in abnormally elevated levels of resting intracellular calcium compared to healthy skeletal muscle, suggestive of damage and increased permeability of the dystrophin deficient sarcolemma (53, 72-75). These increased levels of intracellular calcium in *mdx* muscle correspond with abnormal SR calcium levels, SR calcium leakage, and trans-sarcolemmal calcium fluxes (55). Such varying levels of calcium result in muscle fibre damage, even throughout low force

repeated contractions (55). Importantly, this contraction-induced increase in intracellular calcium is inhibited in *mdx* muscle by the antioxidant, N-acetylcysteine (NAC), suggesting that oxidative stress plays an antagonistic role in the disturbance in calcium homeostasis (76, 77).

Mechanistically, this impairment of calcium homeostasis results in downstream molecular processes which have the potential to activate calcium-activated proteases, known as calpains (78, 79). Calpain activation results in the degradation of cytoplasmic, nuclear and membrane proteins, which further contributes to muscle damage and increased amounts of dysfunctional proteins, and subsequent cellular apoptosis and chronic inflammation (78-80).

4.4.3 Chronic Inflammation

Inflammation is an immune response initiated through the increase of pro-inflammatory cytokines from infiltrating inflammatory cells (81-83). Cytokines, such as interleukins and lymphokines, are small (<40kDa) signalling proteins that bind to surface receptors of both immune and non-immune cells, stimulating regeneration for damaged muscle fibres (81-83). In healthy skeletal muscle, cytokine levels decrease once the muscle fibres are regenerated and functional again (84). This inflammatory response is essential for normal skeletal muscle regeneration of damaged/injured muscle cells, however, in DMD, skeletal muscle inflammation is chronic due to the repeated bouts of damage and regeneration (81-83).

Once pro-inflammatory cytokines are bound to receptors, they have the potential to further increase cytokine levels, resulting in chronic inflammation (81-83). Chronic inflammation can then drive continual cycles of muscle degradation and regeneration leading to muscle wasting, decrease muscle force per fibre, and eventual muscle fibrosis (81-83). These levels of chronic inflammation in DMD directly correlate with the severity of disease progression (81-83). Furthermore, evidence suggests that constant inflammation may eventually impair the ability to repair muscle fibres, resulting in infiltration of both adipose and connective tissue (81, 85).

The culmination of increased ROS production, elevated intracellular calcium and chronic inflammation has the potential to result in an accumulation of damaged, and potentially toxic,

proteins within skeletal muscle (86, 87). These proteins may be detrimental to skeletal muscle function as dysfunctional proteins are unable to carry out their normal cellular function, and have the potential to aggregate within the cell, resulting in the inhibition of essential molecular processes and the initiation of stress responses (86, 87). Because of this, the upregulation of cellular processes, such as macroautophagy (referred to as autophagy), helps to limit the build-up of these toxic proteins and facilitate regeneration by sequestering and degrading damaged proteins and other cellular structures (88, 89).

4.5 Autophagy

Autophagy (self-eating) is a ubiquitous process that breaks down and recycles incorrectly folded or toxic proteins that, if left to build up, would cause damage and impair cell function (88, 90). The importance of autophagy for maintaining normal cellular function is highlighted by studies showing that the upregulation of autophagy increases the lifespan in many different models, such as yeast (91), worms (92), flies (93) and mice (94). Importantly, the upregulation of autophagy has also been shown as a promising pathway to improve the phenotype of muscles from *mdx* mice (89, 95).

Autophagy itself is a multi-stepped sequential process (Fig. 3) that begins with the formation of a double membrane structure known as a phagophore (88, 90, 96). This phagophore elongates around unnecessary or dysfunctional components within the body, encapsulating these components with a complete membrane known as an autophagosome (88, 90, 96). After the completed formation of an autophagosome, a lysosome then fuses, forming an autolysosome (88, 90, 96). This step allows for the release of lysosomal hydrolase enzymes that degrade proteins, and other molecules, within the autophagosome (88, 90, 96). During this process, the inner membrane of the autolysosome is also degraded (88, 90, 96).

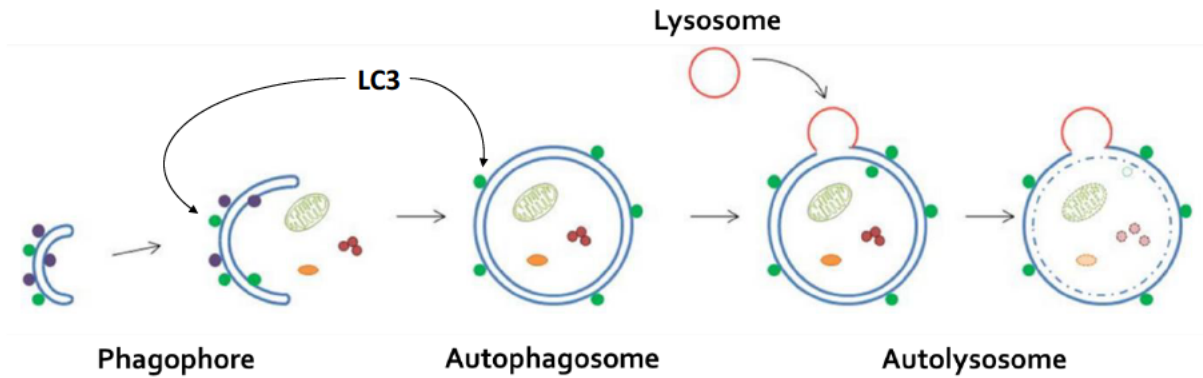


Figure 3. Autophagic Pathway - Elongation and maturation. ULK1 initiates autophagy through the initiation of a double membraned phagophore. The phagophore elongates and encapsulates all components for degradation, and with the lipidation of LC3B-I to LC3B-II, completes the formation of the autophagosome. p62 that is within the inner membrane binds and provides a link between LC3B-II and the proteins for degradation. A lysosome fuses with the autophagosome forming a lysosome, resulting in the secretion of degradative enzymes, breaking down all proteins encapsulated in the structure, including the inner membrane of the autolysosome. (Modified from 94)

More specifically, autophagy is initiated through the serine/threonine specific protein kinase ULK1 (97). ULK1 is present with a protein complex comprised of four proteins (ULK1, FIP200, ATG13 and ATG101) and is responsible for the beginning of phagophore elongation and autophagosome formation (98). ULK1 is either inhibited or activated through its direct phosphorylation by the mammalian/mechanistic target of rapamycin complex 1 (mTORC1) or AMP-activated protein kinase (AMPK), respectively (99). mTORC1 is a master inducer of protein synthesis through its phosphorylation of 4EBP1 and p70^{S6k1} resulting in increased cap-dependant translation (100). When mTORC1 activity is upregulated, it also inhibits autophagy initiation through the phosphorylation of ULK1 at Ser757 whilst also disrupting the interaction of AMPK and ULK1 (99). Conversely, activated AMPK promotes autophagy initiated ULK1 phosphorylation at Ser317, Ser555 and Ser777 (99).

Following the activation of the ULK1 protein complex is the construction of the phosphatidylinositol-3 kinase complex I (PI3KC3-C1). Similar to the ULK1 complex, PI3KC3-C1 is encompassed by 4 different sub-units. These sub-units consist of BECLIN1, PIK3C3, PIK3R4 and ATG14 and are essential in the stages of phagophore elongation at the nucleation stage of autophagy (101-104). As autophagy begins, the PI3KC3-C1 complex converts

phosphatidylinositol (PI) into phosphatidylinositol 3-phosphate (PI3P) at the sites of phagophore nucleation, providing a conjugation scaffold for other essential autophagic proteins to bind (102-104).

One such autophagic protein is the commonly used marker of autophagosome completion, microtubule-associated protein 1A/1B-light chain 3 (LC3B). LC3B is a protein that is present on both the inner and outer membrane of an autophagosome, that is cleaved via ATG4 to produce the cytosolic protein LC3B-I (105). LC3B-I is then lipidated with phosphatidylethanolamine via the ATG5-ATG12 complex, forming the LC3B-phosphatidylethanolamine conjugate (LC3B-II) (106). LC3B-II's formation results in phagophore completion, and subsequent autophagosome formation (106). Thus, an increase in the amount of LC3B-II protein (and/or an increase in the LC3B-II to LC3B-I ratio) is a commonly used marker for the initial activation of autophagy (107).

LC3B-II on the inner membrane of the autophagosome conjugates with another commonly used marker of autophagy completion, the multifunctional protein, p62. p62 is responsible for recognising specific proteins for their breakdown through the autophagic pathway (108, 109). Specifically, p62 binds to ubiquitin labelled aggregates, and then interact with LC3B-II (108, 109). Once p62 is bound to both inner membrane LC3B-II and ubiquitinated aggregates, the autophagosome is then fully formed allowing for the final step of autophagosome-lysosomal fusion (108, 109).

The HOPS complex, consisting of the proteins PLEKHM1 and EPG5, plays a role in autophagosome-lysosome fusion through its ability to react concurrently with proteins on both the lysosomal membrane and the autophagosome membrane (110). Specifically, PLEKHM1 binds to the nucleotide guanosine triphosphate enzyme, RAB7, present on the lysosome, whilst also binding to the LC3B-II on the outer layer of the autophagosome (111). EPG5 plays a similar role, binding to both LC3B-II and RAB7 accordingly. It's the binding of these proteins that allows for lysosomal fusion, resulting in the secretion of lysosomal hydrolase enzymes inside the inner membrane (112). This results in the degradation of proteins, and other

molecules within the autophagosome, while subsequently degrading the inner membrane of the double membrane structure (88, 90, 96). This results in some of LC3B-II, and all of p62, present on the inner membrane being degraded during the completion of autophagy. As such, a decrease in p62 protein is a commonly used marker for the completion of the final steps of autophagy (107).

Importantly, studies have demonstrated that autophagy completion is inhibited in dystrophic skeletal muscle (89). Specifically, data in the *mdx* diaphragm has shown an increase of LC3B-I and a subsequent decrease of LC3B-II, indicating an inhibition of autophagy completion (89). This data is coupled with the increase in p62 levels within the *mdx* tibialis anterior (TA) and diaphragm, suggesting that the incomplete autophagy occurs prior to autolysosome fusion (89). Furthermore, levels of lysosomes within dystrophic *mdx* muscle are decreased, inhibiting autolysosome creation (113). Interestingly, the same study showed that many of the lysosomes that are present in *mdx* mice have been detected in the extracellular space, which could further reduce rates of autophagy completion of dystrophic muscle fibres (113). This data suggests that inhibition of autophagy completion potentially occurs primarily at the autophagosome-lysosome fusion stage. Due to autophagy inhibition within *mdx* mice, there is an abundance of malfunctioning and misfolded proteins within the muscle (26, 89, 114). These proteins can cause further damage to skeletal muscle through aggregating within the cell, negatively impacting skeletal muscle health (26, 89, 114). This increased level of muscle fibre damage results in further instability to the already dystrophin-deficient sarcolemma, potentially negatively affecting muscle function (26, 89, 114).

Because of the ability of autophagy to remove toxic proteins, upregulation of autophagy within DMD skeletal muscle is hypothesised to improve muscle function. Interestingly, a drug that has shown to improve muscle function in dystrophic skeletal muscle, whilst activating autophagy, is rapamycin (95).

4.6 Rapamycin/mTOR/Autophagy Pathway

The lipophilic macrolide antibiotic, rapamycin, is a prominent inducer of autophagy through its inhibitory effect on mTORC1 (95). mTOR, G-protein β -subunit like protein (G β L) and the regulatory associated protein of mTOR (raptor) are the three functional components of the protein complex, mTORC1, which inhibits autophagy through its phosphorylation of ULK1 (99, 115). Rapamycin inhibits the kinase activity of mTORC1 through conjugating with the immunophilin, FKBP12, which binds to mTOR and impedes the mTOR-raptor binding and mTOR substrate phosphorylation (116). Importantly, the rapamycin-induced inhibition of mTORC1, and subsequent activation of autophagy, has been shown to improve *mdx* skeletal muscle force production, indicating autophagy's potential therapeutic effect on dystrophic skeletal muscle (95).

Rapamycin, however, is unlikely to be used clinically in human DMD patients due to the possibility of long-term side effects, in part, because rapamycin is an immune suppressant (117). Because of this, finding a non-toxic long-term activator of autophagy could be important as a therapeutic treatment for dystrophic skeletal muscle. One such potential inducer of autophagy in skeletal muscle is the naturally occurring polyamine, spermidine.

4.7 Spermidine and the Polyamine Pathway

Spermidine is a small ubiquitous molecule that is synthesised within the polyamine pathway (Fig. 4). The first reaction of the polyamine synthesis pathway initiates with the enzyme, ornithine decarboxylase (Odc1) (118). Odc1 synthesises putrescence through the decarboxylation of ornithine (118). Putrescine is then converted into spermidine via the enzyme spermidine synthase (SpdSyn) (118). For this reaction to occur, an aminopropyl group is donated by decarboxylated S-adenosylmethionine (dcSAM), which is catalysed by the enzyme, S-adenosylmethionine decarboxylase (Amd1) (118). Spermidine can be further converted into spermine via the enzyme, spermine synthase (SpmSyn), which requires the same aminopropyl group that is donated via Amd1's reaction product, dcSAM (118). Spermine

can also be reverted back into spermidine via the enzyme, spermine oxidase (Smox), while the enzyme spermidine/spermine N¹-acetyltransferase (Sat1) can remove both spermidine and spermine from the polyamine pathway through their direct acetylation (118).

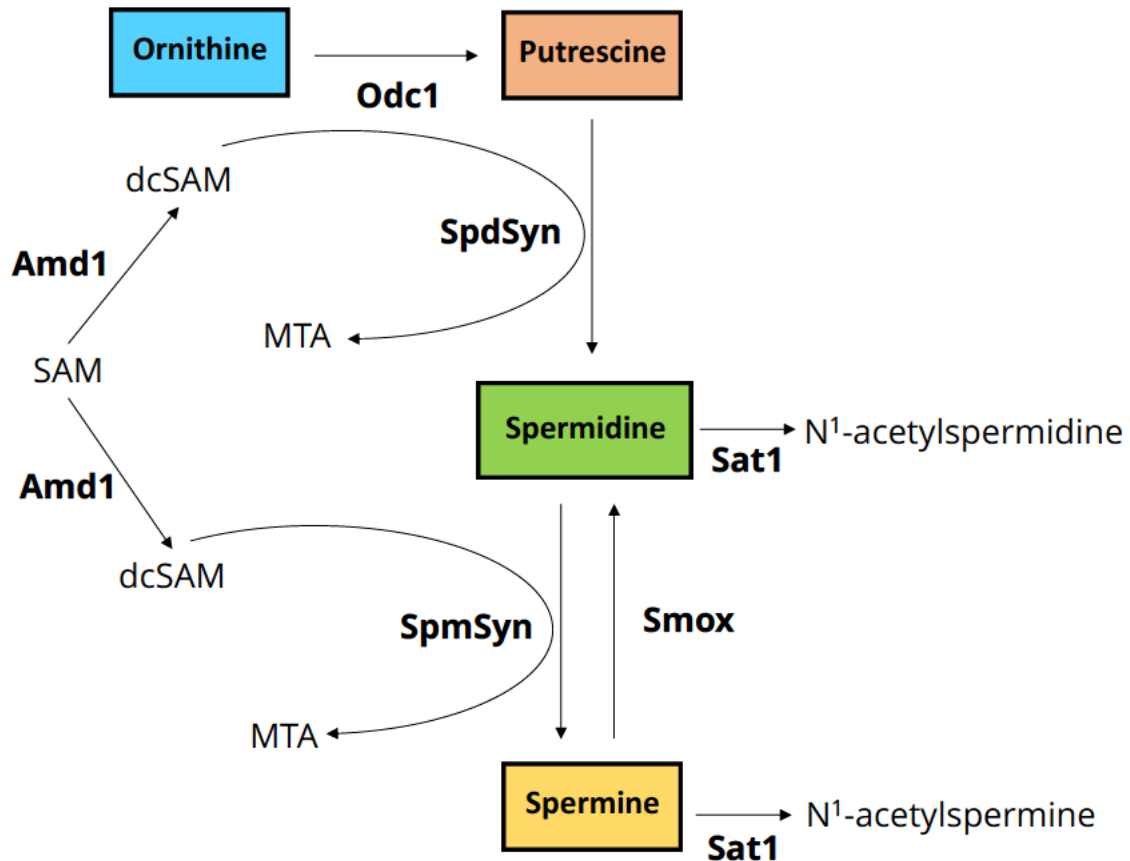


Figure 4. Polyamine Pathway. Ornithine is first converted to putrescine by ornithine decarboxylase 1 (Odc1). Putrescine is converted to spermidine, and then spermine, by spermidine synthase (SpdSyn) and spermine synthase (SpmSyn), respectively. Spermine oxidase (Smox) can regress spermine back into spermidine. AdoMetDC (Amd1) is a regulator of both SpdSyn and SpmSyn through its relation of donating an aminopropyl group from decarboxylated S-adenosylmethionine (dcSAM) while spermidine/spermine N¹-acetyltransferase (Sat1) can eject both spermine and spermidine from the polyamine pathway for bodily use in the form of N¹-acetylspermidine/N¹-acetylspermine respectfully. Solid lines are direct and dotted lines are indirect relations between enzymes. S-adenosylmethionine (SAM), 5-methylthioadenosine (MTE).

Spermidine plays an essential role in cell homeostasis through its impact on autophagy proteins, histone acetylation, DNA synthesis and protein synthesis (119-122). Importantly, spermidine supplementation has been shown to activate autophagy, in many different models, such as yeast, flies, worms, mice and human immune cells, with no long-term toxicity (119, 123).

Recent publications have also suggested a relation between the polyamine pathway and mTORC1 (124). Firstly, in a human prostate cancer cell line (DU145), mTORC1 was shown to reduce proteasome system degradation of Amd1 through the direct phosphorylation of Amd1 (125). Another potential link was that rapamycin was shown to increase Odc1 activity in intestinal IEC-6 cell cultures (126). Furthermore, the transcription factor c-Myc, whose expression is increased via mTORC1 activation, has been shown to regulate the transcription of Odc1, Amd1 and SpdSyn (127-129). Consistent with this, our lab has recently published data showing that Amd1, SpdSyn and c-Myc proteins were upregulated during muscle hypertrophy induced by chronic mechanical overload, and that this was prevented by the mTORC1 inhibitor, rapamycin (130). Lastly, our lab have also shown that food deprivation-induced muscle atrophy was associated with a decrease of Sat1 protein levels, coinciding with decreased protein synthesis, a decrease in a marker of mTORC1 signalling (phosphorylated-p70^{S6K1}/total p70^{S6K1} ratio), and increased LC3B-II/LC3B-I ratio (130).

Despite the data suggesting a link between changes in the expression of polyamine pathway proteins, and mTORC1 signalling during muscle remodelling associated with muscle growth, no studies have thoroughly examined the expression of the polyamine pathway enzymes in dystrophic skeletal muscle. Furthermore, no studies have examined the effect of spermidine supplementation on polyamine pathway protein expression, or on markers of autophagy activation, in normal or dystrophin-deficient muscle.

4.8 Potential mechanisms for spermidine-induced autophagy

One proposed mechanism by which spermidine increases rates of autophagy is through the upregulation of AMP-activated protein kinase (AMPK) activity. AMPK is responsible for the activation of a range of catabolic processes within the cell, including macromolecule degradation via autophagy (99, 131). Importantly, AMPK has been shown to increase rates of autophagy in mouse C2C12 myoblasts, through the inhibition of mTORC1, and corresponding increase in ULK1 activity (Fig. 5) (132). Although an increase in spermidine has been shown to induce autophagy in many different models, there are limited studies that show its molecular

effect within skeletal muscle. Nonetheless, one study has shown that intraperitoneal injections (IP) of spermidine increased the activation of AMPK in aging rat skeletal muscle, resulting in improved muscle function (133). While this study suggests that spermidine has the potential to activate autophagy through AMPK activation, autophagy was not specifically investigated.

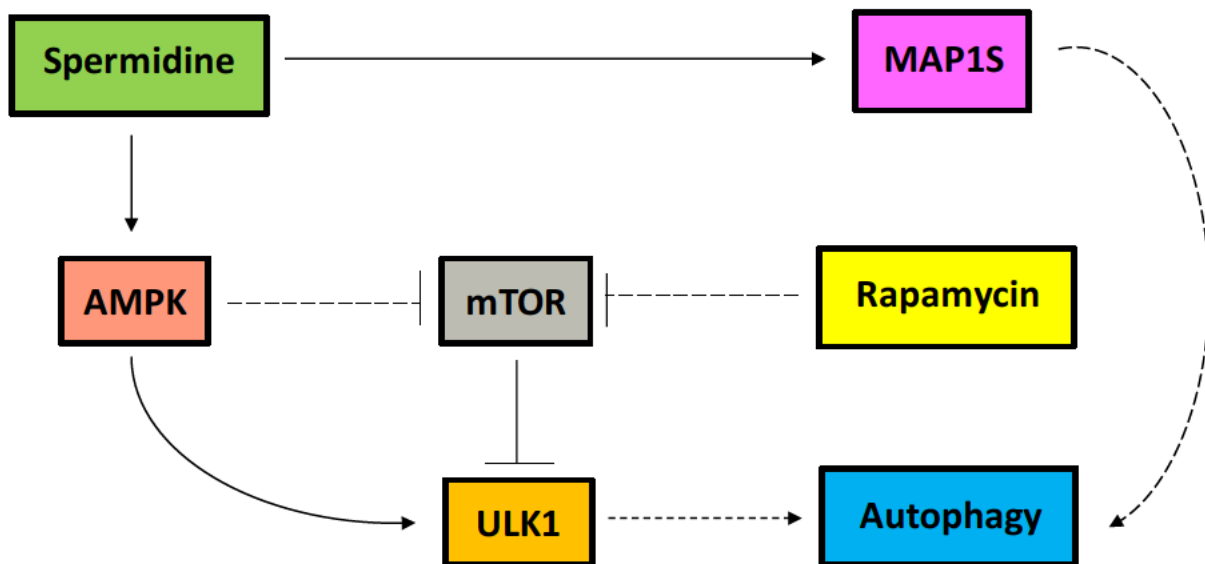


Figure 5. Spermidine/AMPK/Autophagy Pathway. Spermidine has shown to activate AMP-activated protein kinase (AMPK) which results in increased autophagy through mammalian target of rapamycin (mTOR) inhibition and subsequent ULK1 activation. Spermidine has also shown to upregulate Microtubule-associated protein 1S (MAP1S) expression which reacts with microtubule-associated protein 1A/1B-light chain 3 (LC3B-II) to upregulate autophagy. Rapamycin also inhibits mTOR which allows for autophagy activation. Solid lines are direct and dotted lines are indirect relations between proteins.

Another proposed mechanism for a spermidine-induced activation of autophagy is an increase in the abundance of the Microtubule-associated protein 1S (MAP1S), which interacts with microtubules, and a range of autophagy-related proteins, including LC3B-I and LC3B-II, to promote the autophagosome formation and degradation (134). Importantly, spermidine ingestion has been shown to increase MAP1S protein expression in the liver of wild type mice, with spermidine-induced increases in autophagy being dependent on MAP1S expression (135). Interestingly, spermidine was also shown to reduce CCl₄-induced liver fibrosis and oxidative stress in a MAP1S-dependent manner (135). Furthermore, a second study showed that MAP1S is upregulated via spermidine in CCl₄-induced liver fibrosis, also increasing antioxidant production via NRF2, influencing autophagosome formation (136). While MAP1S

is expressed in normal skeletal muscle (137), no studies have examined its expression in dystrophic muscle or potential changes in its expression in response to spermidine.

Regarding spermidine's potential to activate autophagy in a model of muscle dysfunction, one study showed that spermidine (3mM), administered through water supplementation, was able to upregulate rates of autophagy and improve the structure and function of muscle in wild type mice and in a collagen VI-null myopathy mouse model (although AMPK and MAP1S were not examined in this study) (138). This study provides evidence that supports spermidine's therapeutic potential to improve the phenotype of impaired skeletal muscle. However, to date, no studies have examined whether spermidine supplementation has the potential to improve the dystrophic phenotype of *mdx* mice, and whether any positive effect would be associated with increased autophagy. There is also a gap in the literature examining at the polyamine pathway enzymes in dystrophin-deficient skeletal muscle, and whether spermidine supplementation would impact any of their expression.

Therefore, the focus of this master's project can be split into 4 different, yet connected, aims. Firstly is to examine whether there are any genotypic differences in the expression of polyamine pathway proteins in slow- and fast-twitch muscle from wild type (WT) and *mdx* mice. Secondly, to investigate whether spermidine supplementation alters the expression of polyamine pathway proteins in slow and fast-twitch muscle of WT or *mdx* mice. Thirdly, to determine whether spermidine supplementation improves the structure and function of the dystrophic *mdx* mice. And lastly, to document whether any beneficial effects of spermidine supplementation correlate with an upregulation of autophagy initiation/completion.

5. Methodology and Conceptual Framework

5.1 Spermidine supplementation from 3 to 16 weeks of age

The main objective of this experiment was to determine if long term spermidine supplementation improves the structure and function of slow- and fast-twitch *mdx* muscle. The experimental design of this experiment can be seen in Fig. 6. WT (C57/Bl10ScSn) (n=8 per

group) and *mdx* (n=12 per group) mice were divided into vehicle (water) and spermidine supplemented treatment groups. The water-soluble polyamine, spermidine, was delivered through its addition into drinking water at a concentration of 3mM, as this concentration had shown to induce autophagy in the collagen VI-null myopathy mouse model (138). As spermidine is light sensitive, the supplemented water was protected from light with a covering of aluminium foil to limit the rate of spermidine degradation. Spermidine also degrades over time and, as such, spermidine supplemented water was remade every 2 days to ensure the correct concentration of spermidine was being supplemented constantly (119). Mice were housed in a day/night cycle of 12hrs light/12hrs dark.

From all mice, the EDL and SOL muscles were harvested for all analysis. These muscles were chosen as they are composed of different muscle fibre types, with the EDL being fast-twitch and the SOL being predominantly slow-twitch. Mice were then culled under isoflurane anaesthesia via the removal of the heart and diaphragm.

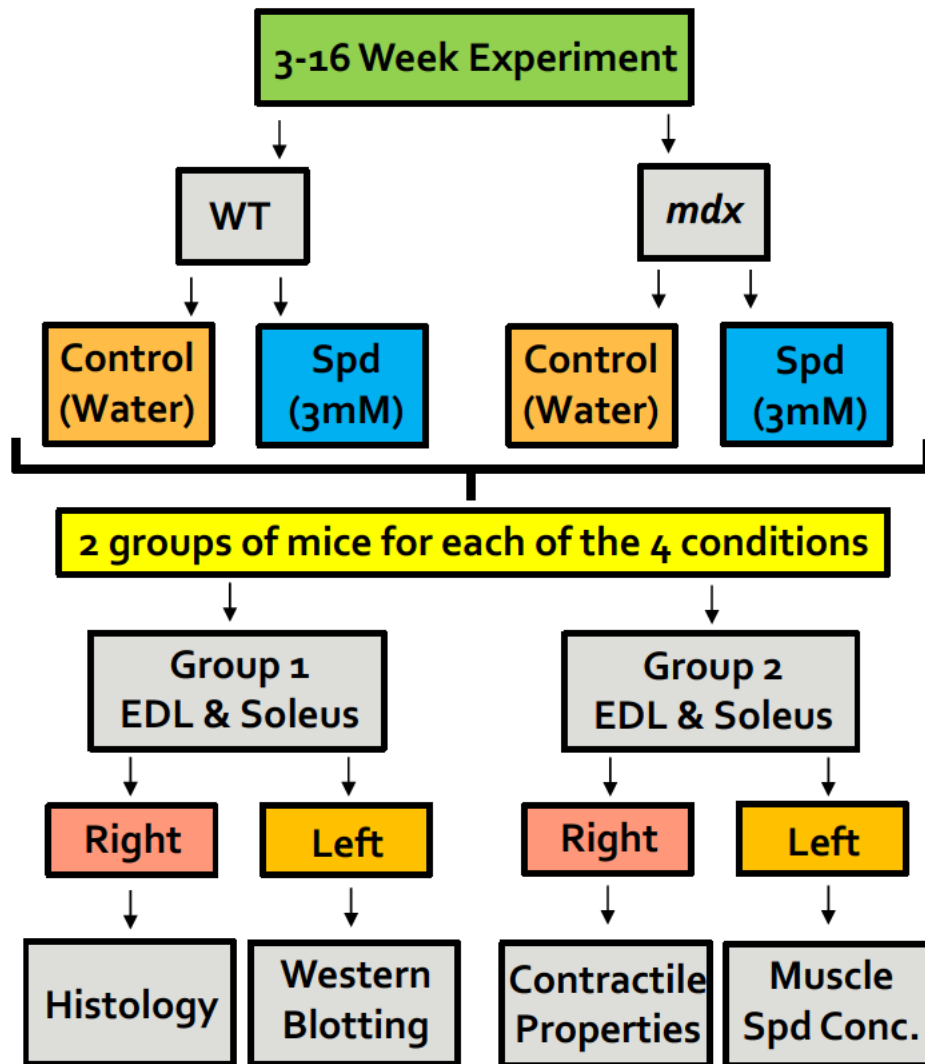


Figure 6. 3–16 week spermidine supplementation animal study. Treatment begins immediately after weaning at 3 weeks of age, and continues until cull date at 16 weeks of age. Both WT and *mdx* strains were used with both receiving either 3mM spermidine within drinking water or control regular water. All groups were separated into 2 identical groups after 13 weeks has completed. After separation, all control and supplemented WT (n=8) and *mdx* (n=12) groups were then culled. Mice in group 1 had the hind limb extensor digitorum longus (EDL) and soleus (SOL) of the right leg taken for histology, with the left legs taken for western blotting. Mice in group 2 had the hind limb EDL and SOL of the right leg taken for contractility properties, with the left leg taken for muscle spermidine concentration at a later date.

Firstly, both the WT and *mdx* mice underwent identical supplementation to allow for comparisons between supplemented WT, non-supplemented WT, supplemented *mdx* and non-supplemented *mdx*. Both the WT and *mdx* groups received one of the following two supplementations.

1. Regular drinking water used as a control for supplementation
2. 3mM of spermidine supplemented into drinking water

Thirteen weeks of 3mM spermidine supplementation, starting at 3 weeks of age when mice were weaned, was completed to target the initiation of aggressive muscle damage that occurs in *mdx* muscles (50). These mice were treated throughout the 13 weeks and were then culled. Group 1 and group 2 are identical with both animals and treatment, but split for different analysis per hindlimb muscle.

After the supplementation period (16 weeks of age), group 1 had the EDL and SOL from the right leg isolated for histology, while the EDL and SOL from the left leg was used for Western blotting (see specific analysis below). Group 2 had the EDL and SOL from the right leg used for assessing contractile function (see below), and the EDL and SOL in the left leg to be used for determining the concentrations of polyamines at a later date.

5.2 7-day Autophagy Flux Assay

The main objective for this experiment was to determine if spermidine supplementation activates the autophagic flux in dystrophic skeletal muscle. Using the drug, colchicine, this experiment aimed to inhibit autophagosome maturation into autolysosomes *in vivo*, resulting in a build-up of autophagosomes, which can be measured as an increased accumulation of p62 and LC3B-II protein over a given period of time. This *in vivo* 'autophagy flux assay' has been used previously as a 'dynamic/static' measurement for rates of autophagy in skeletal muscle (107). The experimental design for this experiment can be seen in Fig. 7. Eight-week-old male WT (n=8 per group) and *mdx* (n=8 per group) mice were used in this study and supplemented with spermidine, or water for controls, for 7 days. 8-week-old mice were chosen to observe any possible spermidine changes at the midpoint of the 3-16 week old experiment. There was also a WT control PBS (n=3) and a *mdx* control PBS (n=3) group used to determine if colchicine had an effect within the muscle.

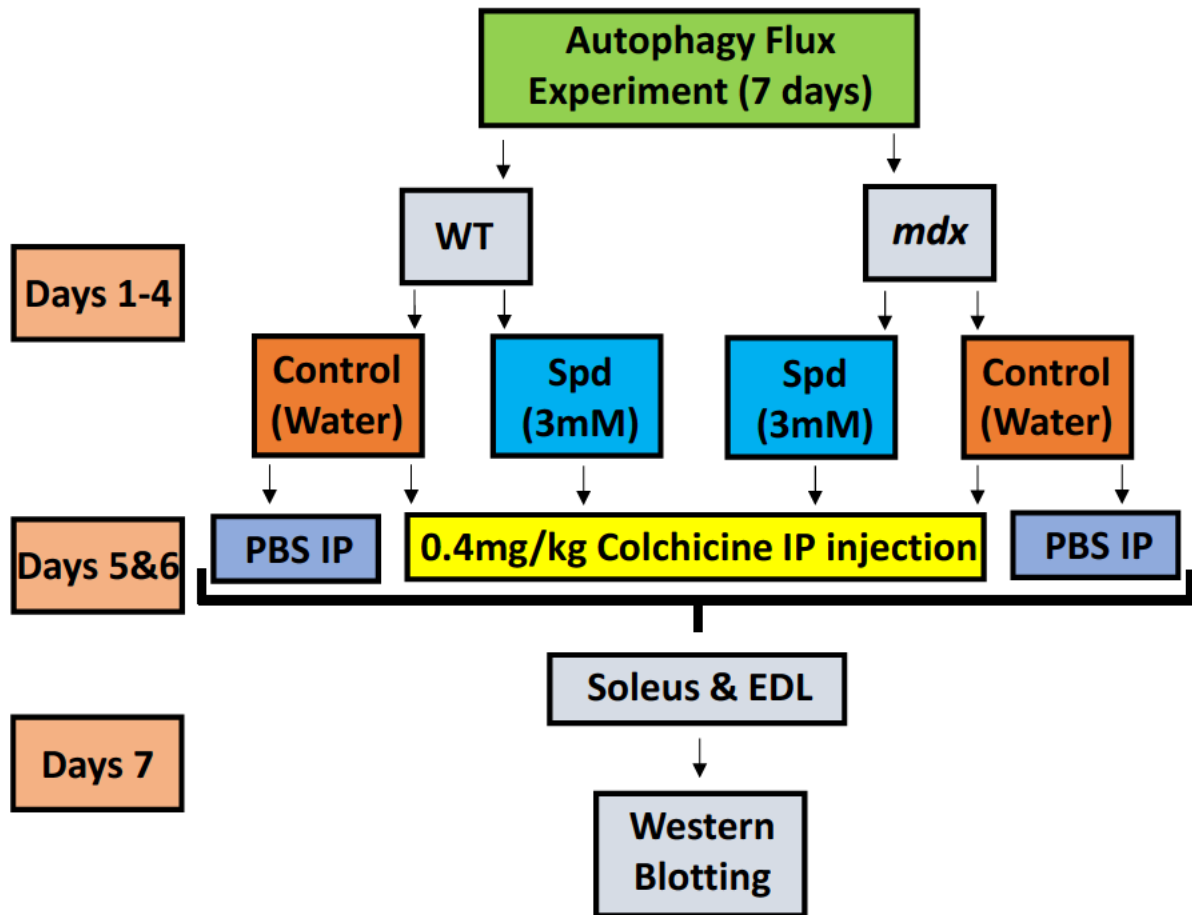


Figure 7. 7-day spermidine supplemented autophagy flux animal experiment. Adult animals (8 weeks old) of both WT and *mdx* strains were used for this study. From day 1-4, both strains were treated with either 3mM spermidine supplementation in drinking water, or control regular drinking water. Supplementation continued until cull date at day 7. On day 5 and 6, both spermidine supplementation and control groups for WT (n=8) and *mdx* (n=8) had 0.4mg/kg IP injections of colchicine within PBS to inhibit autophagy completion. WT controls (n=3) and *mdx* controls (n=3) had control PBS IP injections without colchicine. On day 7 the hindlimb EDL and SOL muscles were taken and used for western blotting.

On days 5 and 6 of spermidine supplementation, mice received an intraperitoneal injection containing 0.4mg/kg of colchicine, suspended in PBS, to inhibit autophagosome maturation into an autolysosome (107). On these days the PBS controls received just PBS for their IP injections. On day 7 the EDL and SOL were harvested and examined for the build-up of p62 and LC3B proteins, via Western blotting, as a marker of the rate of autophagosome formation. It is expected that spermidine supplementation will increase LC3B-II in muscles from both WT and *mdx* mice, indicating increased autophagic flux, with a potential to increase p62 levels with inhibited degradation of the lysosomal inner membrane.

5.3 Contractile Function

Both EDL and SOL muscles were tied tendon to tendon with 4-0 USP black braided silk and placed into a contractile chamber containing Krebs-Henseleit Ringer's solution (118mM NaCl; 4.75mM KCl; 1mM Na₂HPO₄; 1.18mM MgSO₄·7H₂O; 2.5mM CaCl₂; 24.8mM NaHCO₃; 11mM D-Glucose; pH 7.4). Chambers were bubbled with carbogen (5% CO₂ in O₂) with the Krebs-Henseleit Ringer's solution maintained at 30°C. The proximal muscle tendon was hooked onto a calibrated force transducer with the distal tendon being fixed to a micromanipulator with stimulating electrodes positioned to flank the belly of the muscle. All data was collected and analysed using LabChart Pro version 8 software (ADInstruments, New Zealand).

Preceding the contractility experiments, optimal length of each muscle was determined. The muscle was activated through a series of twitch contractions every few seconds at increasing lengths until its twitch force peaked ensuring optimal overlap of the sarcomeric actin and myosin. Supramaximal square wave pulses (0.2ms duration, 100Hz) were delivered to the muscles to produce maximum isometric tetanic contractions. Callipers then measured the muscle to determine the muscles optimal length.

Next, a force-frequency analysis was performed whereby muscles were stimulated at increasingly higher frequencies and the resulting forces were recorded. Muscles were stimulated at 10, 20, 30, 40, 50, 60, 80, 100, 120, 150 and 180 Hz for a duration of 350ms for the EDL and 500ms for the SOL, with a 3 min rest between pulses to prevent fatigue. Absolute peak tetanic force was recorded as the highest force obtained in the force-frequency protocol.

Muscle fatigability was also determined by subjecting muscles to repeated intermittent electrical stimuli for 3 min, resulting in a time-dependent reduction in force production. The EDL was stimulated every 4s at 100 Hz for 350 ms and the SOL every 2s at 80 Hz for 500 ms to factor in muscle fibre type differences, such as differences in near maximal force production,

and gain comparable levels of fatigue. Stimulated forces were averaged over 20s intervals for the EDL, and 30s intervals for the SOL.

The cross-sectional area (CSA) for the EDL was determined with both optimal length and absolute muscle mass. This was done using the equation by Brooks and Faulkner (139), while also assuming muscle density to be 1.06 g/cm³ (140). Specific force was then calculated with the formula (absolute force/1000)/CSA, with CSA calculated as muscle mass in grams/(optimal length in cm x 0.44 x 1.06) for the EDL, and muscle mass in grams/(optimal length in cm x 0.71 x 1.06) for the SOL.

5.4 Histology – Haematoxylin and Eosin (H and E) Stain

Muscles were submerged in Optimal Cutting Temperature (OCT) compound and frozen in isopentane pre-cooled in liquid nitrogen immediately after harvesting. Once frozen, mid-belly 14µm cross-sections of the EDL and SOL were cut on a cryostat at -20°C and mounted onto glass slides. Muscle sections were then fixed in formal calcium fixative (40% Formaldehyde; Calcium chloride; diH₂O) and incubated at room temperature for 10 min. Muscles were then stained in Harris' haematoxylin (Haematoxylin; Absolute alcohol; Ammonium; Mercuric oxide; Glacial acetic acid; diH₂O) for 5 minutes and then washed under tap water. Excess stain was removed through adding 1% acid alcohol and then washed with tap water. Samples were then counterstained with 1% eosin Y for 3 minutes and then washed again with tap water. Samples were then dehydrated with graded alcohols, cleared in xylene and mounted with synthetic resin and covered with a glass slip. Nail polish was used to seal the edges of the plates together to prevent slippage and dehydration.

5.5 Western Blotting

Western blotting was used to determine differences/changes in the abundance of specific muscle proteins that were hypothesised to be differentially expressed in WT vs *mdx* muscle or to be altered through spermidine supplementation, such as; LC3B-I and LC3B-II, p62, total and phosphorylated AMPK (Thr172), MAP1S, Odc1, Amd1, SpdSyn, SpmSyn, Smox, Sat1

total and phosphorylated p70^{S6K1} (Thr387) and total and phosphorylated 4EBP1 (Thr37/46) (Table 1).

Table 1. Western blotting antibodies and dilutions

Antibody	Catalogue Number	Host Species	Dilution
LC3B	CST #2775	Rabbit	1:1000 in 1% BSA
SQSTM1/p62	CST #5114	Rabbit	1:1000 in 1% BSA
p-AMPK	CST #2535	Rabbit	1:1000 in 1% BSA
AMPK	CST #2603	Rabbit	1:1000 in 1% BSA
MAP1S	Precision Plus #AG10006	Mouse	1:3000 in 1% BSA
Odc1	Proteintech 17003-1-AP	Rabbit	1:1000 in 1% BSA
Amd1	sc-166970 SantaCruz	Mouse	1:250 in 1% BSA
SpdSyn	Proteintech #19858-1-AP	Rabbit	1:1000 in 5% Milk
SpmSyn	ab151547 [EPR9253]	Rabbit	1:1000 in 1% BSA
Smox	Proteintech #15052-1-AP	Rabbit	1:1000 in 1% BSA
Sat1	#61586 CST	Rabbit	1:1000 in 1% BSA
c-Myc	ab32072 [Y69]	Rabbit	1:1000 in 1% BSA
p-p70 ^{S6K1}	CST #9234	Rabbit	1:1000 in 1% BSA
p70 ^{S6K1}	CST #2708	Rabbit	1:1000 in 1% BSA
p-4EBP1	CST #2855	Rabbit	1:1000 in 1% BSA
4EBP1	CST #9452	Rabbit	1:1000 in 1% BSA
Rabbit Secondary	Vector Anti-Rabbit IgG (H+L) - Vector Labs VEPI-1000	Rabbit	1:5,000 in 5% Milk
Mouse Secondary	Peroxidase Labelled Anti-Mouse IgG (H+L) - Vector Labs PI-2000	Mouse	1:25,000 in 5% Milk

Sodium Dodecyl Sulphate (SDS)-Polyacrylamide gels were poured and set between 1.5mm glass plates. Equal amounts of muscle protein were added to SDS sample buffer containing dithiothreitol (DTT) and heated at 95°C for 5 min before being loaded onto the gel. The gels were then submerged in running buffer (30g Tris-base; 144g Glycine; 10g SDS; diH₂O) and ran at 115V for 1 h 30 min. Muscles were homogenised in buffer listed in Table 2.

Table 2. Homogenisation buffer composition

Concentration	Compound	Inhibitors
40 mM	Tris-Hydrochloride	B-Glycerophosphate
1 mM	Ethylenediaminetetraacetic acid (EDTA)	Sodium fluoride (NaF)
5 mM	Ethylene glycol tetra acetic acid (EGTA)	Phenylmethylsulfonyl Fluoride (PMSF)
0.5%	Triton X-100	Leupeptin (LEU)
7	pH	Sodium Orthovanadate (Na ₃ VO ₄)
		Western immunoprecipitation kinase assay (WIK) Buffer

After protein separation, the proteins were wet transferred from the gel onto a 0.45µm Polyvinylidene Fluoride (PVDF) membrane in transfer buffer (50g Tris-base; 130g Glycine; 20% Methanol; diH₂O) at 300mA for 1h-1.5h, followed by a 1 h blocking in 5% skim milk/Tris-buffered saline tween 20 (TBST). Membranes were then washed in TBST, sealed in a plastic bag with the appropriate primary antibodies and incubated overnight. Membranes were then washed and probed with the appropriate secondary antibody. Membranes were then incubated for 1 minute with Thermo Scientific's enhanced chemiluminescent reagent ECL and captured on a Fusion FX imaging system, Vilber Lourmat, Germany. The intensity of the band representing the protein of interest was quantified using Viber Lourmat Fusion Imaging Software. To confirm equal loading, membranes were then stained with Coomassie blue. To account for minor loading differences, the intensity of a protein of interest was normalised to the intensity of the entire lane (total protein) on the Coomassie stained membrane using ImageJ software version 1.8 64-bit.

6. Statistical Analysis

Prior to analysis, all data was checked for normality. Data is presented as means ± SEM, with all graphs showing the results for individual samples (black dots for males, white dots for female). Statistical significance was determined through a two-way ANOVA with a Tukey's post hoc analysis (for the 4 groups from the 13-week treatment) or an unpaired, two-tailed t test (between PBS and colchicine groups for the autophagy flux). Differences between groups

were deemed significant when $p < 0.05$ with statistical analysis performed on GraphPad Prism software v9.

Results

7. Genotypic differences in the expression of polyamine pathway proteins and the effect of 13 weeks of spermidine supplementation

7.1 Fast-twitch EDL muscle

The polyamine pathway enzymes Odc1, Amd1, SpdSyn, SpmSyn, Smox, and Sat1, as well as the protein synthesis enzyme c-Myc, were probed for and the results are shown in Fig 8. Interestingly, there was an upregulation of Amd1 (Fig. 8B), SpdSyn (Fig. 8C) and c-Myc (Fig. 8G) expression in the *mdx* EDL muscles, compared to the WT EDL muscles. Conversely, there were no genotypic differences observed for Odc1 (Fig. 8A), SpmSyn (Fig. 8D), Smox (Fig. 8E) and Sat1 (Fig. 8F). Spermidine supplementation did not alter the expression of any of these proteins compared to non-supplemented controls in WT or *mdx* EDL muscles.

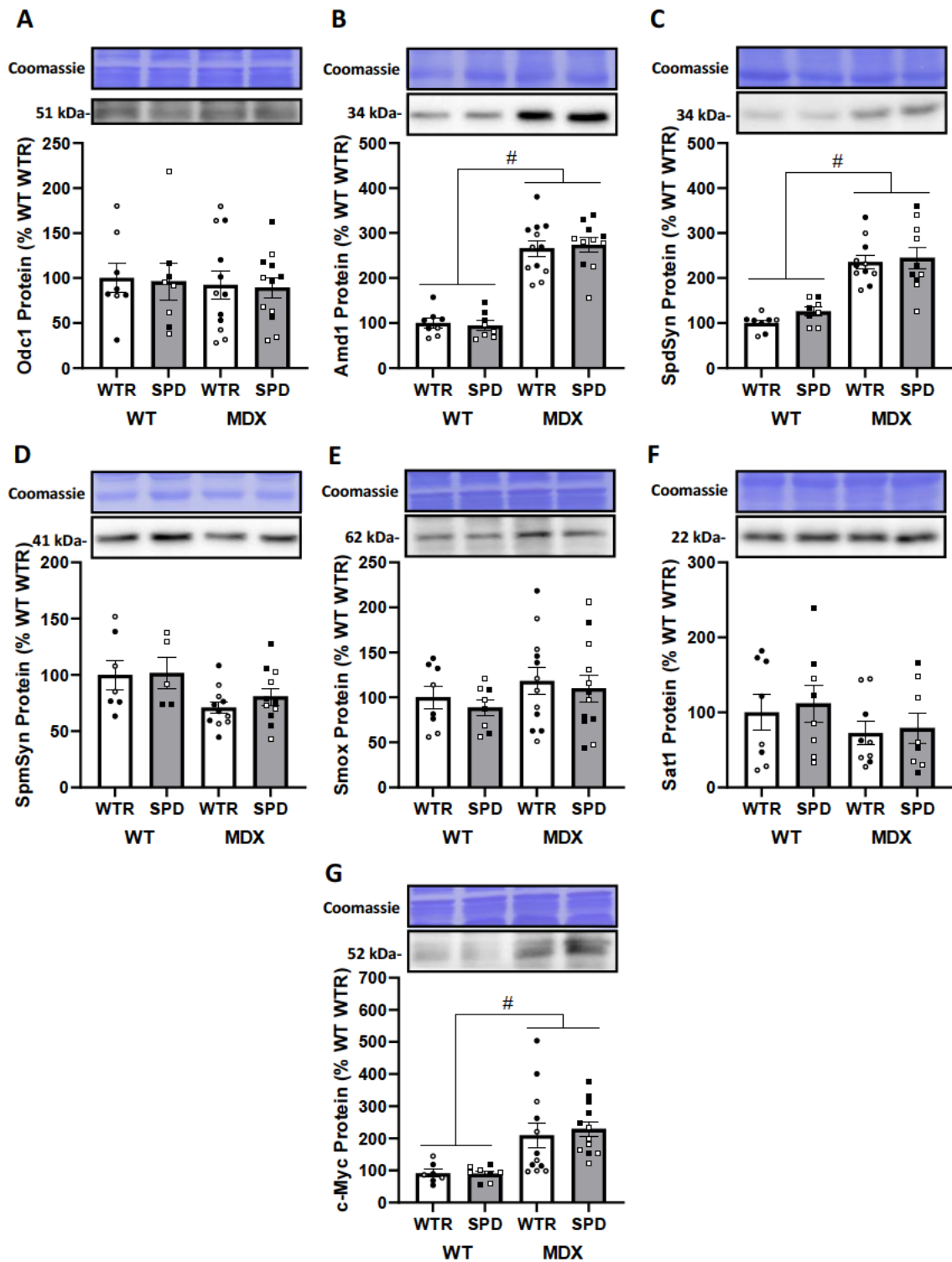


Figure 8. The genotype and spermidine supplementation effect on polyamine pathway proteins within the EDL. 3-week-old mice were supplemented with 3mM spermidine drinking water, or control water for 13 weeks. The EDL was then removed and subjected to western blot analysis for the polyamine pathway enzymes: A) Ornithine decarboxylase (ODC1), B) adenosylmethionine decarboxylase (Amd1), C) spermidine synthase (SpdSyn), D) spermine synthase (SpmSyn), E) spermine oxidase (Smox), F) spermidine/spermine acetyltransferase 1 (Sat1) and G) c-Myc. Amd1, SpdSyn and c-Myc showed upregulation within *mdx* samples compared to WT. No spermidine supplementation effects observed between all groups. Data is presented as means \pm SEM (n=6-8 WT samples per group, n=10-12 *mdx* samples per group). # indicates significant genomic

difference between groups. Black dots are male, white dots are female. $p < 0.05$. Two-way ANOVA with Tukey's post-test.

7.2 Slow-twitch SOL muscle

Similar to the EDL, there was increased expression of Amd1 (Fig. 9B), SpdSyn (Fig 9C) and c-Myc (Fig 9G) in the *mdx* SOL muscles compared to the WT SOL muscles. Interestingly, however, there was a downregulation of Sat1 (Fig. 9F) within the *mdx* SOL muscles compared to WT SOL muscles. There were no genotypic differences in the expression of Odc1 (Fig. 9A), SpmSyn (Fig. 9D) and Smox (Fig. 9E). As with the EDL muscles, spermidine supplementation did not alter the expression of any of the examined proteins compared to non-supplemented controls.

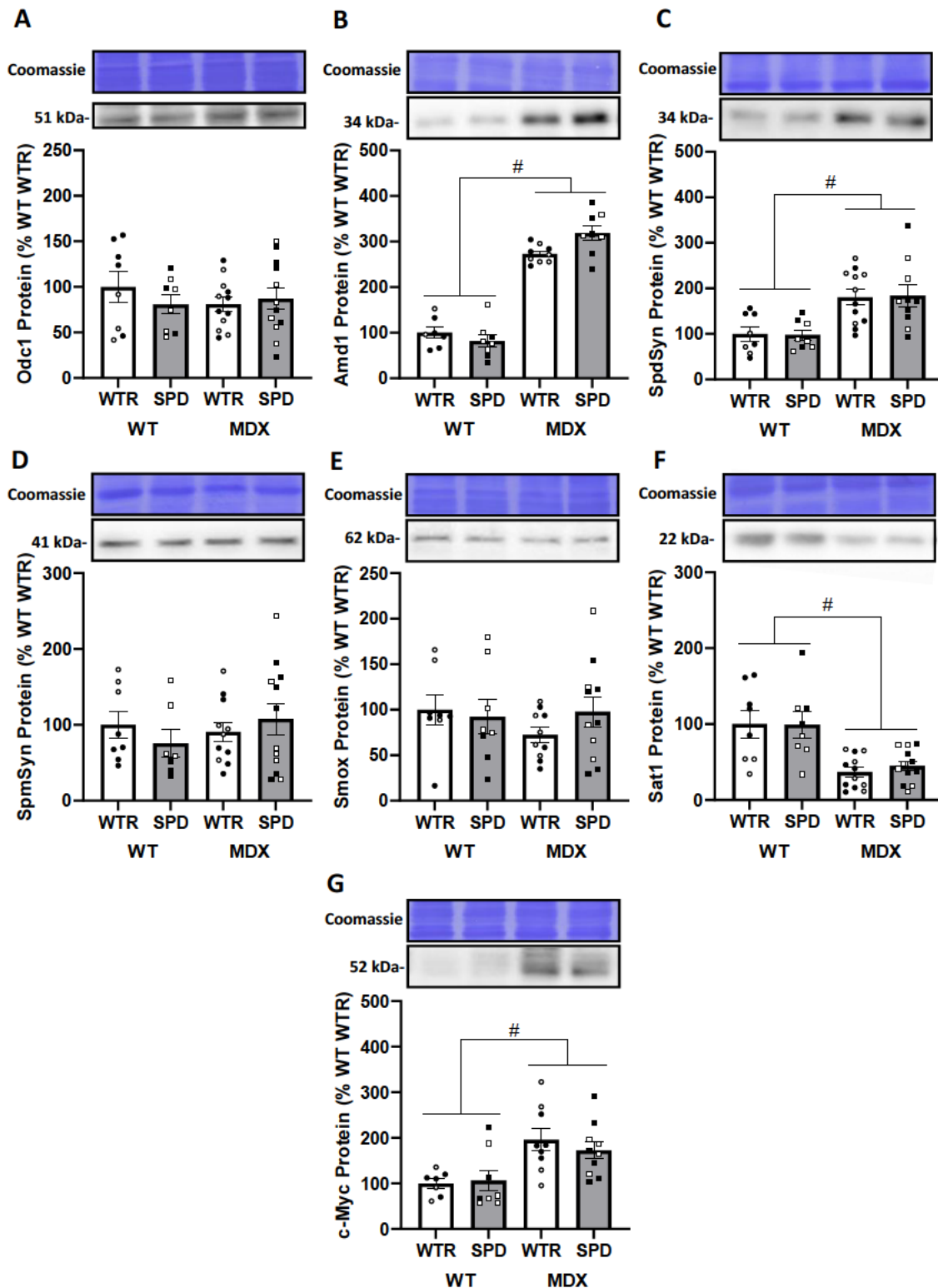


Figure 9. The genotype and spermidine supplementation effect on polyamine pathway proteins within the SOL. 3-week-old mice were supplemented with 3mM spermidine drinking water, or regular water for 13 weeks. The SOL was then removed and subjected to western blot analysis for the polyamine pathway enzymes: A) Ornithine decarboxylase (ODC1), B) adenosylmethionine decarboxylase (Amd1), C) spermidine synthase (SpdSyn), D) spermine synthase (SpmSyn), E) spermine oxidase (Smox), F) spermidine/spermine acetyltransferase 1 (Sat1) and G) c-Myc. Amd1, SpdSyn and c-Myc showed upregulation within *mdx* samples compared to WT, whilst Sat1 showed a downregulation within *mdx* samples compared to WT. No spermidine

supplementation effects observed between all groups. Data is presented as means \pm SEM (n=6-8 WT samples per group, n=10-12 *mdx* samples per group). # indicates significant genomic difference between groups. Black dots are male, white dots are female. p < 0.05. Two-way ANOVA with Tukey's post-test.

8. The effect of spermidine supplementation on body weight, muscle mass, force output and fatigue

8.1 Body Weight

Mice were weighed throughout the treatment with their weight plotted every week and, as shown in Fig 10, there was no difference between genotypes and supplemented groups when expressed as absolute mass (g).

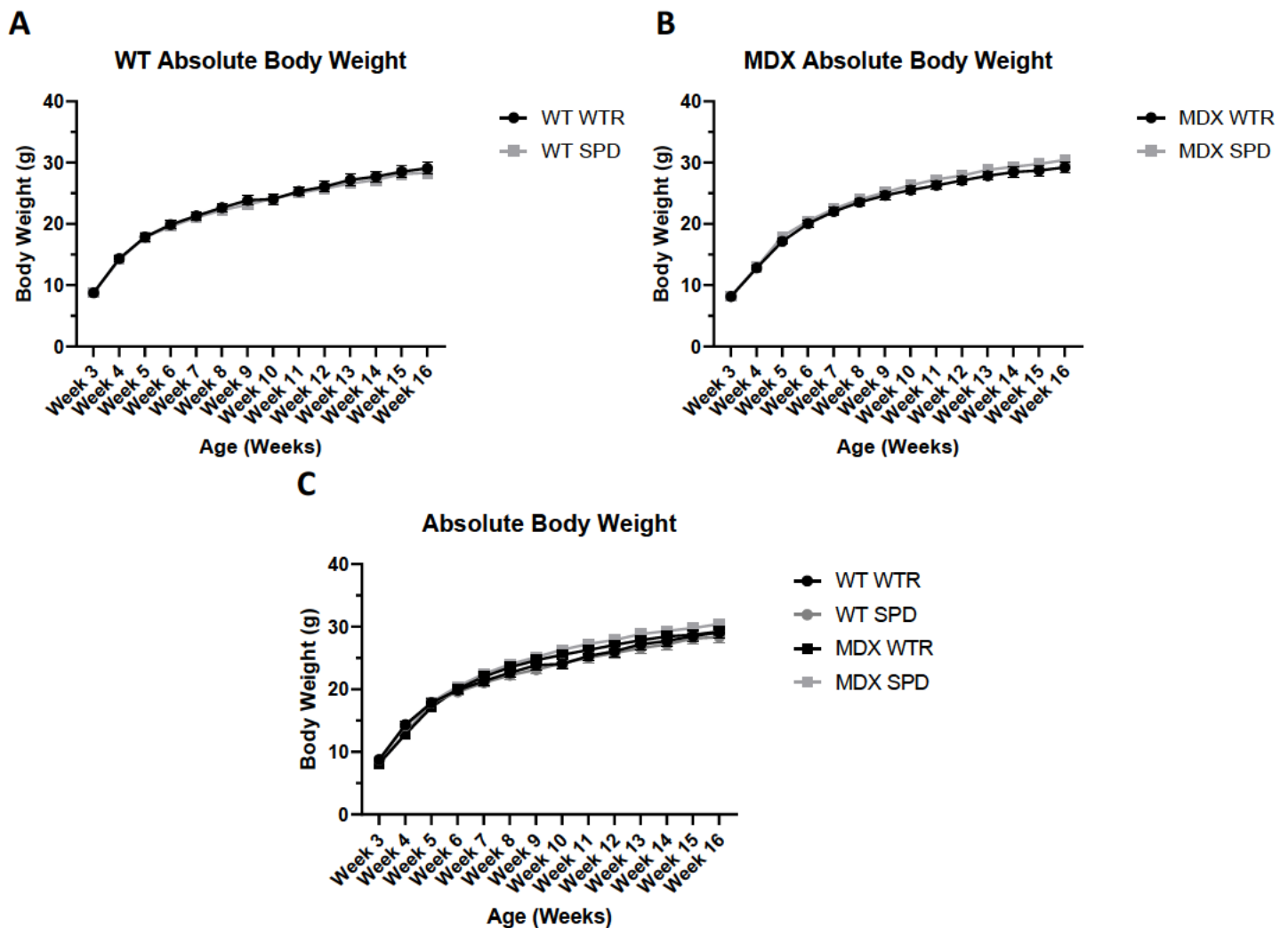


Figure 10. The effect of spermidine supplementation on absolute body weights. The 3-week-old mice were treated with either 3mM spermidine or control drinking water were weighted at the initiation of their treatment, and weekly throughout treatment until cull date at 16 weeks of age. Groups were compared to each other each week for the 13-week period: A) WT absolute body weight (g), B) MDX absolute body weight (g), C) Absolute body weight (g). There were no genotypic or spermidine supplemented effects observed between all groups per week. Data is presented as means \pm SEM (n=16 WT WTR, n=22 WT SPD, n=23 *mdx* WTR, n=24 *mdx* SPD). $p < 0.05$. Two-way ANOVA on each week with Tukey's post-test.

For the weekly relative change in body mass (i.e. body mass expressed as a percentage of body mass from the previous week; Fig 11), consistent with the absolute body weight data (Fig. 10C), there was no effect of spermidine supplementation on the rate of growth for WT (Fig. 11A) and *mdx* (Fig 11.B) mice. Conversely, however, there was a genotypic difference in growth rate change between 4-6 weeks for the *mdx* mice compared to WT mice (Fig. 11C). More specifically, *mdx* mice had a smaller increase in body mass between 3 and 4 weeks (consistent with the level of muscle damage around this time), but then had a larger increase in body mass between weeks 4 and 5, and between weeks 5 and 6 (Fig. 11C).

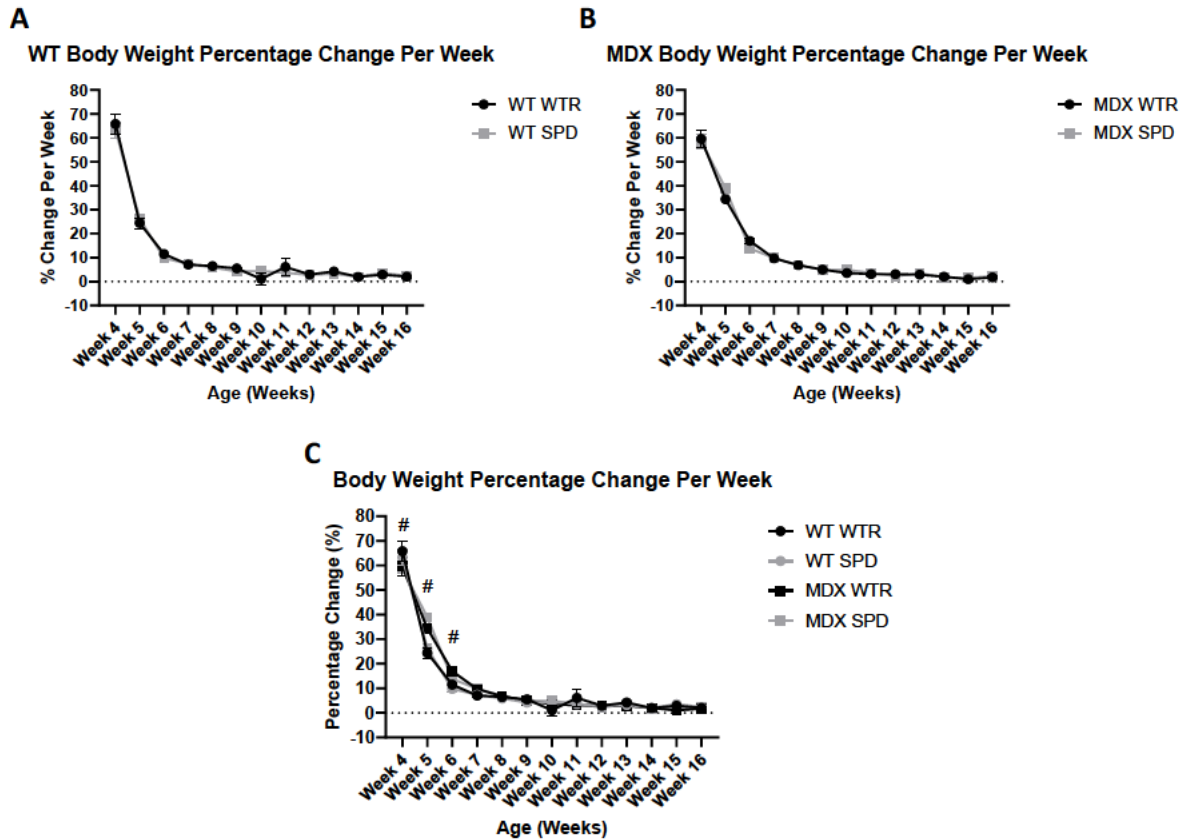


Figure 11. The effect of spermidine supplementation on body weight percentage change. The 3-week-old mice were treated with either 3mM spermidine or regular drinking water were weighted at the initiation of their treatment, and weekly throughout treatment until cull date at 16 weeks of age. Percentage difference in body weight was determined from previous week per mouse for A) WT, B) *mdx* and C) WT and *mdx*, then analysed within each week. Week 4, 5 and 6 showed an *mdx* upregulation in percentage change within weeks compared to the WT groups of the same weeks. No other genomic effects, or any spermidine supplemental effects, were observed within all other percentage change weeks. Data is presented as means \pm SEM (n=16 WT WTR, n=22 WT SPD, n=23 *mdx* WTR, n=24 *mdx* SPD). # indicates significant genomic difference between groups. $p < 0.05$. Two-way ANOVA on each week with Tukey's post-test.

Over the supplementation period, water consumption per mouse per week was monitored (water was changed on day 2, 4 and 7 of each week) by weighing the water bottles pre/post refreshing the drinking water (assuming 1 gram of water equals 1 ml of water), and then dividing the pre/post difference by the number of mice in the cage (n=2/5 per cage). This was important to determine if all mice were ingesting the same amount of water and whether the supplementation groups were ingesting the same amount of spermidine. As shown in Fig 12, there were no significant differences in weekly water consumption between groups.

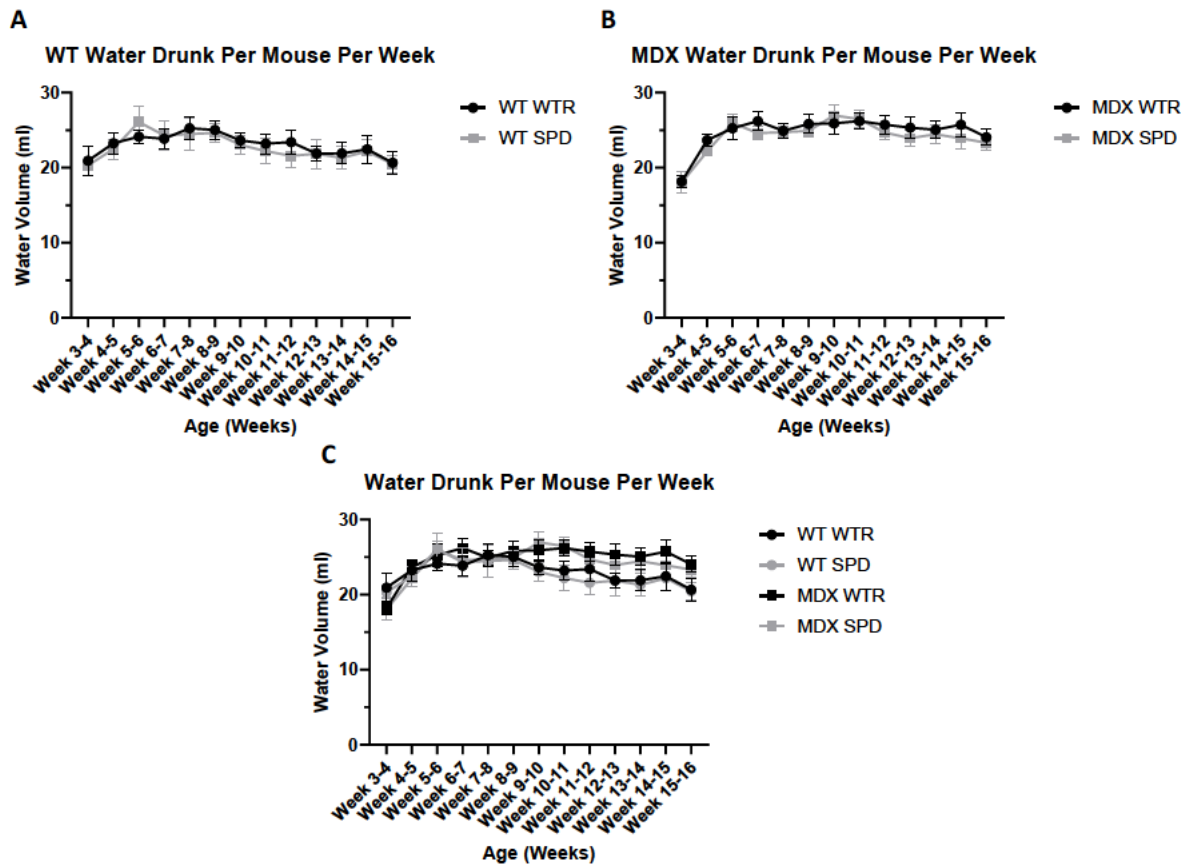


Figure 12. Volume of water ingested throughout 3–16-week animal study. The 3-week-old mice were treated with either 3mM spermidine or regular drinking water were weighted at the initiation of their treatment, and weekly throughout treatment until cull date at 16 weeks of age. Water weights were taken at every changeover 3 times a week, with water drunk calculated every week for A) WT, B) *mdx* and C) WT and *mdx*, and divided my number of mice per cage to get average water intake per mouse per week. No genomic or spermidine supplemental effects were observed with water volume intake per mouse within each week. Data is presented as means \pm SEM (n=16 WT WTR, n=22 WT SPD, n=23 *mdx* WTR, n=24 *mdx* SPD). $p < 0.05$. Two-way ANOVA on each week with Tukey’s post-test.

8.2 EDL – Muscle Mass, absolute/specific forces and fatiguability

The EDL’s that were harvested for contractile function experiments were weighed after completion of the contractile protocol. The absolute EDL weights were plotted, with these values also being normalised to body weight and plotted (Fig 13). For both absolute (Fig. 13A) and normalised (Fig 13B) EDL muscle masses, there was a genotypic difference such that EDL muscle’s from *mdx* mice were larger than WT EDL muscles. This difference is likely due to the pseudohypertrophy that occurs in *mdx* muscles, which is primarily because of their chronic inflammation, increased water content, fibrosis and fat infiltration (28, 59, 82, 84).

Although there was no spermidine supplementation effect on absolute *mdx* EDL mass, interestingly, spermidine supplementation induced a decrease in normalised *mdx* EDL mass compared to EDL muscles from control *mdx* mice, with no effect on WT EDL muscle mass (Fig. 13B). This data could suggest an improvement in the *mdx* phenotype due to decreased levels of muscle damage and repair, bringing the muscle closer to that of WT EDL's.

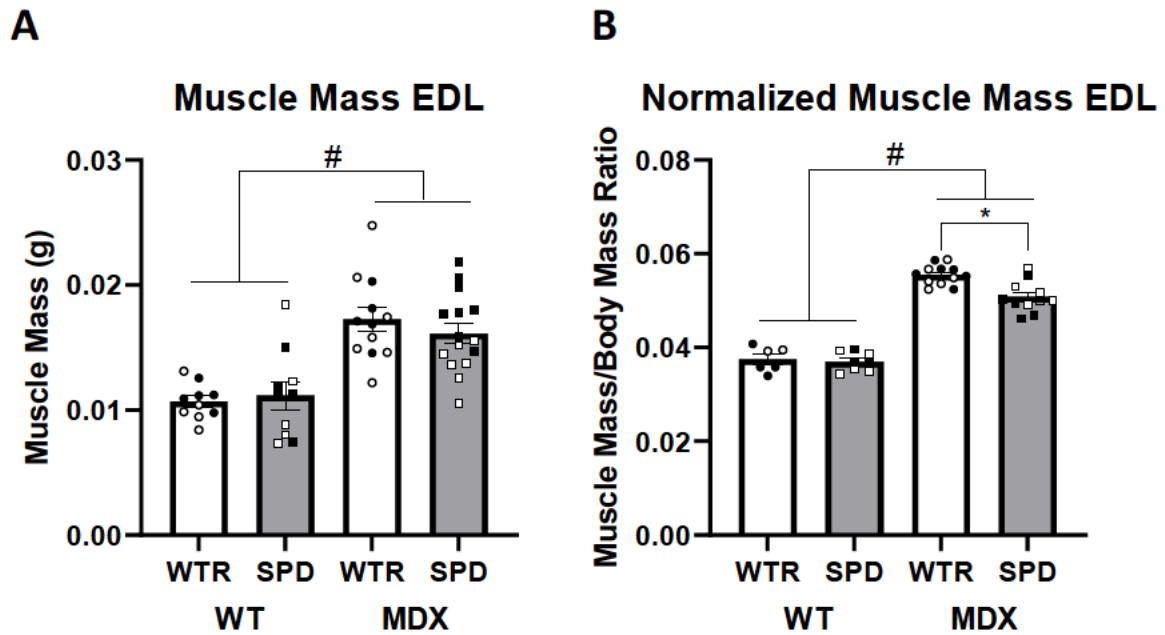


Figure 13. The genotype and spermidine supplementation effects on EDL muscle mass. 3-week-old mice were supplemented with 3mM spermidine drinking water, or regular water for 13 weeks. The EDL's were then removed and weighed to obtain the absolute muscle mass (A). Absolute muscle mass was normalised relative to the mouse's body weight (B). Muscle mass showed an *mdx* upregulation compared to WT with no spermidine supplement changes. Normalised muscle mass showed the same genomic upregulation; however, spermidine supplementation showed a decrease in *mdx* normalised muscle mass when compared to *mdx* controls. Data is presented as means \pm SEM (n=7-10 WT samples per group, n=10-14 *mdx* samples per group). # indicates significant genomic difference between groups, * shows significant supplementation effect between groups. Black dots are male, white dots are female. $p < 0.05$. Two-way ANOVA with Tukey's post-test.

Once optimal length of the EDL was established, repeated twitches seconds apart until maximal twitch force, prior to assessing muscle contractile function, the length of the muscle was measured tendon loop to tendon loop (Fig. 14). There were no changes observed on EDL optimal length between the genotypes or treatment groups. Optimal length, as well as muscle mass, are needed to normalise absolute forces to cross-sectional area (i.e. specific force).

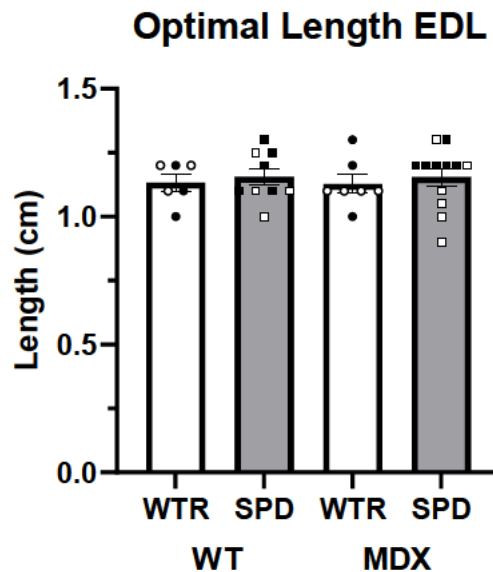


Figure 14. Optimal length of EDL from functional studies. 3-week-old mice were supplemented with 3mM spermidine drinking water, or regular water for 13 weeks. Optimal length of the EDL was achieved and measured tendon to tendon. No genomic or spermidine supplementation effects were observed between all groups. Data is presented as means \pm SEM (n=6-9 WT samples per group, n=6-12 *mdx* samples per group). $p < 0.05$. Two-way ANOVA with Tukey's post-test.

Whilst the EDL's were undergoing their force/frequency contractile protocol, the largest force produced was recorded (usually at a stimulation frequency of 180Hz) and plotted as the muscle's highest absolute force. As shown in Fig. 15A, there was no genotype or treatment difference observed in the maximal absolute force productions.

When absolute force was normalised to the calculated muscle CSA (see methods 5.3), there was a main genotypic effect for specific force to be lower in EDL muscles from *mdx* mice compared to the WT controls (Fig. 15B). This result was expected as, although absolute forces were similar between *mdx* and WT EDL's (Fig. 15A), EDL muscles from *mdx* mice were larger than WT controls (Fig. 13), resulting in less force per unit of area/mass. Interestingly,

spermidine supplementation resulted in a significant increase in *mdx* EDL specific force compared to non-supplemented *mdx* EDL muscles (Fig. 15B). The improved muscle function supports the normalised muscle mass data (Fig. 13B), indicating that spermidine supplementation may improve muscle health through a decreased rate of chronic inflammation.

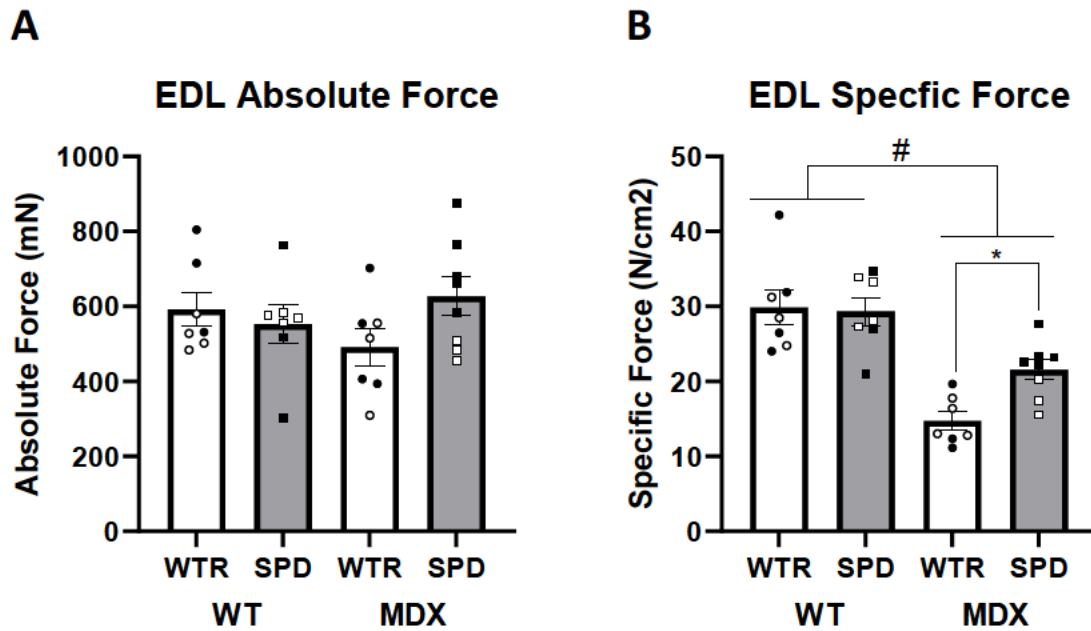


Figure 15. The effect of spermidine supplementation on EDL functionality. 3-week-old mice were supplemented with 3mM spermidine drinking water, or regular water for 13 weeks. EDL's absolute force (A) was the largest force the muscle could produce. There were no genotypic or spermidine effects observed within EDL absolute force. These forces were normalised to CSA (B) which showed that the *mdx* EDL's had a decrease in specific force compared to the WT groups. Spermidine supplementation also showed an improve in *mdx* specific force compared to *mdx* control. Data is presented as means \pm SEM (n=7 WT samples per group, n=7-8 *mdx* samples per group). # indicates significant genomic difference between groups, * shows significant supplementation effect between groups. Black dots are male, white dots are female. $p < 0.05$. Two-way ANOVA with Tukey's post-test.

At the completion of the force/frequency protocol, EDL muscles were then subjected to a fatiguing stimulation protocol. Stimulated forces were averaged over 20s intervals. When comparing the decline in absolute force production (fatigue) between each group, there were no changes observed between any groups (Fig. 16 A and C). Similarly, when force produced in each 20s-time interval was expressed relative to the previous 20s interval, there were no changes observed between any of the genotypic or supplemented groups (Fig. 16B and 16D).

This data suggests that despite an improved muscle mass and specific force, spermidine supplementation does not statistically influence muscle fatiguability within the *mdx* EDL.

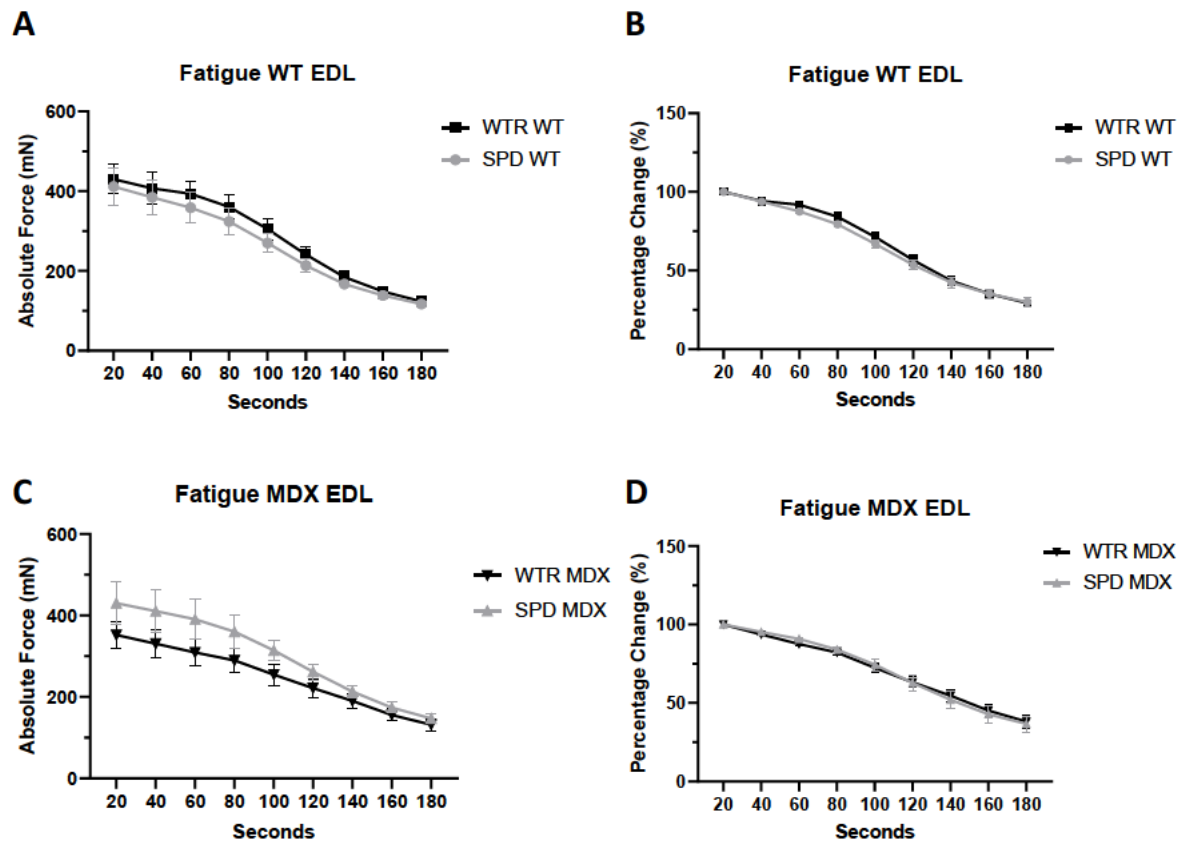


Figure 16. Spermidine supplementations impact on EDL fatigue. 3-week-old mice were supplemented with 3mM spermidine drinking water, or regular water for 13 weeks. Muscles were stimulated repeatedly for 3 minutes, with peaks being grouped into 20 second averages. These averages for absolute force fatigue were compared between each group and showed no genotype or spermidine supplementation effect between A) WT, and C) *mdx*, groups. A fatigue percentage change of the previous block was also plotted between B) WT and D) *mdx*, and showed no genotype or spermidine supplementation effect between any group per block. Data is presented as means \pm SEM (n=6 WT samples per group, n=6 *mdx* samples per group). $p < 0.05$. Two-way ANOVA with Tukey's post-test.

8.3 SOL – Muscle Mass, absolute/specific forces and fatiguability

Absolute and normalised SOL muscle masses essentially mimicked what was found for EDL muscles (Fig. 13), in that there was a genotypic increase in the mass of SOL muscles from *mdx* mice compared to the WT controls (Fig. 17). Although not to the same extent as the EDL, due to the SOL being a more protected muscle in the *mdx* phenotype (139), this result suggests the presence of pseudohypertrophy in SOL muscles from *mdx* mice.

Although there was no spermidine supplementation effect on the absolute mass of SOL muscles from *mdx* mice (Fig. 17A), spermidine supplementation showed a strong trend ($p=0.057$) to decrease normalised *mdx* SOL mass compared to control *mdx* SOL muscles (Fig. 17B), similar to the significant decrease observed in the *mdx* EDL (Fig. 13). This data could suggest a similar improvement in the phenotype of *mdx* SOL muscles due to decreased levels of muscle damage and repair, although not to the same extent as in the *mdx* EDL's (Fig. 13B) as the SOL does not undergo the same degree of damage.

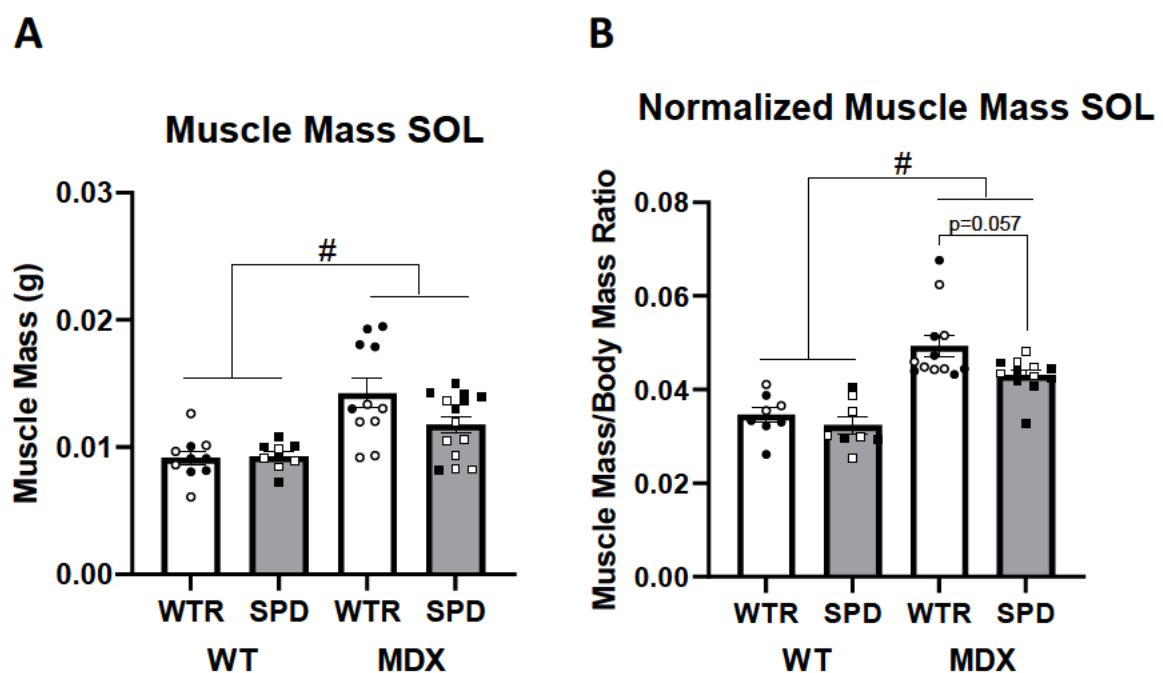


Figure 17. The genotype and spermidine supplementation effects on SOL muscle mass. 3-week-old mice were supplemented with 3mM spermidine drinking water, or regular water for 13 weeks. The SOL's were then removed and weighed to obtain the absolute muscle mass (A). Absolute muscle mass was normalised relative to the mouse's body weight (B). Muscle mass showed an *mdx* upregulation compared to WT with no spermidine supplement changes. Normalised muscle mass showed the same genomic upregulation; however, spermidine supplementation showed a strong trend for decreased *mdx* normalised muscle mass when compared to *mdx* controls. Data is presented as means \pm SEM ($n=8-10$ WT samples per group, $n=11-13$ *mdx* samples per group). # indicates significant genomic difference between groups. Black dots are male, white dots are female. $p < 0.05$. Two-way ANOVA with Tukey's post-test.

Similar to the EDL muscles (Fig. 14), there were no changes observed on SOL optimal length between the genotypes or treatment groups (Fig. 18).

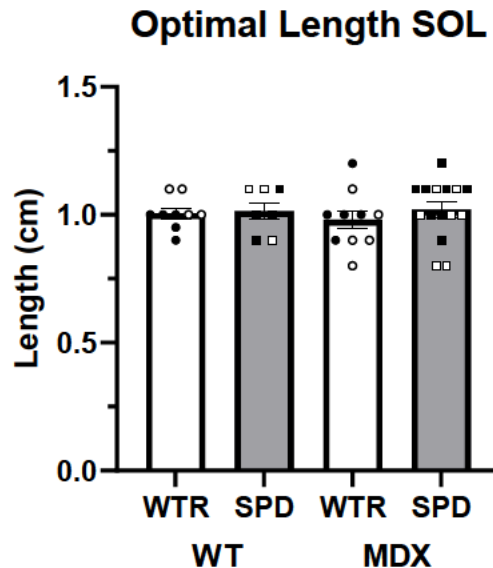


Figure 18. Optimal length of SOL from functional studies. 3-week-old mice were supplemented with 3mM spermidine drinking water, or regular water for 13 weeks. Optimal length of the SOL was achieved and measured tendon to tendon. No genomic or spermidine supplementation effects were observed between all groups. Data is presented as means \pm SEM (n=6-9 WT samples per group, n=10-14 *mdx* samples per group). Black dots are male, white dots are female. $p < 0.05$. Two-way ANOVA with Tukey's post-test.

Interestingly, unlike the EDL (Fig. 15A), there was a genotypic difference in SOL absolute force production, such that SOL muscles from *mdx* mice produced higher absolute forces compared to WT controls (Fig. 19A). Spermidine supplementation had no effect on absolute force production in SOL muscles (Fig. 19A).

Similar to the EDL muscles, when SOL force was normalised to muscle CSA (see methods 5.3), there was a genotypic downregulation in the specific force produced by SOL muscles from *mdx* mice compared to the WT groups (Fig. 19B). Interestingly, despite the strong trend

in decreased SOL muscle mass with spermidine supplementation (Fig. 17B), we did not see a change in *mdx* SOL specific forces compared to control ($p=0.3858$).

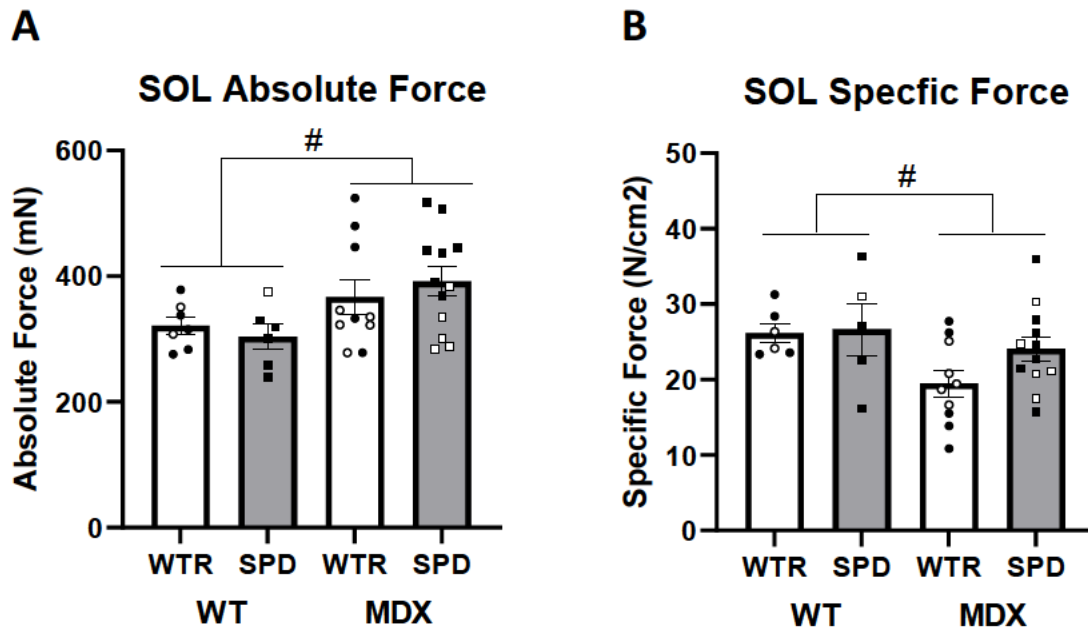


Figure 19. The effect of spermidine supplementation on SOL functionality. 3-week-old mice were supplemented with 3mM spermidine drinking water, or regular water for 13 weeks. SOL's absolute force (A) was the largest force the muscle could produce. There was an *mdx* upregulation in absolute force when compared to the WT groups, although there were no spermidine supplementation effects observed. These forces were then normalised to CSA (B) which showed that the *mdx* SOL's had a decrease in specific force compared to the WT groups. Spermidine supplementation however showed no improvement between all groups. Data is presented as means \pm SEM ($n=6-7$ WT samples per group, $n=10-12$ *mdx* samples per group). # indicates significant genomic difference between groups. Black dots are male, white dots are female. $p < 0.05$. Two-way ANOVA with Tukey's post-test.

For the SOL fatigue protocol, induced forces were grouped for each 30s interval due to the higher fatigue resistance for the SOL compared to EDL muscles. Similar to the EDL results (Fig. 16), there were no changes observed between any groups in fatigue when expressed as absolute force (Fig. 20 A and C) or relative to the previous time interval (Fig. 20 B and D).

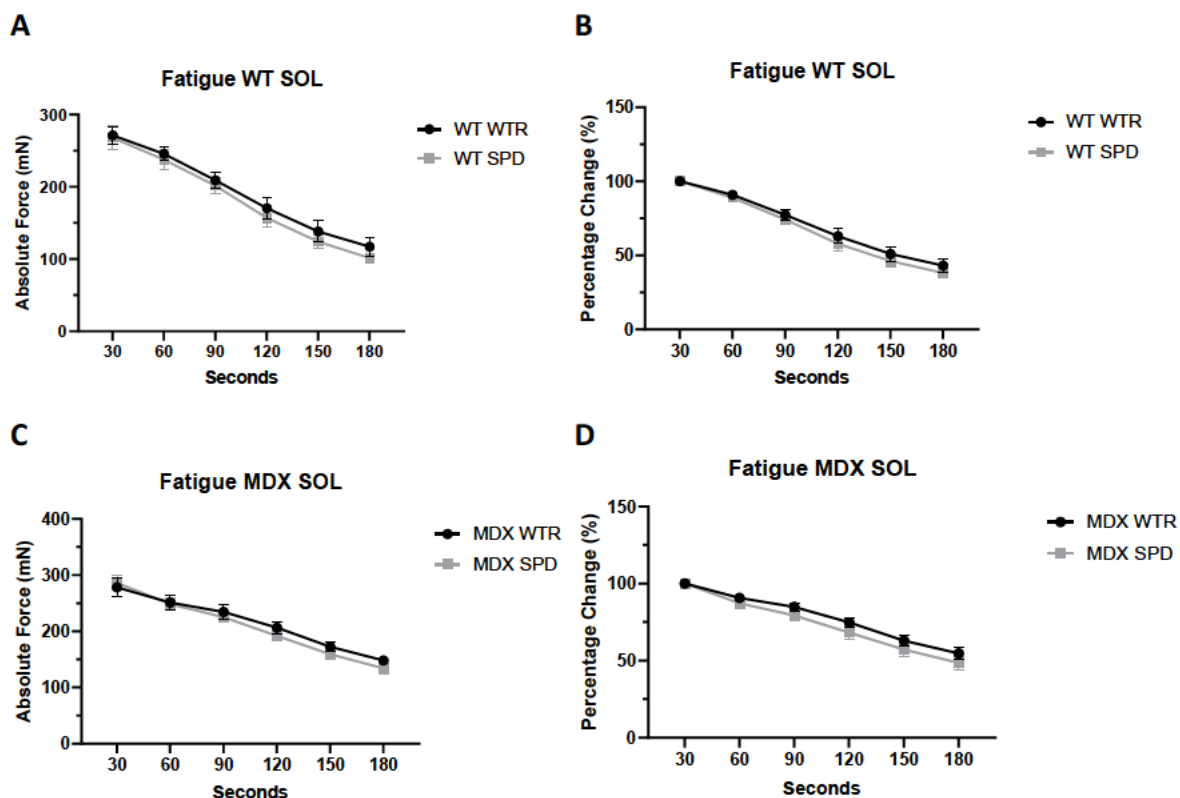


Figure 20. Spermidine supplementations impact on SOL fatigue. 3-week-old mice were supplemented with 3mM spermidine drinking water, or regular water for 13 weeks. Muscles were stimulated repeatedly for 3 minutes, with peaks being grouped into 30 second averages. These averages for absolute force fatigue were compared between each group and showed no genotype or spermidine supplementation effect between A) WT, and C) *mdx*, groups. A fatigue percentage change of the previous block was also plotted between B) WT and D) *mdx*, and showed no genotype or spermidine supplementation effect between any group per block. Data is presented as means \pm SEM (n=8-10 WT samples per group, n=9-12 *mdx* samples per group). $p < 0.05$. Two-way ANOVA with Tukey's post-test

9. The effect of spermidine supplementation on muscle structure

9.1 EDL – Haematoxylin and Eosin (H&E) Stain for muscle fibre size and muscle health

EDL muscles were H&E stained to observe any differences in the number of healthy and damaged/regenerating fibres between groups. A fibre was deemed damaged or regenerating through either the presence of centrally localised nuclei, or being structurally damaged. If a fibre had none of these prerequisites, it was deemed a healthy, non-regenerating muscle fibre.

As expected, there was a genotypic difference in the relative proportion of healthy fibres, with the EDL muscles from *mdx* mice showing a substantial decrease of healthy fibres compared to the WT groups (Fig. 21). This is attributed to the chronic inflammation and cycles of

damaged and repair within the *mdx* phenotype, resulting in constant regenerating fibres within the muscle. Encouragingly, spermidine supplementation induced a significant increase in the proportion of healthy fibres in *mdx* EDL muscles compared to non-supplemented *mdx* EDL muscles (Fig.21). This data suggests that spermidine supplementation may decrease levels of chronic inflammation, and/or improve regeneration of some fibres in *mdx* EDL muscles.

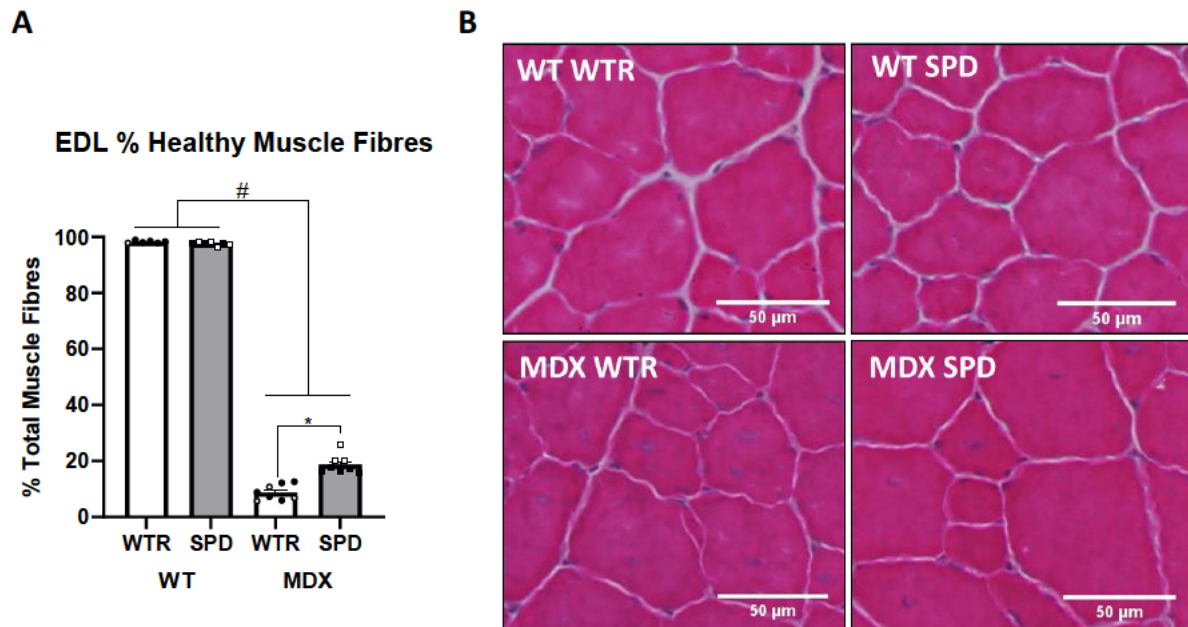


Figure 21. The effect of spermidine supplementation on muscle fibre health in WT and *mdx* EDL muscles. 3-week-old mice were supplemented with 3mM spermidine drinking water, or regular water for 13 weeks. Whole muscle was counted with fibres not containing centrally localised nuclei being deemed healthy fibres, with a percentage taken from total muscle fibres (A). A clear *mdx* downregulation of healthy muscle fibres was observed compared to WT. Spermidine supplementation within the *mdx* EDL also resulted in an increase in healthy muscle fibres compared to *mdx* control. B) representative image. Data is presented as means \pm SEM (n=6-7 WT samples per group, n=8 *mdx* samples per group). # indicates significant genomic difference between groups, * shows significant supplementation effect between groups. Black dots are male, white dots are female. $p < 0.05$. Two-way ANOVA with Tukey's post-test. Scale bar = 50 μ m.

H&E stains were also analysed for levels of unhealthy muscle tissue, as determined by selecting the area of all fatty tissue infiltration or fibrotic enveloped fibres. The percentage of unhealthy muscle tissue was normalised to total muscle area to determine the percentage of unhealthy muscle tissue.

As expected, there was a genotypic difference in the level of unhealthy muscle tissue with the EDL muscles from *mdx* mice displaying a greater proportion of unhealthy tissue compared to

the WT groups (Fig. 22). Importantly, spermidine supplementation decreased the percentage of unhealthy muscle tissue in *mdx* EDL muscles compared to non-supplemented *mdx* controls (Fig. 22). These data suggest that spermidine supplementation had the potential to decrease unhealthy muscle tissue levels in fast twitch dystrophic skeletal muscle.

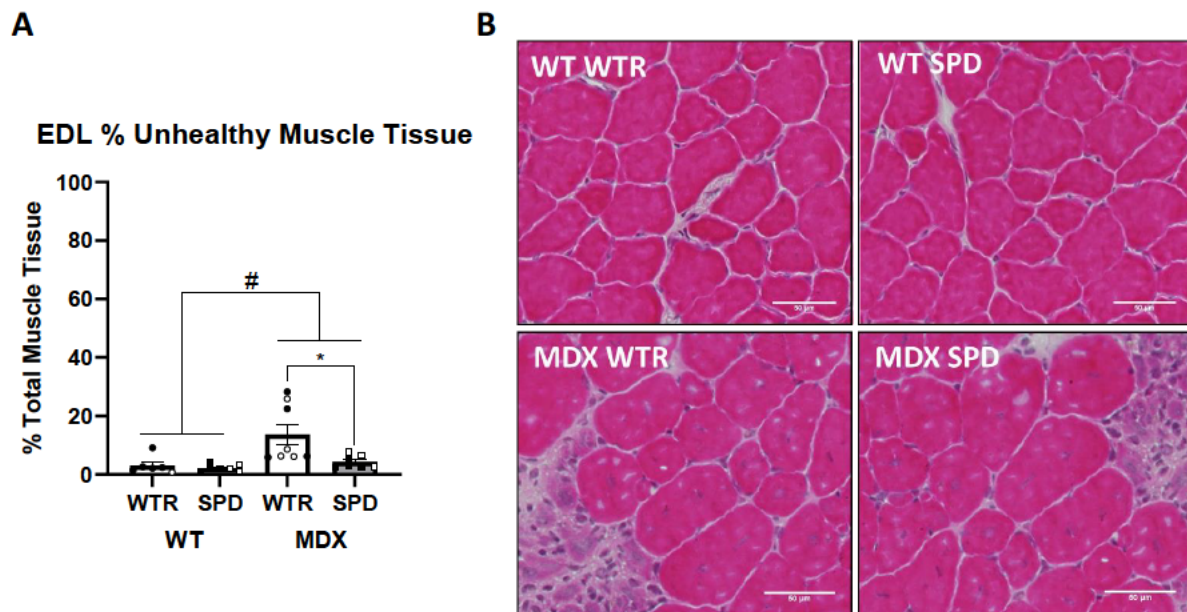


Figure 22. The effect of spermidine supplementation on muscle tissue health in WT and *mdx* EDL muscles 3-week-old mice were supplemented with 3mM spermidine drinking water, or regular water for 13 weeks. Whole muscle was counted with areas of fatty infiltration and fibrotic enveloped fibres being deemed unhealthy tissue, with a percentage taken from total muscle area (A). A clear *mdx* upregulation of unhealthy tissue was observed compared to WT. Spermidine supplementation within the *mdx* EDL also resulted in a decrease in unhealthy muscle tissue compared to *mdx* control. B) representative image. Data is presented as means \pm SEM (n=6-7 WT samples per group, n=8 *mdx* samples per group). # indicates significant genomic difference between groups, * shows significant supplementation effect between groups. $p < 0.05$. Black dots are male, white dots are female. Two-way ANOVA with Tukey's post-test. Scale bar = 50 μ m.

Next, the H&E sections were analysed for differences in muscle fibre size. The CSA of all fibres from each muscle section were averaged and plotted as a single data point, as well as being placed into bin sizes increasing in 250 μ m increments. As shown in Fig. 23A, there was a genotypic difference in average muscle fibre CSA with *mdx* EDL muscles fibres being larger than fibres from WT muscles.

Interestingly, although spermidine supplementation increased the proportion of healthy muscle fibres, and decreased the level of unhealthy muscle tissue, it had no effect on average

fibre size or on the relative distribution of muscles fibre sizes in WT (Fig. 23B) or *mdx* (Fig.23C) EDL muscles.

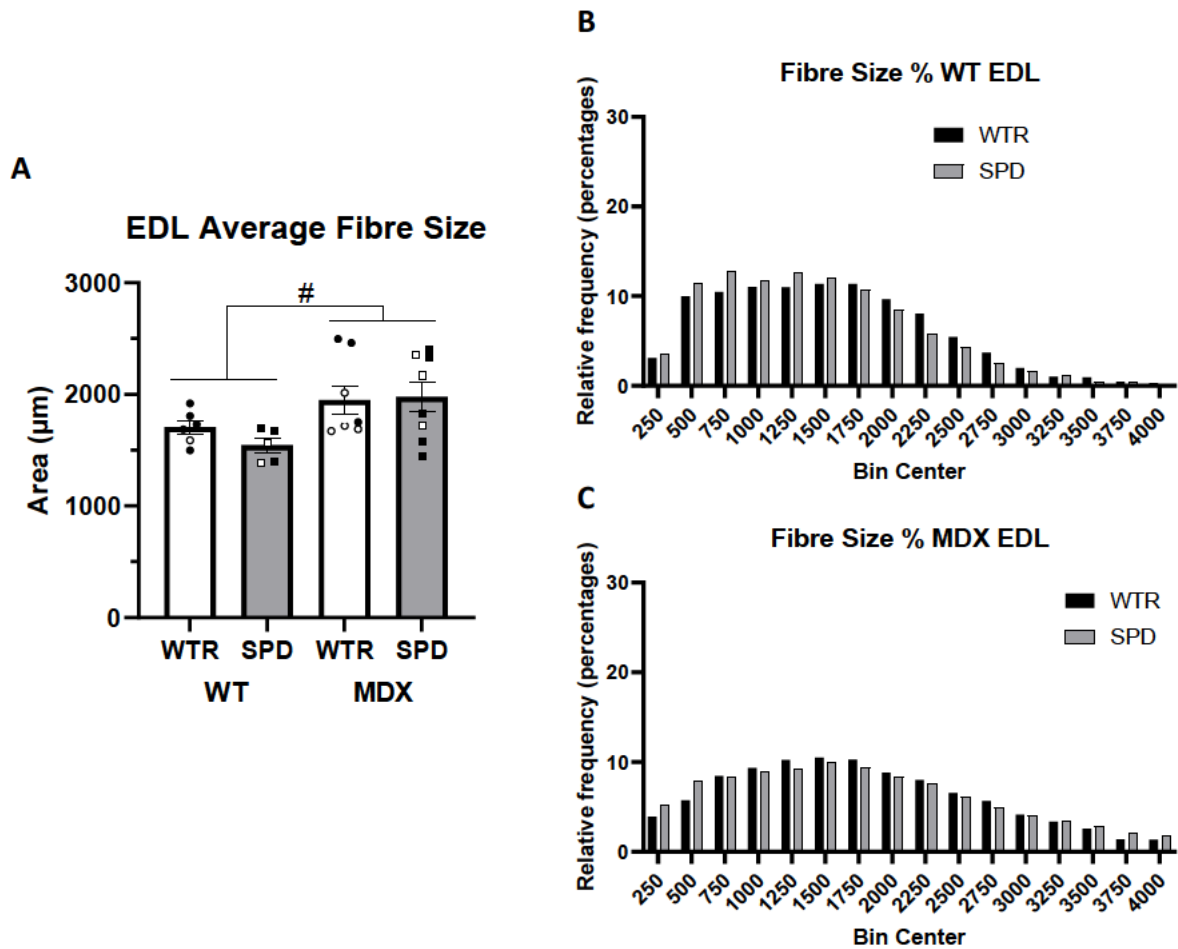


Figure 23. The effect of spermidine supplementation on muscle fibre size in WT and *mdx* EDL muscles. 3-week-old mice were supplemented with 3mM spermidine drinking water, or regular water for 13 weeks. Whole muscle was counted with all fibre sizes placed in bin sizes of 250 μm for WT (B) and *mdx* (C), as well as plotted as an average fibre size (A). All groups were compared between each bin and saw no genotype or spermidine supplementation differences between groups. Average fibre size showed an upregulation within *mdx* samples compared to WT, although no changes were observed with spermidine supplementation. Data is presented as means \pm SEM (n=6-7 WT samples per group, n=8 *mdx* samples per group). # indicates significant genomic difference between groups. Black dots are male, white dots are female. $p < 0.05$. Two-way ANOVA with Tukey's post-test.

9.2 SOL – Haematoxylin and Eosin (H&E) Stain for muscle fibre size and muscle health

SOL muscles were also H&E stained to observe the levels of healthy and regenerating fibres between groups. As expected, there was a genotypic difference in the proportion of healthy

muscle fibres with the *mdx* SOL muscles showing a substantial lower number of healthy muscle fibres compared to the WT groups. Interestingly, although spermidine supplementation induced an increase in the number of healthy muscle fibres in the *mdx* EDL muscles, there was no effect of spermidine on the *mdx* SOL muscles. This suggests that the beneficial effect of spermidine supplementation may be muscle/fibre-type specific.

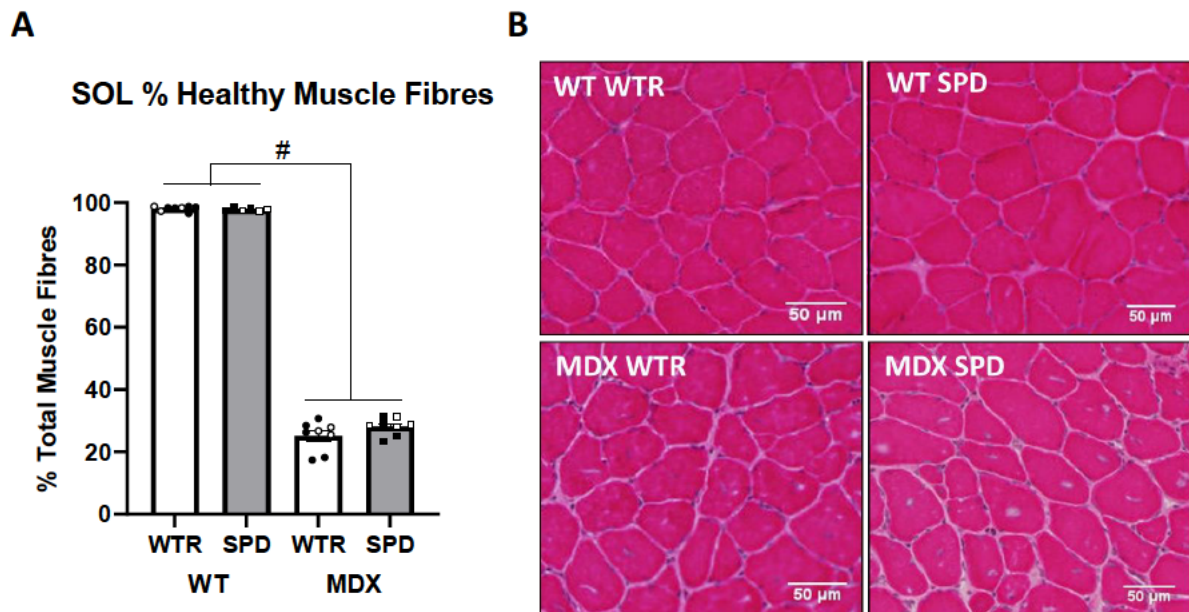


Figure 24. The effect of spermidine supplementation on muscle fibre health in WT and *mdx* SOL muscles. 3-week-old mice were supplemented with 3mM spermidine drinking water, or regular water for 13 weeks. Whole muscle was counted with fibres not containing centrally localised nuclei or tissue/fibrotic infiltration being deemed healthy fibres, with a percentage taken from total muscle fibres (A). A clear *mdx* downregulation of healthy muscle fibres was observed compared to WT. Spermidine supplementation had no effect on any group. B) representative image. Data is presented as means ± SEM (n=6-8 WT samples per group, n=8 *mdx* samples per group). # indicates significant genomic difference between groups. Black dots are male, white dots are female. $p < 0.05$. Two-way ANOVA with Tukey's post-test. Scale bar = 50μm.

Mirroring what we saw in the EDL muscles (Fig. 22), there was a genotypic difference in level of unhealthy muscle tissue with *mdx* SOL muscles showing a higher level of unhealthy tissue compared to the WT groups (Fig. 25). Unlike the EDL muscles, however, spermidine supplementation did not decrease the proportion of unhealthy tissue within the *mdx* SOL muscles compared to non-supplemented *mdx* controls, further exemplifying that the beneficial effect of spermidine may be fibre-type specific.

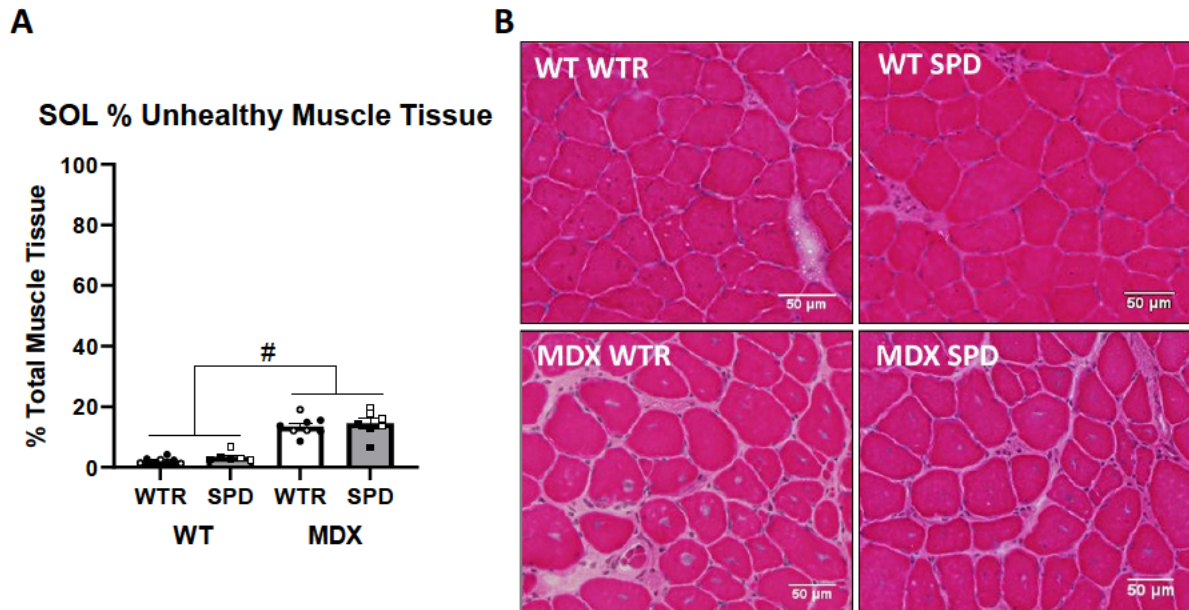


Figure 25. The effect of spermidine supplementation on muscle tissue health in WT and *mdx* SOL muscles. 3-week-old mice were supplemented with 3mM spermidine drinking water, or regular water for 13 weeks. Whole muscle was counted with areas of fatty infiltration and fibrotic enveloped fibres being deemed unhealthy tissue, with a percentage taken from total muscle area (A). A clear *mdx* upregulation of unhealthy tissue was observed compared to WT. Spermidine supplementation showed no effect on any groups. B) representative image. Data is presented as means \pm SEM (n=6-8 WT samples per group, n=8 *mdx* samples per group). # indicates significant genomic difference between groups. Black dots are male, white dots are female. $p < 0.05$. Two-way ANOVA with Tukey's post-test. Scale bar = 50 μ m.

Regarding average SOL fibre size, there was a main genotypic effect with fibres from *mdx* muscles being larger compared to WT controls (Fig. 26A). However, there were no effect of spermidine supplementation SOL muscle fibre CSA compared to non-supplemented controls for both WT (Fig. 26B) and *mdx* (Fig. 26C) groups.

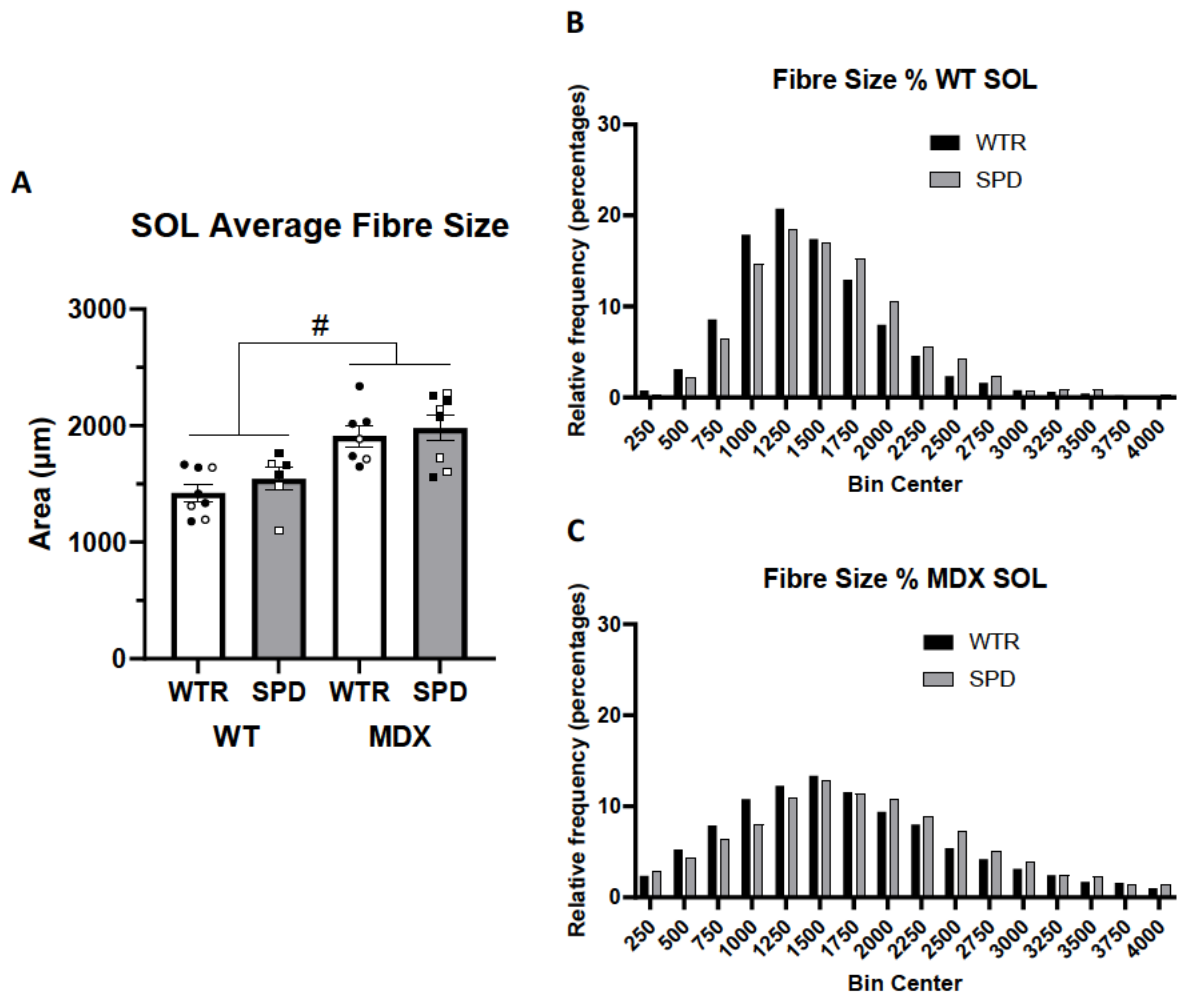


Figure 26. The effect of spermidine supplementation on muscle fibre size in WT and *mdx* SOL muscles. 3-week-old mice were supplemented with 3mM spermidine drinking water, or regular water for 13 weeks. Whole muscle was counted with all fibre sizes placed in bin sizes of 250 μm for WT (B) and *mdx* (C), as well as plotted as average fibre size (A). All groups were compared between each bin and saw no statistical genotype or spermidine supplementation differences between groups. Average fibre size showed an upregulation within *mdx* samples compared to WT, although no changes were observed with spermidine supplementation. Data is presented as means \pm SEM (n=6-8 WT samples per group, n=8 *mdx* samples per group). # indicates significant genomic difference between groups. Black dots are male, white dots are female. $p < 0.05$. Two-way ANOVA with Tukey's post-test.

10. The effect of spermidine supplementation on autophagy-related proteins

Spermidine supplementation has been shown to activate autophagy, in many different models, such as yeast, flies, worms and mice, with no long-term toxicity (119, 123). Rapamycin-induced autophagy has been shown to improve muscle strength in *mdx* mice (95). To date, however, no study has looked at the ability for spermidine to regulate autophagy or autophagy-

related proteins, such as MAP1S, AMPK, p70^{s6k1}, 4EBP1, p62 and LC3B-II/LC3B-I within the *mdx* mouse skeletal muscle.

10.1 Fast-twitch EDL muscle

MAP1S interacts with LC3B-I and LC3B-II, promoting autophagosome formation and subsequent completion of autophagy (134). Specifically, spermidine ingestion has shown to increase autophagy in the liver of wild type mice, through the dependant increase in MAP1S expression (135). Furthermore, spermidine-induced autophagy upregulation was dependant of MAP1S expression, highlighting its importance within the autophagy pathway (135). Total MAP1S is expressed in both full length (120kDa) and heavy chain (100kDa) bands, with the total intensity of both quantified together for analysis (141).

As shown in Fig. 27, there was a genotypic difference in MAP1S expression, with MAP1S being higher in EDL muscles from *mdx* mice compared to the EDL muscles of WT controls. Promisingly, spermidine supplementation further increased MAP1S expression in *mdx* EDL muscles when compared to *mdx* EDL controls (Fig. 27), suggesting that the supplemented spermidine was biologically active in *mdx* skeletal muscle and potentially indicating an increased rate of autophagy.

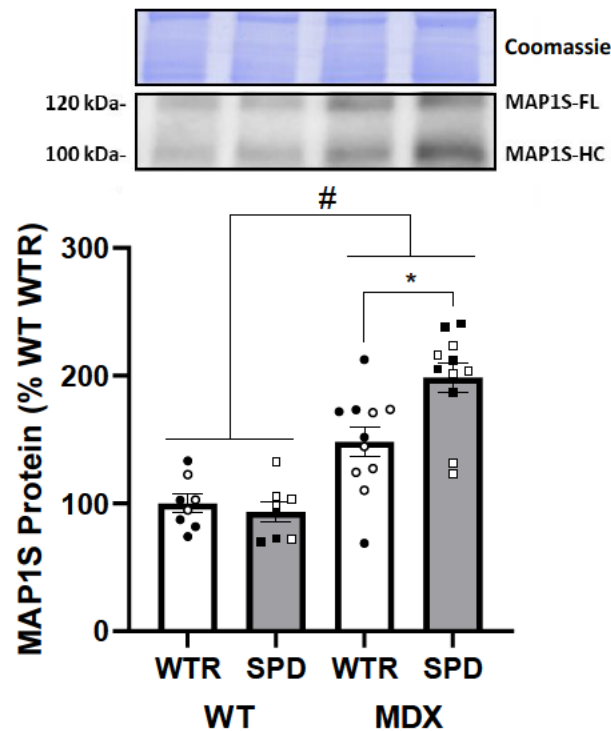


Figure 27. The effect of spermidine supplementation on MAP1S in EDL muscles. 3-week-old mice were supplemented with 3mM spermidine drinking water, or control water for 13 weeks. EDL muscles were removed and subjected to western blot analysis for MAP1S. A genomic upregulation is observed in *mdx* groups compared to WT, with a spermidine supplemental change upregulating MAP1S expression in *mdx* EDL's compared to *mdx* controls. Data is presented as means \pm SEM (n=7-8 WT samples per group, n=11 *mdx* samples per group). # indicates significant genomic difference between groups, * shows significant supplementation effect between groups. Black dots are male, white dots are female. $p < 0.05$. Two-way ANOVA with Tukey's post-test.

Another proposed mechanism of spermidine-induced autophagy upregulation is the activation of the AMPK pathway. AMPK activation plays a role in macromolecule degradation, with p-AMPK being shown to inhibit mTORC1 activity, and upregulate ULK1, in C2C12 mouse myoblasts (99, 131, 132).

There were genotypic differences observed in the active phosphorylated form of AMPK (p-AMPK), with p-AMPK being decreased in the *mdx* EDL muscles, compared to the WT EDL muscles (Fig. 28A). Interestingly, spermidine supplementation induced an increase in p-AMPK *mdx* EDL expression compared to EDL muscles from control *mdx* mice (Fig. 28A). Conversely, there were no differences in total AMPK expression in EDL muscles for both genotype and spermidine supplementation groups (Fig. 28B). Despite the genotypic and spermidine-induced

differences in p-AMPK (Fig. 28A), when p-AMPK was expressed as a ratio with total AMPK, there were no differences between any group (Fig. 28C).

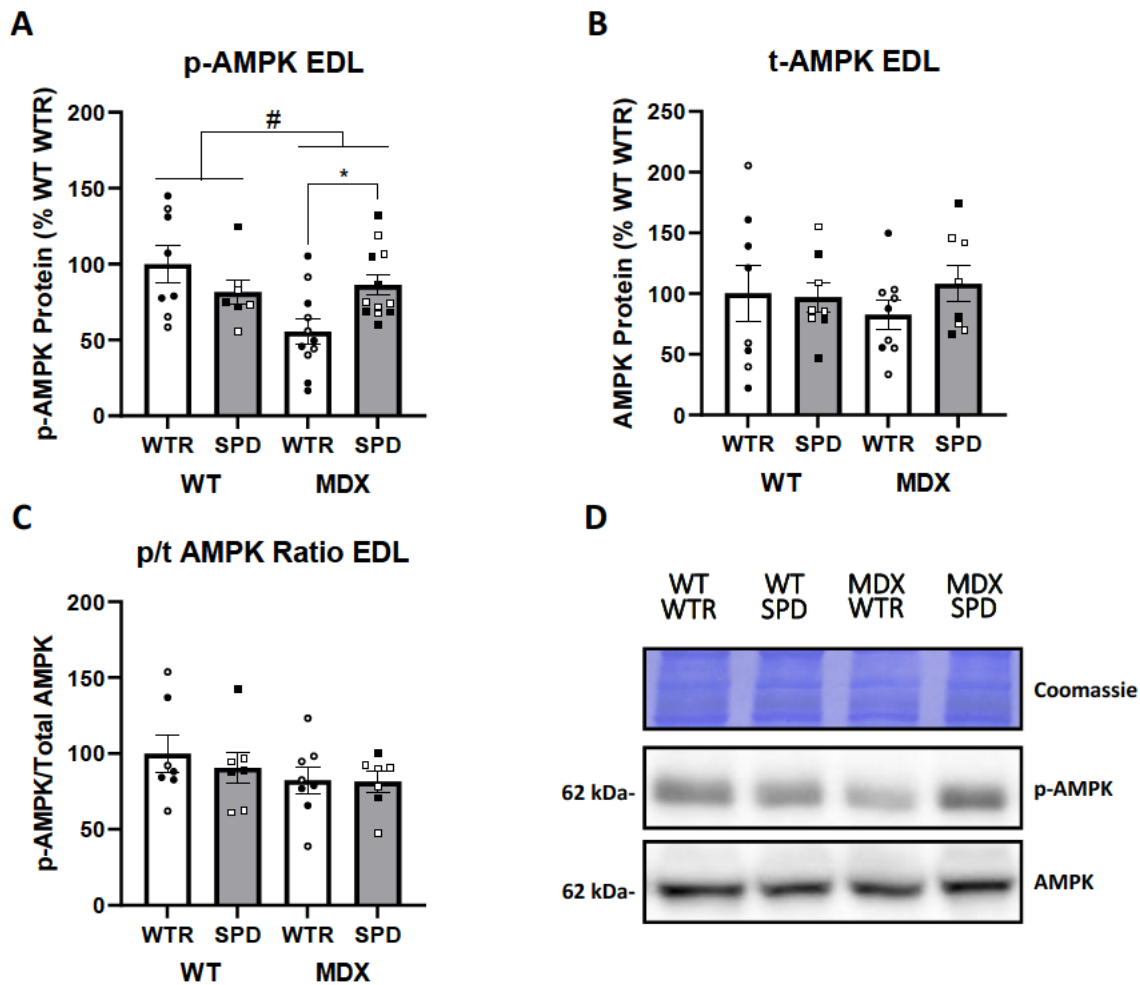


Figure 28. The effect of spermidine supplementation on phosphorylated and total AMPK in EDL muscles. 3-week-old mice were supplemented with 3mM spermidine drinking water, or control water for 13 weeks. EDL muscles were removed and subjected to western blot analysis for A) p-AMPK, B) total AMPK and C) their ratio (p-AMPK/AMPK). There was a genomic downregulation in *mdx* p-AMPK compared to WT, with a spermidine supplementation effect upregulating p-AMPK in *mdx* EDL's compared to *mdx* control. Total AMPK and the p-AMPK/AMPK ratio showed no differences between genotype or spermidine supplementation. D) representative image. Data is presented as means \pm SEM (n=7-8 WT samples per group, n=8-12 *mdx* samples per group). # indicates significant genomic difference between groups, * shows significant supplementation effect between groups. Black dots are male, white dots are female. p < 0.05. Two-way ANOVA with Tukey's post-test.

mTORC1 is a master inducer of protein synthesis, through its ability to facilitate cap dependent translation through the phosphorylation of p70^{S6k1} and 4EBP1 (100). The upregulation of mTORC1 activity corresponds with a decrease in autophagy through the phosphorylation, and subsequent inhibition, of the autophagy initiator ULK1 (99). Conversely, the inhibition of

mTORC1 results in an increased rate of autophagy through ULK1, and subsequent decrease in cap dependant translation expressed in decreased phosphorylation of p70^{s6k1} and 4EBP1 (99, 100). As such, phosphorylation of p70^{s6k1} and 4EBP1 are commonly used markers of mTORC1 activation.

As shown in Fig. 29, there was a genotype difference observed for p-p70^{s6k1} (Fig. 29A), total p70^{s6k1} (Fig. 29B) and p-p70^{s6k1}/total p70^{s6k1} ratio (Fig. 29C), with *mdx* EDL muscles showing higher levels compared to WT EDL groups. Spermidine supplementation, however, had no effect on p-p70^{s6k1} (Fig. 29A), total p-70^{s6k1} (Fig. 29B) and p-p70^{s6k1}/total p70^{s6k1} ratio (Fig. 29C) expression in WT and *mdx* muscles, indicating that spermidine supplementation had no impact on mTORC1 activity at this time point.

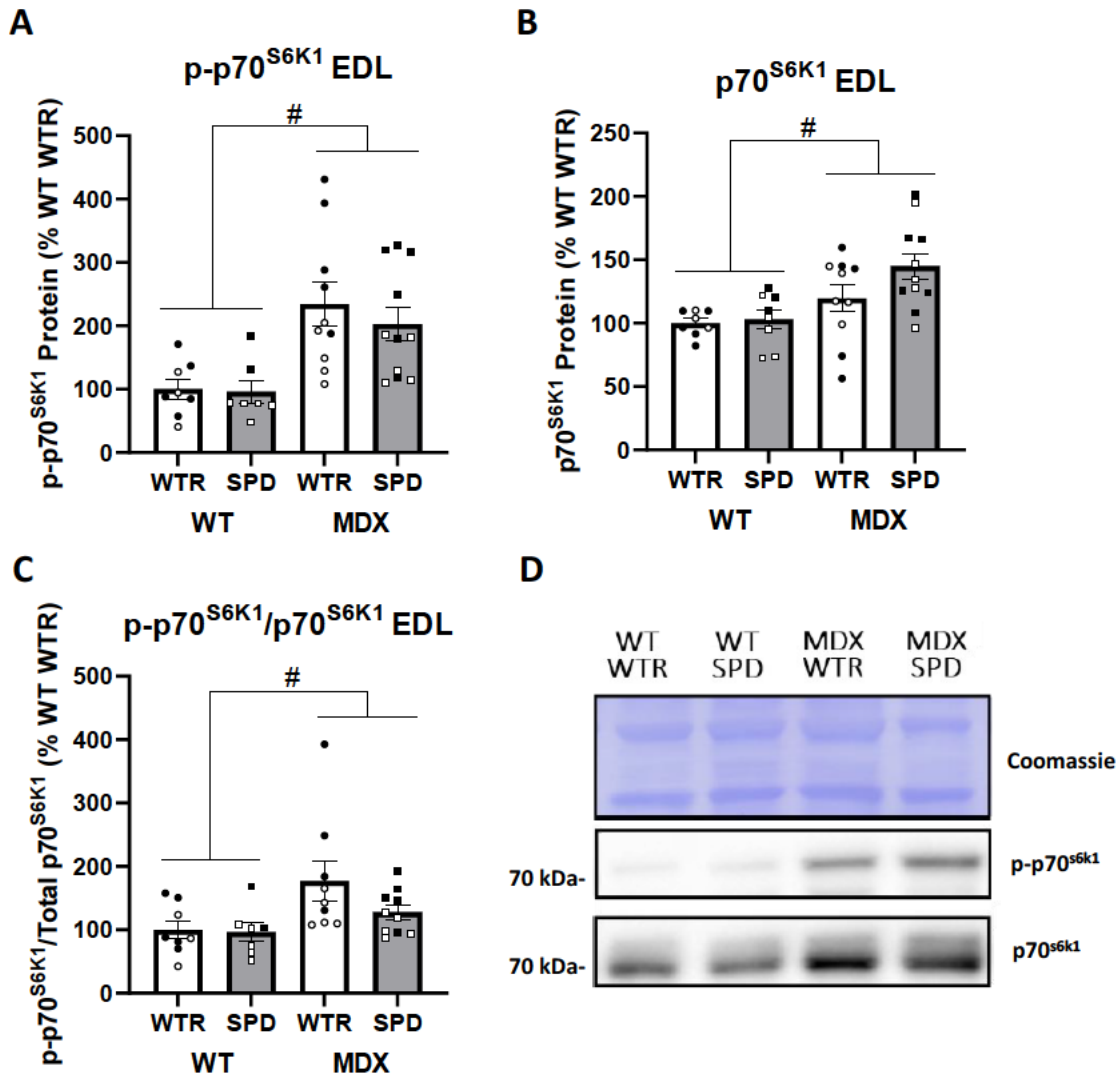


Figure 29. The effect of spermidine supplementation on phosphorylated and total p70^{S6K1} in EDL muscles. 3-week-old mice were supplemented with 3mM spermidine drinking water, or control water for 13 weeks. EDL muscles were removed and subjected to western blot analysis for A) p-p70^{S6K1}, B) total p70^{S6K1} and C) their ratio (p-p70^{S6K1}/p70^{S6K1}). p-p70^{S6K1}, total p70^{S6K1} and the p-p70^{S6K1}/total p70^{S6K1} ratio all showed an *mdx* genotype upregulation when compared to WT groups, however there were no spermidine supplementation effects observed between any groups. D) representative image. Data is presented as means \pm SEM (n=6-7 WT samples per group, n=9-11 *mdx* samples per group). # indicates significant genomic difference between groups. Black dots are male, white dots are female. $p < 0.05$. Two-way ANOVA with Tukey's post-test.

Regarding 4EBP1, there was a genotypic difference observed with p-4EBP1 expression being upregulated in the *mdx* EDL muscles, compared to the WT EDL muscle groups (Fig. 30A). Unexpectedly, spermidine supplementation induced an increase in p-4EBP1 expression within *mdx* EDL muscles, compared to the *mdx* EDL control group (Fig. 30A). These genotypic and spermidine-induced differences were mimicked in total 4EBP1 expression, with increases in

mdx EDL groups compared to WT EDL groups (Fig. 30B), resulting in no genotypic or spermidine supplemented changes observed in the p-4EBP1/total 4EBP1 ratio between all EDL muscle groups (Fig. 30C). This novel data suggest spermidine may increase mTORC1 signalling to 4EBP1 and/or that spermidine enhances the expression of 4EBP1 protein.

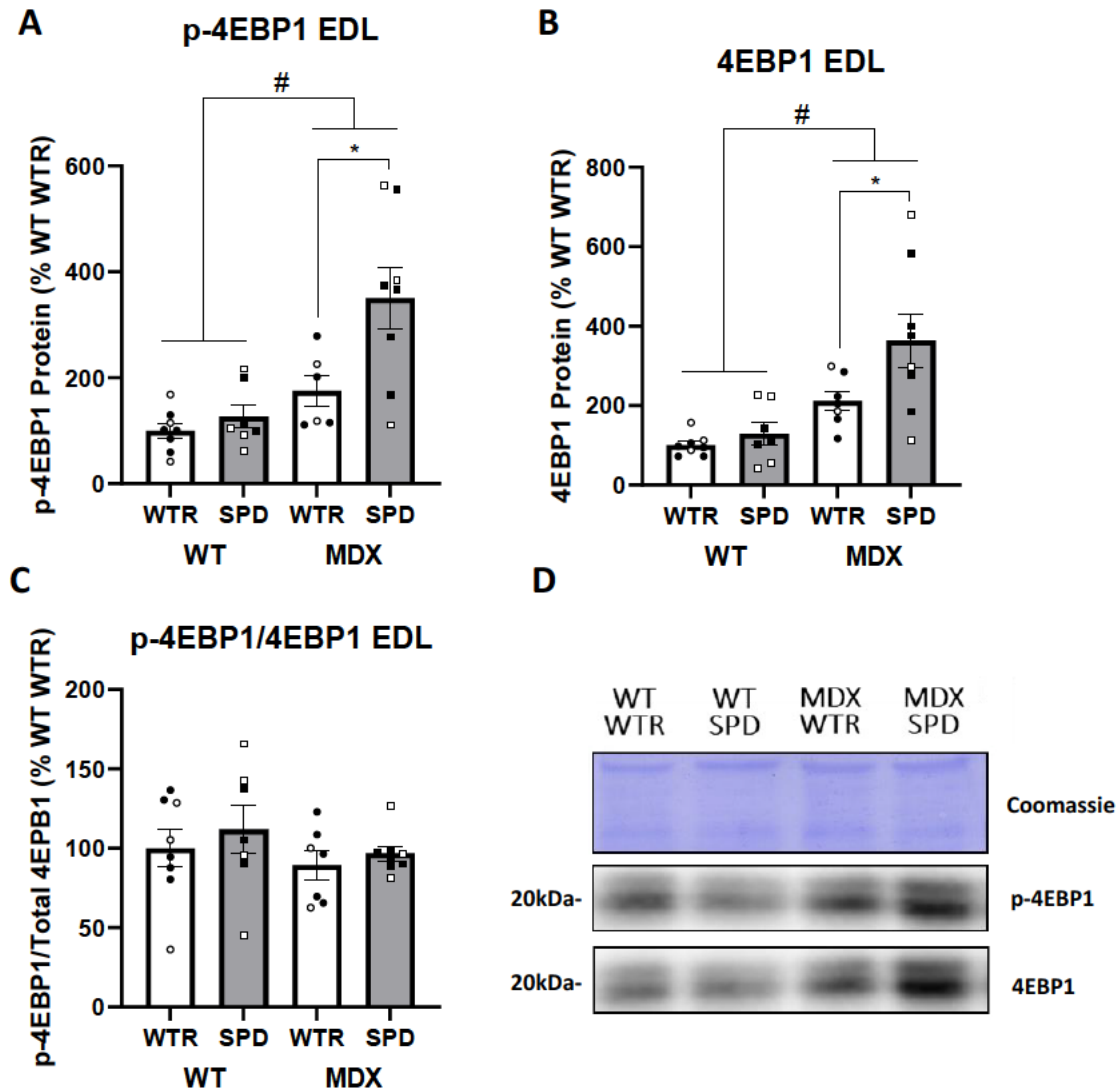


Figure 30. The effect of spermidine supplementation on phosphorylated and total 4EBP1 in EDL muscles. 3-week-old mice were supplemented with 3mM spermidine drinking water, or control water for 13 weeks. EDL muscles were removed and subjected to western blot analysis for A) p-4EBP1, B) total 4EBP1 C) their ratio (p-4EBP1/4EBP1). p-4EBP1 and total 4EBP1 showed an *mdx* upregulation when compared to WT groups. For both p-4EBP1 and total 4EBP1 also had a spermidine supplementation effect in the *mdx* EDL's compared to *mdx* controls. There were no genotypic changes or spermidine supplementation effects on the p-4EBP1/4EBP1 ratio. D) representative image. Data is presented as means \pm SEM (n=7 WT samples per group, n=6-8 *mdx* samples per group). # indicates significant genomic difference between groups, * shows significant supplementation effect between groups. Black dots are male, white dots are female. p < 0.05. Two-way ANOVA with Tukey's post-test.

There were no genotypic differences observed for LC3B-I or LC3B-II levels between all EDL muscle groups (Fig. 31A and 31B), resulting in no genotype differences in the LC3B-II/LC3B-I ratio (Fig. 31C). Spermidine supplementation had no effect on LC3B-I (Fig. 31A), LC3B-II (Fig. 31B) and LC3B-II/LC3B-I ratio (Fig. 31C) in both WT and *mdx* groups, suggesting no changes to rates of autophagy completion.

As expected, there was a genotypic difference in p62 expression of EDL muscles, with *mdx* mice showing elevated p62 expression compared to the EDL muscles of WT controls (Fig. 31E). Coinciding with the LC3B-I (Fig. 31A), LC3B-II (Fig. 31B) and LC3B-II/LC3B-I (Fig. 31C) data, spermidine supplementation did not alter the expression of p62 in both WT and *mdx* EDL muscles (Fig. 31E), again suggesting no changes to autophagy completion rates.

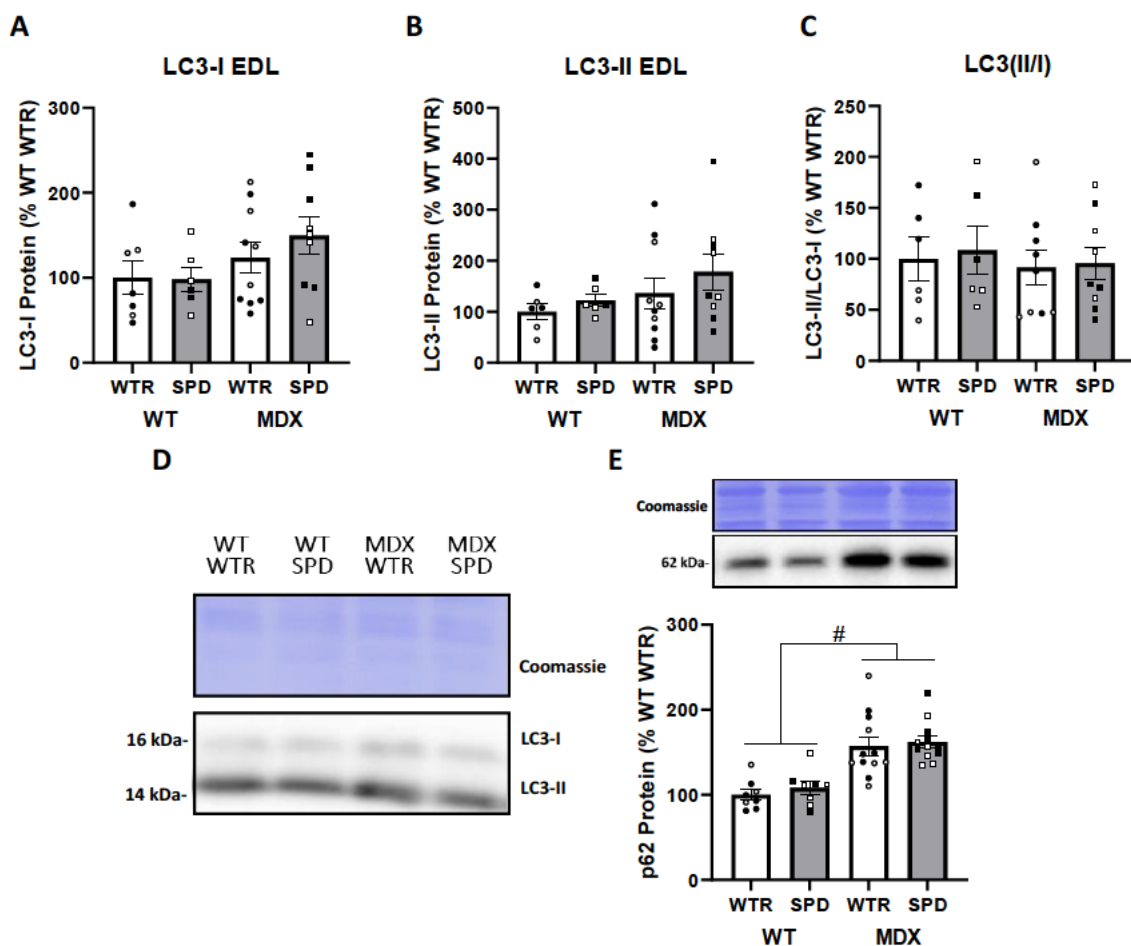


Figure 31. The effect of spermidine supplementation on LC3B and p62 in EDL muscles. 3-week-old mice were supplemented with 3mM spermidine drinking water, or control water for 13 weeks. EDL muscles were removed and subjected to western blot analysis for A) LC3B-I, B) LC3B-II C) their ratio (LC3B-II/LC3B-I) and E) p62. For

LC3B-I, LC3B-II and the LC3B-II/LC3B-I ratio, there were no genomic or spermidine supplementation effects between any group. For p62, a genomic upregulation is observed in *mdx* groups compared to WT, with no spermidine supplementation effects observed. D) representative image. Data is presented as means \pm SEM (LC3B n=6-7 WT samples per group, n=8-10 *mdx* samples per group) (p62 n=8 WT samples per group, n=12 *mdx* samples per group). # indicates significant genomic difference between groups. Black dots are male, white dots are female. $p < 0.05$. Two-way ANOVA with Tukey's post-test.

10.2 Slow-twitch SOL muscle

Similar to results in the EDL muscles (Fig. 27A), a genotypic difference in MAP1S expression was observed, with *mdx* SOL muscles showing increased levels compared to WT SOL muscles (Fig 32A). Furthermore, similar to EDL muscles (Fig. 27A), spermidine supplementation resulted in a strong trend of $p=0.0844$ for an increase in MAP1S protein in *mdx* SOL muscles compared to non-supplemented *mdx* SOL muscles (Fig. 32A).

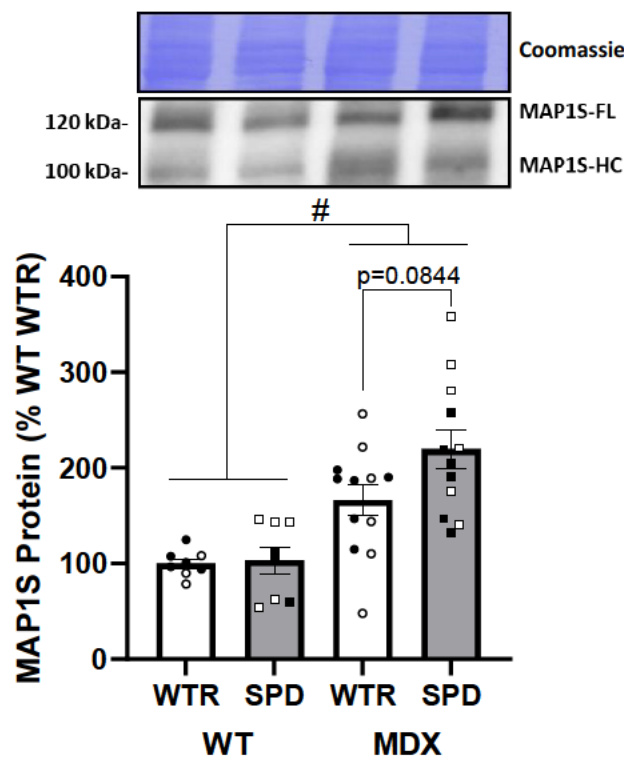


Figure 312. The effect of spermidine supplementation on MAP1S in SOL muscles. 3-week-old mice were supplemented with 3mM spermidine drinking water, or control water for 13 weeks. SOL muscles were removed and subjected to western blot analysis for MAP1S. For MAP1S, a genomic upregulation is observed in *mdx* groups compared to WT, with a spermidine supplemental showing an upregulation trend on MAP1S expression in *mdx* SOL's compared to *mdx* controls. Data is presented as means \pm SEM (n=7-8 WT samples per group, n=11 *mdx* samples per group). # indicates significant genomic difference between groups. Black dots are male, white dots are female. $p < 0.05$. Two-way ANOVA with Tukey's post-test.

Unlike in the EDL muscles (Fig. 28A), there were no genotypic differences observed between the *mdx* SOL muscles and WT SOL muscles in p-AMPK expression (Fig. 33A), nor was there an increase in p-AMPK with spermidine supplementation (Fig. 33A). This suggests that the effect of spermidine on AMPK phosphorylation may be muscle/fibre-type specific. Interestingly, despite no genotypic difference in total AMPK between the EDL muscle groups (Fig. 28B), a genotypic increase in total AMPK was observed within *mdx* SOL muscles compared to WT SOL muscles (Fig. 33B). Despite this, there were no significant effect of spermidine supplementation on total AMPK expression on *mdx* SOL muscles compared to non-supplemented controls. Moreover, there was no effect of spermidine supplementation on the p-AMPK/total AMPK ratio between both WT and *mdx* SOL muscle groups (Fig. 33C).

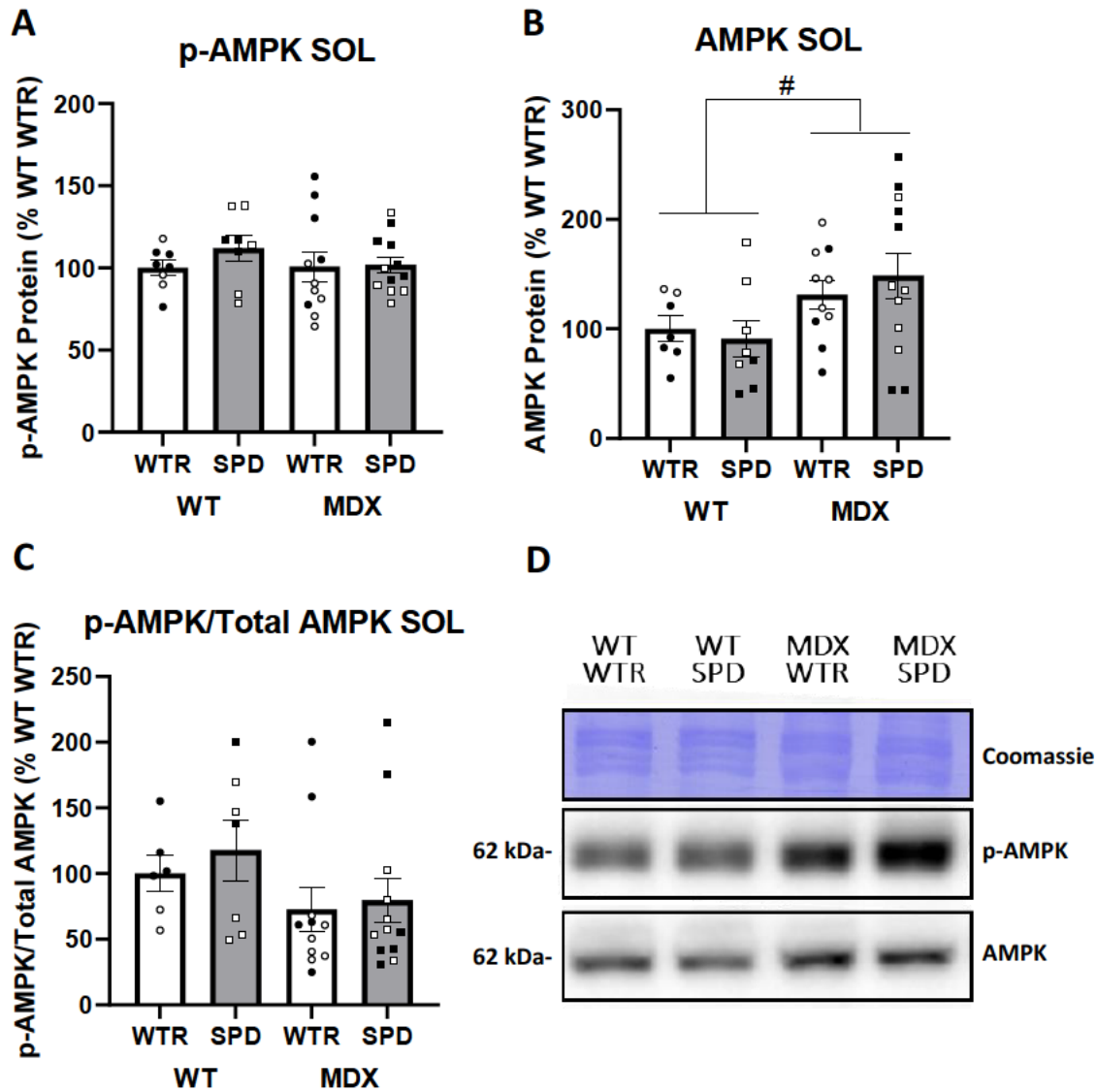


Figure 323. The effect of spermidine supplementation on phosphorylated and total AMPK in SOL muscles. 3-week-old mice were supplemented with 3mM spermidine drinking water, or control water for 13 weeks. SOL muscles were removed and subjected to western blot analysis for A) p-AMPK, B) total AMPK and C) their ratio (p-AMPK/AMPK). p-AMPK and the p-AMPK/AMPK ratio showed no genotype or spermidine supplementation effects between each group. Total AMPK showed an upregulation in *mdx* SOL samples compared to WT groups, however there were no spermidine supplement effects observed between all groups. D) representative image. Data is presented as means \pm SEM (n=7-8 WT samples per group, n=8-12 *mdx* samples per group). # indicates significant genomic difference between groups. Black dots are male, white dots are female. $p < 0.05$. Two-way ANOVA with Tukey's post-test

The level of p-p70^{S6k1} essentially mirrored the findings in the EDL muscles (Fig. 29A), with *mdx* SOL muscles showing increased levels compared to the WT SOL muscle groups (Fig. 34A). Furthermore, again mirroring the EDL findings (Fig. 29B), total levels of p70^{S6k1} varied between genotypes, with the *mdx* SOL muscles also exhibiting higher levels compared to WT SOL

muscles (Fig. 34B). Interestingly, despite seeing an elevation in the p-p70^{S6K1}/total p70^{S6K1} ratio within the EDL (Fig. 29C), there were no genotypic changes observed on the p-p70^{S6K1}/total p70^{S6K1} ratio in all SOL muscle groups (Fig. 34C). Spermidine supplementation also had no effect on the levels of p-p70^{S6K1} (Fig. 34A), total p70^{S6K1} protein (Fig. 34B) or the p-p70^{S6K1}/total p70^{S6K1} ratio (Fig. 34C) between all SOL muscle groups, indicating that spermidine did not influence mTORC1 activity within the SOL at this time point.

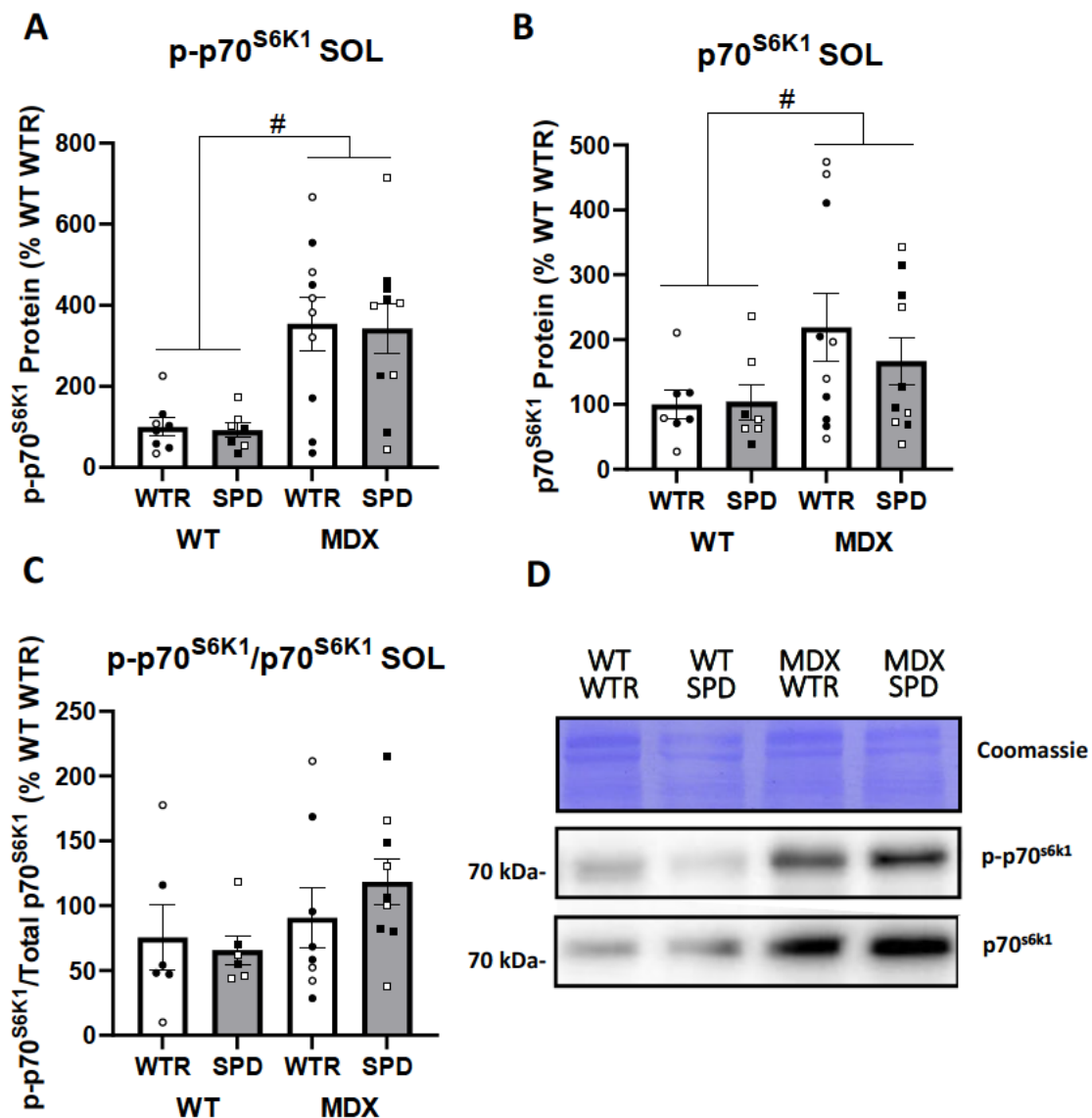


Figure 334. The effect of spermidine supplementation on phosphorylated and total p70^{S6K1} in SOL muscles. 3-week-old mice were supplemented with 3mM spermidine drinking water, or control water for 13 weeks. SOL muscles were removed and subjected to Western blot analysis for A) p-p70^{S6K1}, B) total p70^{S6K1} and C) their ratio (p-p70^{S6K1}/total p70^{S6K1}). p-p70^{S6K1} and total p70^{S6K1} showed an *mdx* genotype upregulation when compared to WT groups, however there were no spermidine supplementation effects observed between any groups. The p-

p70^{s6k1}/ p70^{s6k1} ratio showed no changes between groups both genotypically and with spermidine supplementation. D) Representative image. Data is presented as means \pm SEM (n=6-8 WT samples per group, n=8-11 *mdx* samples per group). # indicates significant genomic difference between groups. Black dots are male, white dots are female. $p < 0.05$. Two-way ANOVA with Tukey's post-test.

Similarly to findings within the EDL (Fig. 30A), p-4EBP1 levels were genotypically different, with *mdx* SOL muscles showing increased levels compared to WT SOL muscles (Fig. 35A). Furthermore, as also shown in within the EDL muscles (Fig. 30B), total 4EBP1 levels were increased in the *mdx* SOL muscles compared to the WT SOL muscle groups (Fig. 35B). Interestingly, despite a spermidine supplementation effect on both p-4EBP1 (Fig. 30A) and total 4EBP1 (Fig. 30B) within the *mdx* EDL muscles, there were no spermidine supplementation effects observed on p-4EBP1 (Fig. 35A), and total 4EBP1 (Fig. 35B) expression between *mdx* SOL muscles and non-supplemented *mdx* SOL controls. Again, similar to EDL muscles (Fig. 30C), there were no genotypic or spermidine supplementation-induced changes observed on the p-4EBP1/total 4EBP1 ratio in all SOL muscle groups (Fig. 35C).

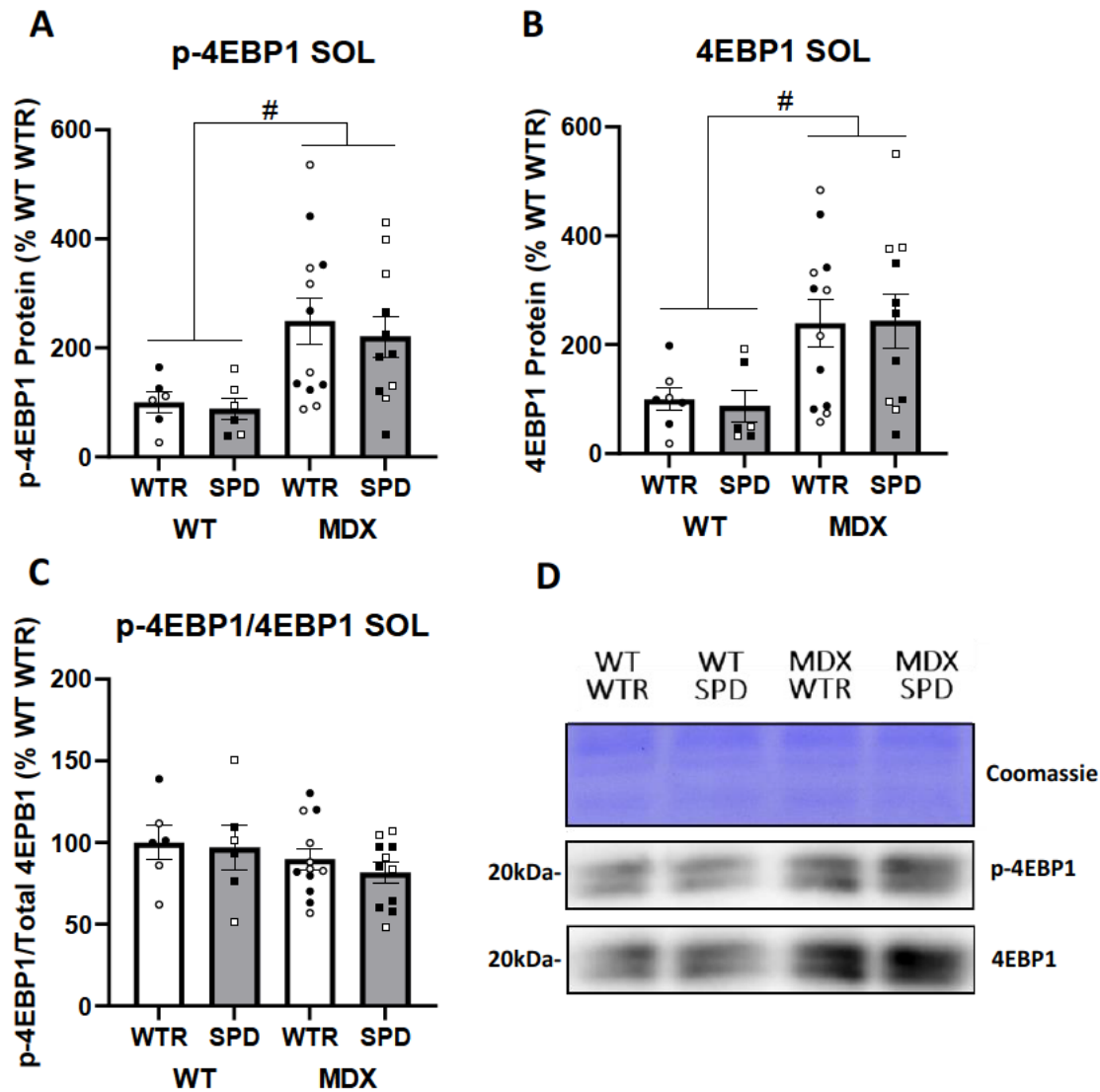


Figure 345. The effect of spermidine supplementation on phosphorylated and total 4EBP1 in SOL muscles. 3-week-old mice were supplemented with 3mM spermidine drinking water, or control water for 13 weeks. SOL muscles were removed and subjected to western blot analysis for A) p-4EBP1, B) total 4EBP1 C) their ratio (p-4EBP1/4EBP1). p-4EBP1 and total 4EBP1 showed an *mdx* upregulation when compared to WT groups, however showed no changes between spermidine supplementation between groups. The p-4EBP1/4EBP1 ratio showed no genotypic or spermidine supplementation changes. D) Representative image. Data is presented as means \pm SEM (n=6 WT samples per group, n=11-12 *mdx* samples per group). # indicates significant genomic difference between groups. Black dots are male, white dots are female. $p < 0.05$. Two-way ANOVA with Tukey's post-test.

Unlike in the EDL muscles (Fig. 31A), there was a genotypic difference in LC3B-I expression, with *mdx* SOL muscles showing increased levels compared to WT SOL muscles (Fig. 36A). Spermidine supplementation, however, had no impact on LC3B-I levels between any SOL muscle groups (Fig. 36A). Consistent with EDL muscles (Fig. 31B), there were no genotypic or spermidine supplementation effects on LC3B-II expression in any of the SOL muscle groups

(Fig. 36B). The genomic difference observed in LC3B-I expression (Fig. 36A) was also reflected in the LC3B-II/LC3B-I ratio, with *mdx* SOL muscles showing a lower ratio than the WT SOL muscles (Fig. 36C), indicating potentially decreased rates of autophagy in the *mdx* SOL muscles.

As seen in the EDL (Fig. 31E), there was also an elevated p62 expression in *mdx* SOL muscles compared to the WT SOL groups (Fig. 36E). However, spermidine supplementation showed no effect on p62 expression between any of the SOL muscle groups, further indicating that spermidine supplementation may not impact autophagy completion (Fig. 36E).

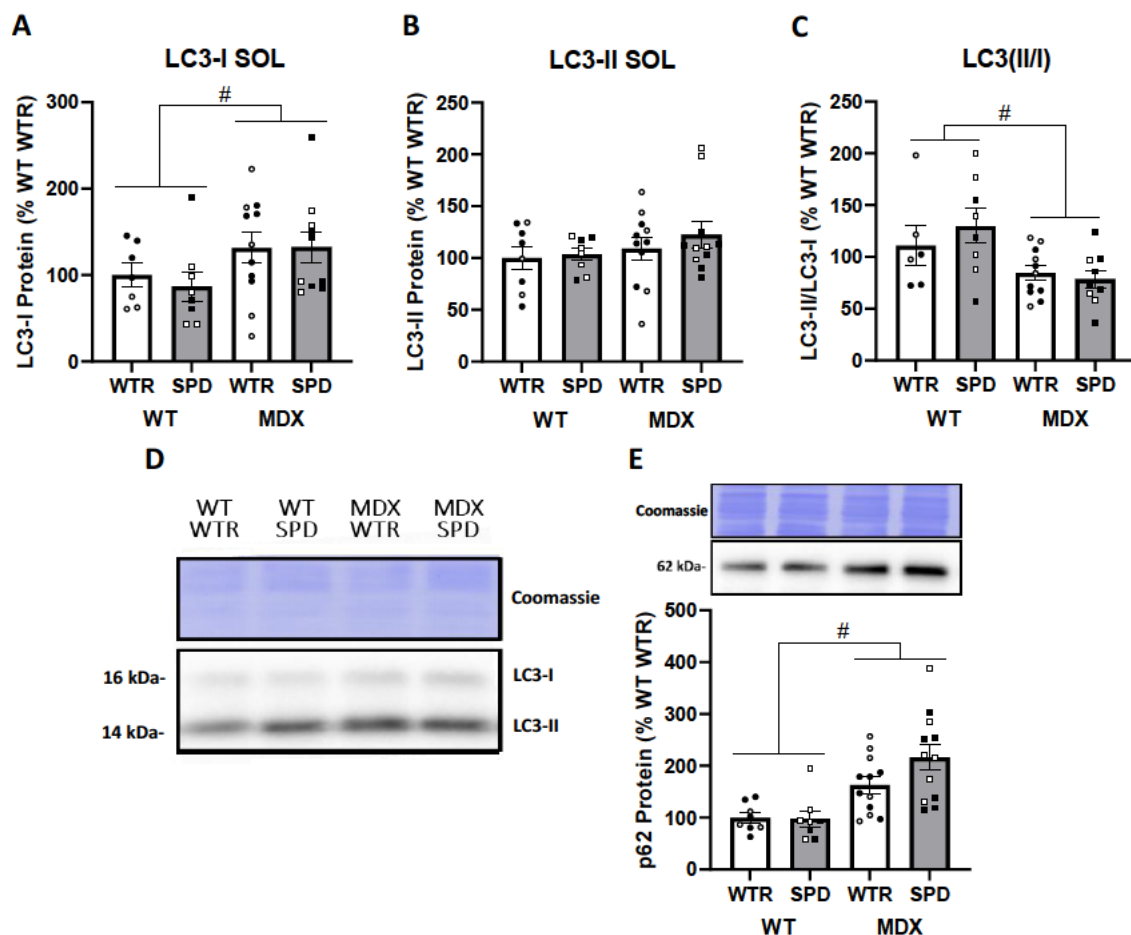


Figure 356. The effect of spermidine supplementation on LC3B and p62 in SOL muscles. 3-week-old mice were supplemented with 3mM spermidine drinking water, or control water for 13 weeks. SOL muscles were removed and subjected to western blot analysis for A) LC3B-I, B) LC3B-II C) their ratio (LC3B-II/LC3B-I) and E) p62. LC3B-I showed a genotypic upregulation of LC3B-I in *mdx* groups compared to WT groups, although there were no spermidine supplementation effects between groups. LC3B-II showed no genotype or spermidine supplementation effects between groups. LC3B-II/LC3B-I ratio showed a genomic downregulation in *mdx* groups compared to WT, whilst also showing no changes between groups for spermidine supplementation. For p62, a

genomic upregulation is observed in *mdx* groups compared to WT, with no spermidine supplementation effects observed. D) representative image. Data is presented as means \pm SEM (LC3B n=6-8 WT samples per group, n=9-11 *mdx* samples per group) (p62 n=8 WT samples per group, n=12 *mdx* samples per group). # indicates significant genomic difference between groups. Black dots are male, white dots are female. $p < 0.05$. Two-way ANOVA with Tukey's post-test.

Overall, these data suggest that, despite the spermidine-induced increase in the autophagy-related protein, MAP1S, spermidine appears to have not induced an activation of autophagy, as assessed by levels of LC3B and p62 at this time point. As this data was from a single static timepoint, observing LC3B and p62 levels in a model catered to observing the dynamic rate of autophagy would further support these findings.

11. The effect of spermidine supplementation on the autophagy flux assay

11.1 Fast-twitch EDL muscle

As autophagy is a dynamic multi stepped process, looking at a static timepoint of its markers LC3B and p62 is not the most accurate depiction of this process. Because of this, an autophagy flux assay animal study was used to determine the overall rate of autophagy through these same LC3B and p62 markers. The administration of colchicine, inhibits the formation of autolysosomes, resulting in the build-up of autophagosomes (107). As there are no autolysosomes formed, there is no breakdown of the inner membrane of the autophagosome resulting in an increase in LC3B-II and p62 levels (107). Because of this, if the autophagy process is upregulated, there would be an increase in LC3B-II and p62 due to their breakdown being inhibited via the colchicine (107). This allows for a 'dynamic/static' measure of autophagy when probing these markers via Western blotting.

The EDL's that were harvested from mice that underwent the 7-day autophagy flux experiment were probed via Western blotting for the autophagy marker p62 (Fig. 37). Importantly, colchicine induced an accumulation of p62 in WT muscles compared to EDL muscles from PBS treated mice control muscles (Fig. 37), demonstrating that the injected colchicine was biologically active, inhibiting autophagosome lysosome fusion and/or autolysosome-mediated degradation (107). Although not significant, there was a relatively strong trend ($p=0.0833$)

found for colchicine to also induce an accumulation of p62 *mdx* EDL muscles compared to PBS controls (Fig. 37). This could suggest that colchicine's inhibitory effect on autolysosome formation is lower in the *mdx* skeletal muscle phenotype. Interestingly, there was no effect of spermidine supplementation on the colchicine-induced accumulation of p62 in either WT or *mdx* EDL muscles (Fig. 37).

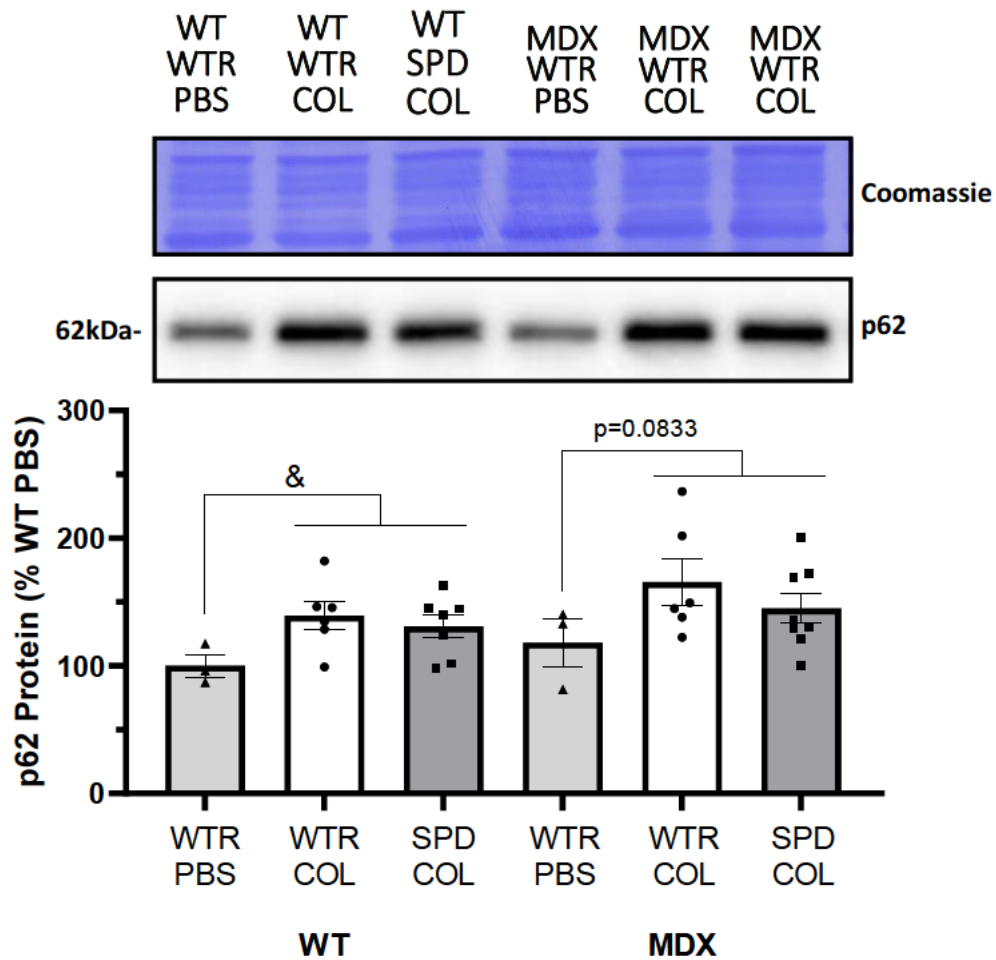


Figure 367. The effect of spermidine supplementation on p62 in 7-day autophagy flux EDL muscles. 8-week-old male mice were supplemented with 3mM spermidine drinking water, or control water for 7 days. On day 5 and 6, the WT and *mdx* groups received a 0.4mg/kg IP injection of colchicine, with 3 WT and *mdx* controls getting an IP injection of PBS. The EDL was then removed and subjected to western blotting for p62. Colchicine within the WT groups showed an upregulation of p62 when compared to WT PBS controls. Colchicine within the *mdx* groups showed a trend for the upregulation of p62 when compared to the *mdx* PBS controls. There were no genotypic or spermidine supplemented changes observed between any groups. Data is presented as means \pm SEM (n=3 for WT and *mdx* PBS samples per group, n=6 WT samples per group, n=7-8 *mdx* samples per group).

& indicates significant colchicine difference between groups. $p < 0.05$. Unpaired, two-tailed t test and two-way ANOVA with Tukey's post-test.

Similar to p62, a colchicine effect was observed in WT EDL muscles, with colchicine inducing an increase in LC3B-I and LC3B-II compared to muscles from the PBS treated WT control mice (Fig. 38A), again confirming the biological activity of the colchicine *in vivo*. Unlike for p62, there was no trend for a colchicine effect on LC3B-I or LC3B-II accumulation in *mdx* EDL muscles compared to *mdx* PBS treated controls (Fig. 38A and 38B). Interestingly, unlike at 16 weeks of age (Fig. 29A), there was a main genotype effect of LC3B-I expression, with *mdx* EDL muscles exhibiting higher levels compared to other WT EDL groups (Fig. 38A) but not for LC3B-II. Again, similar to p62, spermidine supplementation had no effect on EDL LC3B-I or LC3B-II levels in both *mdx* and WT colchicine treated groups (Fig. 38A and 38B).

Given the larger relative colchicine-induced increase in LC3B-II compared to the increase in LC3B-I, there was a significant colchicine-induced increase in the LC3B-II/LC3B-I ratio in WT EDL muscles compared to the WT EDL PBS controls (Fig. 38C). Despite no changes in LC3B-I (Fig. 38A) and LC3B-II (Fig. 38B) with colchicine in *mdx* EDL muscles, there was a strong trend ($p=0.0781$) for an increase in LC3B-II/LC3B-I ratio in *mdx* EDL muscles compared to PBS treated *mdx* muscles (Fig. 38C). These data suggest that *mdx* EDL muscles are relatively resistant to the effect of colchicine in inhibiting autophagy, possibly due to the already elevated levels of autophagy in *mdx* muscles in the basal state. Lastly, no spermidine supplementation effects were observed within all WT and *mdx* colchicine muscle groups within their LC3B-II/LC3B-I ratio (Fig. 38C), suggesting that spermidine is unable to increase the *in vivo* rate of autophagy in EDL muscles from either WT or *mdx* mice.

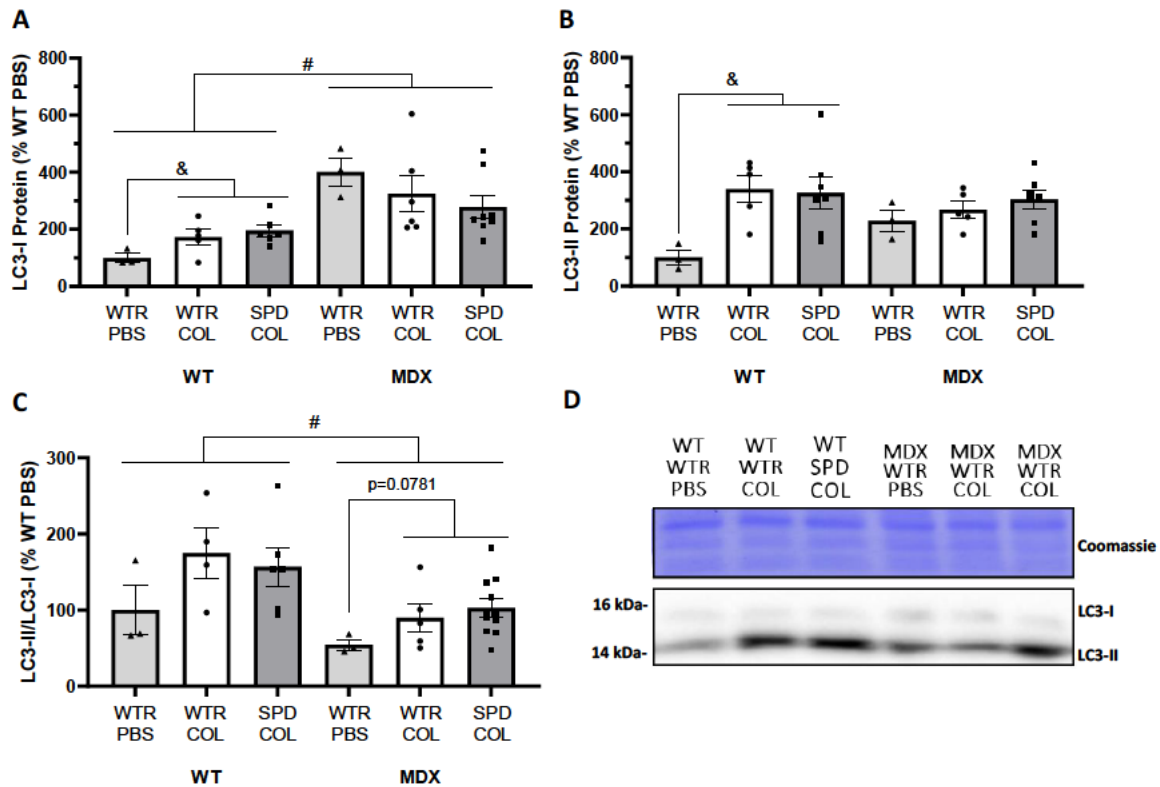


Figure 378. The effect of spermidine supplementation on LC3B in 7-day autophagy flux EDL muscles. 8-week-old male mice were supplemented with 3mM spermidine drinking water, or control water for 7 days. On day 5 and 6, the WT and *mdx* groups received a 0.4mg/kg IP injection of colchicine, with 3 WT and *mdx* controls getting an IP injection of PBS. The EDL was then removed and subjected to western blotting for A) LC3B-I, B) LC3B-II and C) their LC3B-II/LC3B-I ratio. Levels of LC3B-I were increased in WT colchicine samples when compared to WT PBS controls. There were no colchicine changes observed within the *mdx* groups. For LC3B-I, the *mdx* groups did have an upregulation of LC3B-I compared to the WT groups, although no groups showed a spermidine supplementation effect. Levels of LC3B-II were increased in WT colchicine samples compared to WT PBS controls. For LC3B-II, there were no colchicine changes observed within the *mdx* groups. All other groups showed no difference in genotype and spermidine supplementation for LC3B-II. WT groups showed no colchicine effect between all groups for the LC3B-II/LC3B-I ratio, with a trend observed for the LC3B-II/LC3B-I ratio upregulation in *mdx* colchicine samples compared to *mdx* PBS controls. There was a genotypic downregulation in *mdx* groups compared to WT groups for the LC3B-II/LC3B-I ratio, although there were no spermidine supplementation effects between all groups. D) Representative image. Data is presented as means \pm SEM (n=3 for WT and *mdx* PBS samples per group, n=4-6 WT samples per group, n=5-8 *mdx* samples per group). & indicates significant colchicine difference between groups, # indicates significant genotypic difference between groups. $p < 0.05$. Unpaired, two-tailed t test and two-way ANOVA with Tukey's post-test.

11.2 Slow-twitch SOL muscle

Unlike findings within the EDL (Fig. 37), there was no effect of colchicine on p62 levels in WT or *mdx* SOL muscles compared to SOL muscles from PBS controls (Fig. 39). This suggests that fast-twitch muscle fibres may be more sensitive to the action of colchicine than slow-twitch

muscles fibres. Despite the lack of colchicine effect, a genotypic difference in p62 level was present with p62 being higher in *mdx* SOL muscles compared to the WT SOL muscles (Fig. 39). Spermidine supplementation had no effect on p62 levels in WT and *mdx* SOL muscles (Fig. 39).

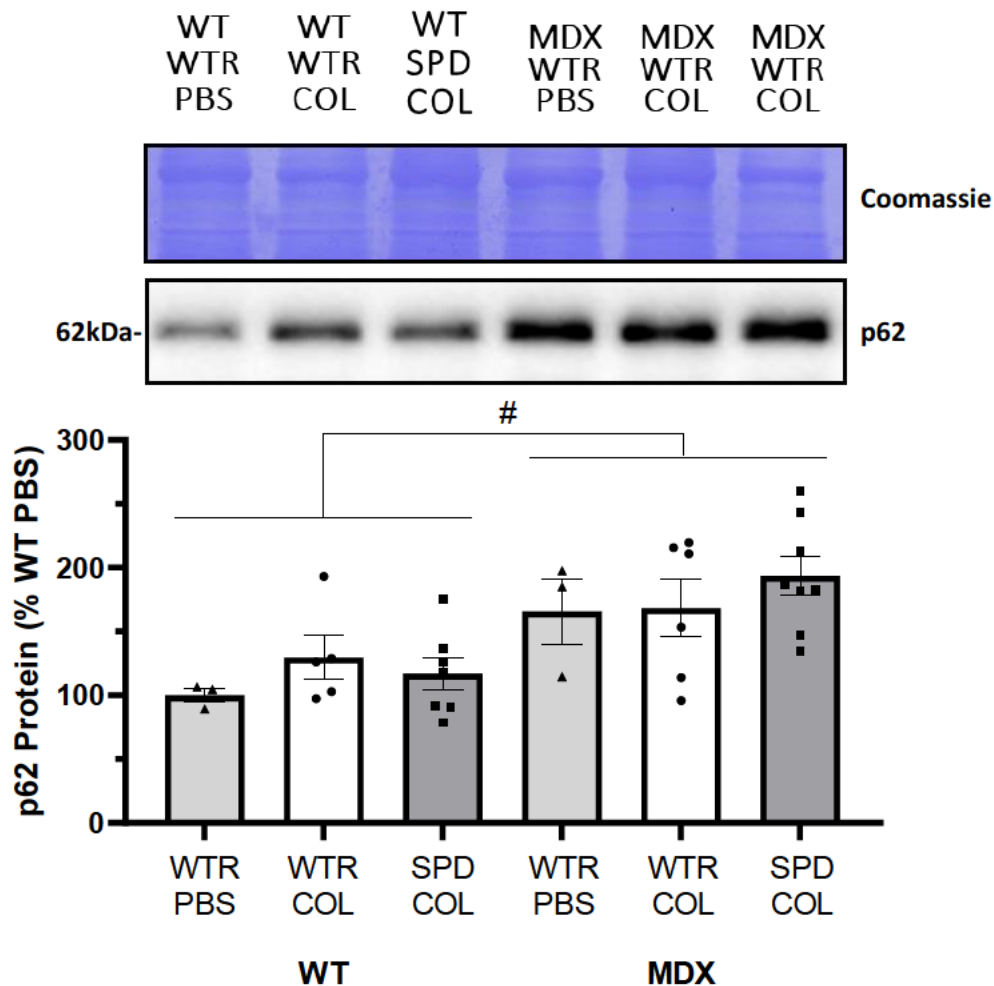


Figure 389. The effect of spermidine supplementation on p62 in 7-day autophagy flux SOL muscles. 8-week-old male mice were supplemented with 3mM spermidine drinking water, or control water for 7 days. On day 5 and 6, the WT and *mdx* groups received a 0.4mg/kg IP injection of colchicine, with 3 WT and *mdx* controls getting an IP injection of PBS. The SOL was then removed and subjected to western blotting for p62. There were no colchicine effects observed in both WT and *mdx* groups when compared to their PBS controls. A genotypic upregulation was shown in the *mdx* samples compared to the WT groups. There were no spermidine supplementation effects observed between any groups. Data is presented as means \pm SEM (n=3 for WT and *mdx* PBS samples per group, n=5-6 WT samples per group, n=6-8 *mdx* samples per group). # indicates significant genomic difference between groups. $p < 0.05$. Unpaired, two-tailed t test and two-way ANOVA with Tukey's post-test.

Consistent with the SOL p62 data (Fig. 39), colchicine had no effect on LC3B-I levels in WT or *mdx* SOL muscles compared to the PBS controls (Fig. 40A). Furthermore, there were no genotypic or spermidine supplementation effects on LC3B-I expression between WT and *mdx* muscle groups (Fig. 40A).

Interestingly, despite no difference in LC3B-I expression (Fig. 40A), a colchicine effect was observed with LC3B-II being increased by colchicine in WT SOL muscles compared to WT PBS controls (Fig. 40B), suggesting that WT SOL muscles are not completely unresponsive to the actions of colchicine. No colchicine effect was, however, detected for LC3B-II levels in *mdx* SOL muscles (Fig. 40B). Furthermore, there was no genotypic difference or effect of spermidine supplementation on LC3B-II levels in WT or *mdx* SOL muscles (Fig. 40B).

Despite the colchicine-induced increase in LC3B-II in WT SOL muscles (Fig. 40B), this did not translate into a significant increase in the LC3B-II/LC3B-I ratio for WT or *mdx* SOL groups compared to their PBS controls (Fig. 40C). Furthermore, there was no genotypic difference or spermidine supplementation effect on the LC3B-II/LC3B-I ratio between all WT and *mdx* SOL groups (Fig. 40C).

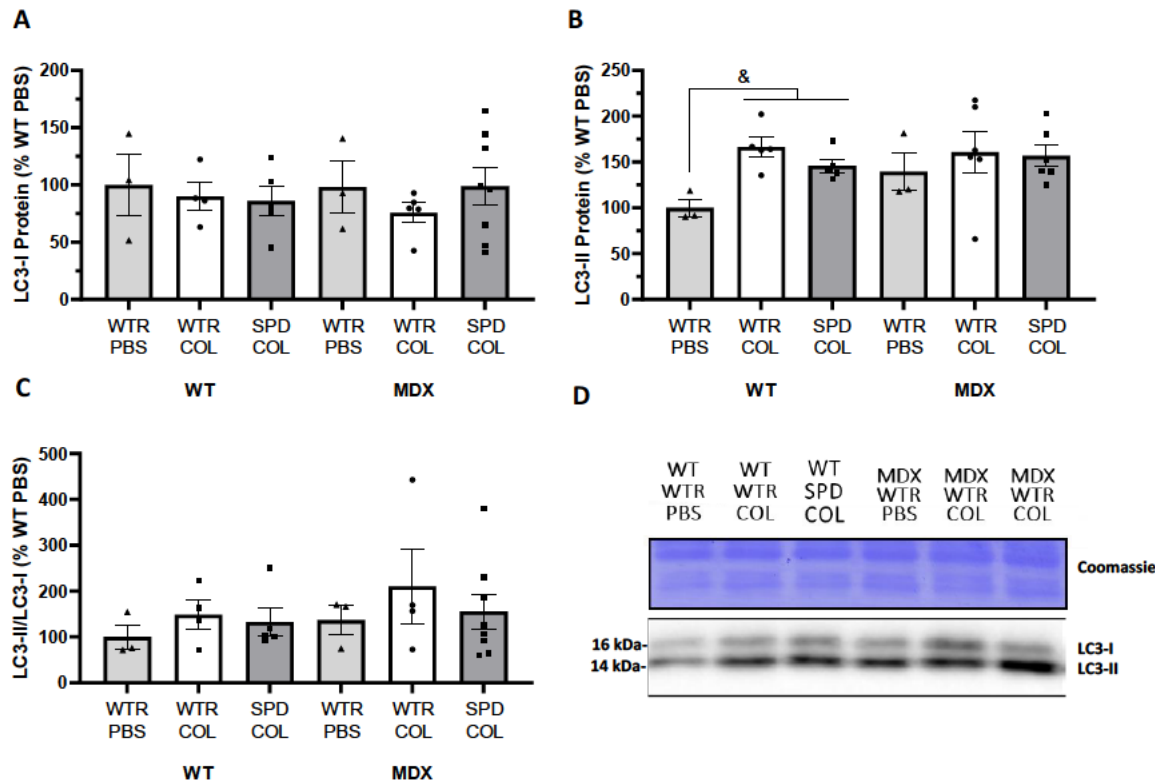


Figure 4039. The effect of spermidine supplementation on LC3B in 7-day autophagy flux SOL muscles. 8-week-old male mice were supplemented with 3mM spermidine drinking water, or control water for 7 days. On day 5 and 6, the WT and *mdx* groups received a 0.4mg/kg IP injection of colchicine, with 3 WT and *mdx* controls getting an IP injection of PBS. The SOL was then removed and subjected to western blotting for A) LC3B-I, B) LC3B-II and C) their LC3B-II/LC3B-I ratio. There were no colchicine, genotype or spermidine supplementation effects observed on LC3B-I levels between any groups. LC3B-II levels were upregulated with colchicine within the WT groups compared to WT PBS controls. There was no colchicine effect within the *mdx* groups. There was also no effect of spermidine supplementation on LC3B-II levels between all groups. The LC3B-II/LC3B-II ratio shows no colchicine, genotype or spermidine supplementation effect between all groups. D) Representative image. Data is presented as means \pm SEM (n=3 for WT and *mdx* PBS samples per group, n=4-6 WT samples per group, n=5-8 *mdx* samples per group). & indicates significant colchicine difference between groups. $p < 0.05$. Unpaired, two-tailed t test and two-way ANOVA with Tukey's post-test.

When combined, these data suggest that fast-twitch EDL muscles are more sensitive to colchicine's action in inhibiting autophagy compared to slow-twitch SOL muscles, and that spermidine does not appear to activate autophagy *in vivo* in either EDL or SOL muscles from WT or *mdx* mice.

Discussion

This is the first study to determine genotypic differences in, and spermidine supplemented changes to, polyamine pathway enzyme expression in wild type and *mdx* skeletal muscle. Furthermore, this is the first study to investigate the potential therapeutic effect of spermidine supplementation on *mdx* skeletal muscle structure and function. Promisingly, spermidine supplementation led to improvements in *mdx* skeletal muscle, indicating that spermidine may indeed have a therapeutic impact on the mouse model of skeletal muscle dystrophy.

12. Expression of polyamine pathway enzymes in wild type vs *mdx* skeletal muscle

This is the first study to have compared the expression of polyamine pathway proteins in fast-twitch (EDL) and slow-twitch (SOL) muscles from WT and dystrophic *mdx* mice. Furthermore, no studies have examined whether spermidine supplementation has an impact on the polyamine pathway enzymes in either WT or *mdx* muscle. To this end, 3-week-old mice were supplemented with spermidine for 13 weeks (discussed in methods 5.1), after which EDL and SOL muscles were analysed via Western blotting for differences in the levels of polyamine enzyme protein expression.

In the EDL and SOL muscles (Fig. 8 and 9), there was an upregulation of Amd1 (Fig. 8B and 9B) and SpdSyn (Fig. 8C and 9C) in the *mdx* samples compared to the WT muscles, suggesting the potential for increased polyamine production and, in particular, spermidine, in *mdx* muscle. This result is consistent with data showing that DMD boys have increased muscle spermidine content in the vastus lateralis compared to healthy boys (142). Furthermore, spermidine content has been shown to be 2-3 times higher in *mdx* mouse gastrocnemius muscles compared to WT muscle (143). This data prompts the question as to why Amd1, SpdSyn and spermidine are elevated within the *mdx* genotype, and are these beneficial adaptations in the context of DMD.

Interestingly, Amd1 and SpdSyn were recently reported to be upregulated in WT muscles subjected to chronic mechanical overload, a model that induces muscle hypertrophy that is associated with elevated mTORC1 activation (130). Moreover, the overload-induced increase in these proteins was inhibited by the mTORC1 inhibitor, rapamycin, suggesting that mTORC1 may directly, or indirectly, play a role in the regulation of Amd1 and SpdSyn expression (130). In this current study, and in agreement with previous studies (89, 144), two key markers of mTORC1 signalling (p-p70^{s6k1} and p-4EBP1) were also found to be elevated in *mdx* EDL (Fig. 29A and 30A) and SOL (Fig. 34A and 35A) muscles, suggesting that AMD1 and SpdSyn expression may also be regulated by mTORC1 in dystrophic skeletal muscle. To more definitively confirm this hypothesis, future studies should treat *mdx* mice with an mTORC1 inhibitor, such as rapamycin, to determine whether Amd1 and SpdSyn expression is reduced.

Regarding how mTORC1 might regulate the level of Amd1 and SpdSyn proteins, mTORC1 has been shown to directly phosphorylate Amd1, resulting in decreased levels of proteasome-mediated Amd1 degradation in prostate cancer cells (125). Furthermore, SpdSyn mRNA has the potential to form secondary structures, due to its high G-C content in its 5'-untranslated region (5'-UTR), resulting in impaired translation initiation (145, 146). As such, when mTORC1 activity is increased, stimulating an increase in cap-dependant translation which involves the recruitment of the RNA helicase, eIF-4A, to assist in unwinding mRNA secondary structures, SpdSyn mRNA will be translated with increased efficiency, promoting increased SpdSyn protein synthesis (147). Lastly, mTORC1 activation has been shown to increase the expression of the transcription factor c-Myc (148), with previous studies showing c-Myc's ability to upregulate the transcription of both Amd1 and SpdSyn (128, 129). Strengthening this hypothesis, in the current study, c-Myc expression was found to be elevated in *mdx* EDL (Fig. 29G and 30G) and SOL (Fig. 34G and 35G) muscles.

As to whether there is any benefit to having increased polyamine levels in *mdx* muscle, current evidence suggests that spermidine may play an essential role in protein synthesis and cell growth. Specifically, spermidine is the precursor molecule for the production of hypusine,

which is used for the unique post-translational modification of eukaryotic translation initiation factor 5a (eIF5a), referred to as hypusination (149). Importantly, the inhibition of eIF5A hypusination in cultured muscle cells has been shown to inhibit protein synthesis rates, demonstrating that spermidine has an indirect impact on protein synthesis (150). This is important because rates of protein synthesis are known to be elevated in *mdx* skeletal muscle (50, 151), presumably due to increased rates of protein turnover with the cycles of damage and regeneration. As such, the increased expression of SpdSyn and elevated spermidine content in DMD muscles would assist in enabling increased rates of protein turnover.

Intriguingly, the expression of polyamine enzyme, Sat1, was decreased in *mdx* SOL samples compared to the WT SOL muscles. Sat1 expression is regulated, in part, by polyamine levels (152). Specifically, when polyamine levels are elevated, Sat1 transcription and mRNA translation are increased (152). Conversely, decreased polyamine levels result in decreased Sat1 expression (152). These data suggest the possibility that polyamine levels may be lower in the *mdx* SOL muscles compared to WT SOL muscles. This is unlikely, however, as the current study found increased Amd1 (Fig. 9B) and SpdSyn (Fig. 9C) expression levels in *mdx* SOL muscles, suggesting that polyamine levels would be increased. Another potential option is that Sat1 expression is dysregulated and/or independent of polyamine levels in *mdx* SOL muscles. As such, a decrease in Sat1 expression could lead to an accumulation of polyamines due to decreased polyamine removal of spermidine and spermine. To further explore these possibilities, future studies would need to quantify polyamine levels within *mdx* SOL muscles.

Interestingly, spermidine supplementation had no effect on the expression of any of the polyamine pathway enzymes in either WT or *mdx* EDL (Fig. 8) and SOL (Fig. 9) muscles. These data could indicate that polyamine enzyme expression was not responsive to changes in spermidine levels. This seems unlikely, however, as Sat1 expression is known to be regulated by polyamine levels (152), and Amd1 expression is known to be negatively regulated by spermine (derived from its precursor spermidine) (153).

Another possibility is that the supplemented spermidine was rapidly metabolized/removed prior to impacting the expression of polyamine pathway enzymes, or it was unable to be transported into the muscles. Indeed, this current study provides no evidence that spermidine supplementation had any impact on WT skeletal muscles. Nonetheless, spermidine supplementation did result in changes to *mdx* skeletal muscle function, health, and both MAP1S and 4EBP1 expression, suggesting that the supplemented spermidine was able to at least impact *mdx* muscle. Potentially *mdx* skeletal muscle have greater levels of polyamine transporters to allow for increased uptake of exogenous spermidine compared to WT skeletal muscle. Clearly, further studies are required to investigate these possibilities more thoroughly.

Overall, these results show the novel findings that Amd1 and SpdSyn levels are upregulated in EDL and SOL *mdx* muscles compared to EDL and SOL WT muscles, likely due to elevated mTORC1 signalling. This study also showed a muscle/fibre-type specific difference with Sat1 being downregulated in *mdx* SOL, but not *mdx* EDL muscles. Future studies are required to correlate differences in polyamine enzymes with polyamine content in both WT and *mdx* muscle. Lastly, future studies are required to investigate whether exogenous spermidine is able to be taken up by WT and *mdx* muscles, and whether the differences in polyamine enzyme expression in *mdx* muscles is a beneficial adaptation or if they could play a role in the DMD pathology.

13. The effect of spermidine supplementation on body weight, muscle force output and fatigue

The activation of autophagy in *mdx* skeletal muscle, via the rapamycin-induced inhibition of mTORC1, has been shown to improve *mdx* muscle health and force production (95). Recently, supplementation with 3mM spermidine in drinking water was shown to activate autophagy and improve muscle health in a collagen VI-null myopathy mouse model (138). This study concluded that: “The beneficial effects of spermidine, together with it being easy to administer and the lack of overt side effects, open the field for the design of novel nutraceutical strategies for the treatment of muscle diseases characterized by autophagy impairment” (138). Given

the strong evidence that autophagy is impaired in DMD muscle (89), a major aim of this thesis was to examine whether spermidine supplementation could improve overall muscle health and function of *mdx* mouse muscles. To achieve this, 3-week-old mice were supplemented with spermidine (3mM) for 13 weeks (discussed in methods 5.1) and weighed each week until the end point when EDL and SOL muscles were dissected, weighted and subjected to *ex vivo* muscle function studies.

Spermidine supplemented and water control WT (Fig. 12A) and *mdx* muscles (Fig. 12B) showed no difference in level of water consumption within each week (Fig. 12C). This infers that all mice ingested similar amounts of water and supplemented mice consumed similar amounts of spermidine. As expected, from 3 to 6 weeks of age, body weight of *mdx* mice was shown to have an increased rate of body weight gain compared to WT mice (Fig. 11C). Spermidine supplementation had no effect on the rate of body weight gain of both *mdx* and WT mice, indicating no negative effect of spermidine intake on *mdx* phenotype (Fig. 11C).

Regarding muscle mass, as expected, the EDL (Fig. 13) and SOL (Fig. 17) muscles were heavier than those from WT mice. DMD skeletal muscle exhibits 'pseudohypertrophy' resulting in increased skeletal muscle weight, despite an impairment in muscle function and health (154). Specifically, skeletal muscle enlargement occurs when *mdx* muscle is progressively infiltrated with adipose and fibrotic tissue during the extensive muscle regeneration required, resulting in unhealthy tissue that negatively impacts both skeletal muscle function and health (154). As such, a decrease to muscle mass is commonly associated with improvement of the DMD phenotype (154).

Importantly, while spermidine supplementation had no effect on normalised muscle mass in WT muscle, it did result in a lowering of *mdx* EDL normalised muscle mass (Fig. 13B) and a strong trend ($p=0.057$) to reduce *mdx* SOL normalised muscle mass (Fig. 17B). These findings suggest that spermidine supplementation may have reduced the pseudohypertrophy of *mdx* skeletal muscle, which is indicative of an improved muscle health. One potential reason for this spermidine-induced decrease in *mdx* skeletal muscle mass is reduced muscle damage,

resulting in reduced requirement for muscle regeneration. Another potential reason could be a decrease in the level of oedema/water content within *mdx* skeletal muscle. The exact mechanisms, however, remain to be determined and would need to be addressed in future studies.

Consistent with the hypothesis that spermidine may have improved the phenotype of *mdx* muscles, spermidine supplementation led to an increase in tetanic specific force production in the *mdx* EDL muscles (Fig. 15B), although there was no effect on *mdx* SOL muscles (Fig. 19B). An obvious reason for improved function would be increased autophagy, thus reducing the accumulation of damaged components in the cell. However, as will be discussed in Section 15 and 16, while there was potential for increased initiation of autophagy, it did not appear that autophagy completion was altered by spermidine supplementation.

One potential reason for spermidine improving *mdx* EDL tetanic specific force is through the decrease of oxidative stress within the muscle. Although the exact mechanism remains to be determined, recent studies have shown that spermidine may have antioxidant effects, with spermidine decreasing ROS levels in both zebrafish (155) and transgenic plants (156). With levels of ROS production being elevated in both the *mdx* mouse model (64, 65), and human DMD muscle (66), spermidine supplementation may have decreased levels of oxidative stress, potentially improving muscle contractile function (61). The reason improvements may have been seen in the *mdx* EDL and not SOL muscles is that the fast-twitch fibres are more preferentially affected in dystrophic muscle, likely leading to more oxidative stress (157).

Another potential reason for spermidine to positively impact *mdx* EDL muscle force production is through improved calcium homeostasis and sarcolemmal stability. Data gathered from the *mdx* mouse has shown that damage/increased permeability of the dystrophin deficient sarcolemma results in abnormally elevated levels of resting intracellular calcium (53, 72-75). Furthermore, impaired calcium homeostasis can activate calpain proteases which result in breakdown of cytoplasmic, nuclear and membrane proteins, promoting chronic inflammation and cellular apoptosis within the muscle (78-80). As this increase in intracellular calcium is

decreased by the antioxidants, N-acetylcysteine (NAC) (76, 77) and melatonin (158), there is the potential for spermidine's antioxidant effect to positively impact intracellular calcium levels and sarcolemmal stability within *mdx* skeletal muscle. The exact mechanisms for this effect on tetanic specific force improvement in fast-twitch muscle would need to be addressed in future studies.

Lastly, spermidine supplementation had no effect on resistance to fatigue in either EDL (Fig. 16) or SOL (Fig. 20) muscles from both WT and *mdx* mice during prolonged, repeated, intense *ex vivo* stimulation. These results suggest that despite the improvement in specific force production of the EDL (Fig. 15B), spermidine supplementation is unlikely to have had an effect on energy metabolism, muscle membrane excitability or sarcoplasmic reticulum function during the repeated contraction.

In summary, this data shows that spermidine supplementation had a positive impact on dystrophic *mdx* skeletal muscle by reducing the mass of both fast (Fig. 13) and slow-twitch (Fig. 17) muscles, despite no apparent difference in body weight (Fig. 11). Furthermore, spermidine supplementation improved muscle force production in a muscle/fibre-type dependant mechanism, with the fast-twitch EDL (Fig. 15B), but not the slow-twitch SOL (Fig. 19B), muscle having an improved specific tetanic force production. Lastly, despite improving tetanic force production, spermidine supplementation had no impact on fatigue resistance in EDL (Fig. 16) or SOL (Fig. 20) muscles from either WT or *mdx* mice.

14. The effect of spermidine supplementation on muscle morphology

The DMD pathology is characterised by muscle fibres that are constantly undergoing repeated cycles of damage/repair, even in response to very mild contractions, resulting in chronic muscle inflammation (59, 82). The extent of damage and regeneration is typically assessed as the number of muscle fibres with centrally localised nuclei (in healthy muscle fibres, the myonuclei are located on the fibre periphery), with the presence of focal areas of overt damage/necrosis and infiltration of inflammatory cells (159). As such, if spermidine

supplementation had a beneficial effect on DMD pathology, we would expect to find a reduction in the number of muscle fibres with centralised nuclei, and a reduction in the relative area of 'unhealthy' tissue. Thus, a H&E stain was used to determine any changes in muscle fibre morphology in response to spermidine supplementation.

As expected, *mdx* EDL and SOL muscles had a markedly lower proportion of healthy muscle fibres (i.e. a higher number of muscles fibres with centrally localised myonuclei) compared to WT EDL and SOL muscles (Fig. 21 and 25). Furthermore, spermidine supplementation resulted in a significant increase in the proportion of healthy fibres in *mdx* EDL muscles (Fig. 21) but not in the *mdx* SOL muscles (Fig. 21), which is consistent with the improved specific force output observed in the EDL only (Fig. 15B). When the relative area of unhealthy tissue (i.e. overt regions of damage/necrosis and infiltration of inflammatory cells) was analysed, *mdx* EDL and SOL muscles (Fig. 22 and 26) had a higher proportion than in WT muscles. While, similar to the healthy tissue analysis, spermidine reduced the area of unhealthy tissue in the EDL (Fig. 22) muscles from *mdx* mice, but not SOL muscles (Fig. 26). These novel findings again suggest a muscle/fibre type-dependent action of spermidine on *mdx* muscles and are consistent with the spermidine-induced improvement on EDL normalised muscles mass (Fig. 13B) and specific force production (Fig. 15B).

This data suggests that spermidine supplementation may improve muscle health of fast-twitch DMD muscles, potentially due to fast-twitch fibres being predominantly affected in the DMD pathology compared to slow-twitch fibres (157). Furthermore, this data could indicate decreased levels of muscle inflammation and requirement for regeneration, potentially through the decrease in cytokine levels decreasing muscle oxidative stress. For example, the antioxidant NAC has shown to suppress mRNA expression of proinflammatory cytokines (160), with decreased cytokine expression also reducing rates of muscle chronic inflammation (84). As spermidine has previously shown antioxidant properties (155, 156), there is the potential for spermidine to be decreasing levels of chronic inflammation through the suppression of proinflammatory cytokines. Additionally, the expression of the regulator of

fibrosis TGF- β (161), has been shown to be sensitive to polyamine levels, with decreased levels of polyamines increasing TGF- β expression and promoting fibrosis (162). Therefore, spermidine supplementation could potentially decrease TGF- β expression, reducing levels of fibrosis in *mdx* EDL muscle (Fig. 22). Future studies are required to investigate spermidine's effect on immune cell infiltration, inflammatory cytokine levels and TGF- β expression in *mdx* skeletal muscle.

Lastly, we analysed whether spermidine had an effect on muscle fibre size in WT and *mdx* muscles. As *mdx* muscles undergo pseudohypertrophy (154) and chronic inflammation (81-83), it can be expected that *mdx* muscle fibres would be larger in cross-sectional area (CSA) when compared to muscle fibres from WT muscles. Indeed, this analysis found that *mdx* EDL (Fig. 23A) and SOL (Fig. 26A) muscle fibres were, on average, significantly larger than those from WT muscles. Interestingly, despite the improvement to levels of healthy muscle fibres (Fig. 21) and unhealthy muscle tissue (Fig. 22), spermidine supplementation had no effect on average fibre size (Fig. 23 and 26). This indicates that despite the spermidine-induced improvements to amount of healthy muscle fibres (Fig. 21) and unhealthy muscle tissue (Fig. 22) in *mdx* EDL muscles, it has no impact on muscle fibre size. This suggests that spermidine may have reduced the amount of non-muscle fibre cells/tissue within the whole *mdx* EDL muscle that contributes to pseudo hypertrophy (i.e. fibrotic and adipose tissue infiltration, chronic inflammation and oedema), thus reducing overall muscle mass and unhealthy areas, without impacting individual muscle fibre size. Further studies are now required to determine spermidine's therapeutic effect on fibrosis/fatty tissue, and the muscle/fibre type specific effect on *mdx* skeletal muscle.

In summary, this data shows that spermidine supplementation had an impact on dystrophic *mdx* EDL muscles by improving the number of healthy muscle fibres (Fig. 21) and decreasing unhealthy muscle tissue (Fig. 22). Furthermore, despite these morphological improvements, spermidine supplementation had no effect on muscle fibre size (Fig. 23A and 26A). Lastly, despite spermidine-induced improvements on *mdx* EDL morphology, no changes were

observed on *mdx* SOL muscles (Fig. 24 and 25), indicating a potential muscle/fibre-type specificity with spermidine treatment.

15. The effect of spermidine supplementation on key autophagy-related proteins and autophagy-regulating signalling pathways

3mM spermidine supplementation has been shown to upregulate autophagy in a collagen VI-null myopathy model of skeletal muscle dysfunction, indicated by an increase in the LC3B-II/LC3B-I ratio (138). As such we investigated whether the spermidine-induced improvements to *mdx* EDL muscle mass (Fig. 13B), tetanic force production (Fig. 15B) and tissue health (Fig. 22) might be associated with markers of increased autophagy. Spermidine has also been proposed to regulate the signalling of two key enzyme pathways that, in turn, regulate autophagy i.e. AMPK (99, 132, 133) and mTORC1 (121, 130). Furthermore, it has recently been shown that spermidine upregulates the expression of the autophagy-related protein, microtubule-associated protein 1S (MAP1S) (135, 136). To date, however, no study has investigated whether spermidine supplementation can impact these key proteins in WT or *mdx* skeletal muscle. Thus, 3-week-old WT and *mdx* mice were supplemented with 3mM spermidine for 13 weeks (discussed in methods 5.1), with the EDL and SOL muscles from these mice being analysed via Western blotting for changes in markers of autophagy, AMPK activation, mTORC1 signalling and MAP1S abundance.

This is the first study to compare MAP1S protein abundance between WT and *mdx* muscle, and whether spermidine can increase MAP1S expression. The results of this study found that MAP1S levels were upregulated in *mdx* EDL (Fig. 27) and SOL (Fig. 32) muscles compared to WT muscles. As MAP1S expression has been shown to be upregulated by spermidine (135, 136), this finding could be related to the previously reported higher levels of spermidine in *mdx* muscle (142, 143). Moreover, this genotypic difference in MAP1S protein abundance may help support the reported increased rate of autophagy initiation in *mdx* muscle (89), as MAP1S promotes autophagosome formation and degradation through its interaction with LC3B-I and

LC3B-II (134). Interestingly, spermidine supplementation induced a further upregulation of MAP1S expression in *mdx* EDL muscles (Fig. 27), with a trend ($p=0.0844$) for it to be increased by spermidine in *mdx* SOL muscles (Fig. 32). This finding is in agreement with the two previous non-muscle studies showing that spermidine upregulates MAP1S expression in models of liver fibrosis (135, 136). Importantly, spermidine was also shown to increase autophagy through a MAP1S-dependant mechanism (135). These data suggest that spermidine supplementation has the potential to have some impact on the regulation of autophagy in *mdx* skeletal muscle.

The enzyme, AMPK, is a known regulator of autophagy via its ability to inhibit mTORC1, and correspondingly increase ULK1 activity (132). Furthermore, activation of AMPK in the *mdx* diaphragm, via treatment of the AMPK stimulant AICAR, showed increased levels of autophagy activation, providing some evidence that activation of AMPK could be beneficial for *mdx* muscle (163). Importantly, a recent study found that spermidine may increase phosphorylated AMPK in ageing rat gastrocnemius (133). Thus, a marker of AMPK activation, AMPK Thr172 phosphorylation (p-AMPK), was examined in the supplemented *mdx* muscles and compared to non-supplemented muscle.

This analysis found that the abundance of p-AMPK was lower in *mdx* EDL muscles compared to WT muscles (Fig. 28A), but not in *mdx* SOL muscles (Fig. 33A). However, when EDL p-AMPK was normalised to total AMPK protein, this genotypic difference was lost (Fig. 29C). Nonetheless, this suggests that *mdx* EDL muscles have lower levels of the active form of AMPK (i.e. p-AMPK). This downregulation of p-AMPK in *mdx* EDL muscle potentially correlates with the reported elevation of mTORC1 activity in *mdx* skeletal muscle (89). Thus, lower p-AMPK in *mdx* EDL muscle may facilitate the inhibition of autophagy in *mdx* muscle.

Encouragingly, spermidine supplementation resulted in an upregulation of p-AMPK in *mdx* EDL muscles (Fig. 28A) compared to dystrophic controls, with no effect on p-AMPK in *mdx* SOL muscles (Fig. 33A). This data could suggest that the positive changes induced by spermidine on EDL muscle structure and function may, in part, be contributed to increased active p-AMPK, leading to downregulated mTORC1 signalling and activation of autophagy.

Moreover, this data further reinforces the hypothesis that the positive effect of spermidine is specific to fast-twitch muscles/fibres.

Another major regulator of autophagy is mTORC1 via its ability to inhibit the induction and elongation steps of autophagosome formation (99). As such, two common downstream targets of mTORC1, p70^{S6K1} Thr389 (p-p70^{S6K1}) and 4EBP1 Thr37/46 (p-4EBP1) phosphorylation, were probed as markers of mTORC1 activity. When p70^{S6K1} and 4EBP1 are phosphorylated, cap dependant translation is enhanced, resulting in upregulated rates of protein synthesis (100). In agreement with a previous study (89), there were higher levels of p-p70^{S6K1} (Fig. 29A), total p70^{S6K1} (Fig. 29AB) and the p-p70^{S6K1}/total p70^{S6K1} ratio (Fig. 29C) in *mdx* EDL muscles compared to WT EDL muscle, while p-p70^{S6K1} (Fig. 34A) and total p70^{S6K1} (Fig. 34B) were also elevated in *mdx* SOL muscles; however, spermidine supplementation had no effect on any of these in EDL (Fig. 29) or SOL (Fig. 34) muscles from WT or *mdx* mice.

Similar to p70^{S6K1}, p-4EBP1 and total 4EBP1 were significantly higher in *mdx* EDL (Fig. 30A and 30B) and SOL (Fig. 35A and 35B) groups compared to WT muscles; however, there were no difference in the p-4EBP1/total 4EBP1 ratio between the two strains (Fig. 30C and 35C). Regardless, an increase in the amount of p-4EBP1 should still facilitate elevated rates of cap-dependant translation, which is consistent with previous reports of elevated rates of protein synthesis in *mdx* muscle (50, 151, 164). Unexpectedly, spermidine supplementation induced an upregulation of both p-4EBP1 (Fig. 30A) and total 4EBP1 (Fig. 30B) in *mdx* EDL, but not in the *mdx* SOL muscle (Fig. 35A and 35B) compared to non-supplemented *mdx* controls, again suggesting a muscle/fibre type-specific effect of spermidine in *mdx* muscle.

Given that there was no corresponding spermidine-induced activation of p70^{S6K1} phosphorylation, it seems unlikely that spermidine would increase mTORC1 signalling to 4EBP1 alone. One possibility is that 4EBP1 was phosphorylated via a mTOR-independent pathway. Indeed, one study that used the different mTORC1 inhibitors (i.e. rapamycin, BEZ235, PP242 and WYE354) on the SW620 cancer cell line over a 6-hour time course found that all four mTORC1 inhibitors reduced p-p70^{S6K1} for the entire time course, while p-4EBP1

was only momentarily inhibited, with p-4EBP1 levels re-emerging to initial levels of phosphorylation throughout the remainder of the time course despite continued mTORC1 inhibition (165). Similar results were obtained using siRNA-mediated knockdown of mTORC1 (165). Although not in skeletal muscle, this study suggests the potential for 4EBP1 to be phosphorylated via an mTORC1-independent pathway during mTORC1 inhibition.

Another possible explanation for the spermidine-induced increase in p-4EBP1 and total 4EBP1 is that somehow spermidine activated the expression of the 4EBP1 gene leading to increased 4EBP1 protein, with the basal activity of mTORC1 continuing to phosphorylate this extra 4EBP1, resulting in no change to the p-4EBP1/total 4EBP1 ratio. Thus, in this scenario, the elevated p-4EBP1 is simply due to an increase in total 4EBP1 and not to an increase in mTORC1 signalling *per se*. Clearly, further studies are required to determine the cause of this spermidine-induced increase in p-4EBP1 and total 4EBP1, and whether this change confers some benefit to *mdx* EDL muscle function and/or structure.

The findings that spermidine supplementation increased autophagy-related markers, MAP1S (Fig. 27) and p-AMPK (Fig. 28A) in EDL muscles from *mdx* mice, without an apparent change in mTORC1 signalling, suggests that spermidine has the potential to activate autophagy within *mdx* EDL muscles. To assess this hypothesis more directly, levels of LC3B-I, LC3B-II, LC3B-II/LC3B-I ratio and p62 were analysed. While p62 expression was found to be elevated in *mdx* EDL (Fig. 31E) and SOL (Fig. 36E) muscles compared to WT muscles, spermidine had no effect on p62 expression in either muscle. In regard to LC3B, in EDL muscles there was no effect of genotypic or spermidine supplementation on LC3B-I (Fig. 31A), LC3B-II (Fig. 31B) or the ratio of LC3B-II/LC3B-I (Fig. 31C). In the SOL muscles, there was a genotype effect for LC3B-I (Fig. 36A) to be higher, and the ratio of LC3B-II/LC3B-I to be lower (Fig. 36C), in *mdx* muscles compared to WT muscles possibly indicating lower rates of autophagy in *mdx* SOL muscles; however, spermidine had no effect on either of these measures. These data suggest that spermidine supplementation does not impact rates of autophagy within *mdx* muscle, despite increased levels of MAP1S (Fig. 27) and p-AMPK (Fig. 28A) within *mdx* EDL muscles.

Consistent with the finding of no genotypic differences in LC3B-II/LC3B-I ratio in both EDL and SOL muscles, a previous study has also observed that LC3B-II/LC3B-I ratio was no different between *ad libitum* fed 16-week-old *mdx* mice and WT tibialis anterior (TA) muscles (166). However, after fasting for 24 h, the LC3B-II/LC3B-I ratio increased in WT but not in the *mdx* TA muscles, suggesting that levels of LC3B within *mdx* skeletal muscle can remain consistent despite an intervention that can alter rate of LC3B-I lipidation to form LC3B-II (166). This could explain the lack of changes observed in LC3B, despite the genotypic and spermidine-induced increases in MAP1S abundance in *mdx* skeletal muscle (Fig. 27 and 32), and the spermidine-induced increase in p-AMPK specifically in the *mdx* EDL (Fig. 28A).

Another potential explanation for the lack of genotypic and spermidine-supplemented differences in autophagy markers, is that the analysis of LC3B and p62 levels are static measures, at a particular timepoint, of a dynamic process. Specifically, as autophagy is a multi-stepped dynamic process, quantifying markers at a static timepoint may not be a true depiction of the process. For example, the formation of LC3B-II and increased expression of p62 may be matched by the degradation of these proteins during the final steps in the autophagosome, leading to no change in the steady state levels of these proteins. As such, a measure of flux through the autophagy pathway (i.e. 'autophagy flux') may be a more appropriate approach for detecting an increase in autophagy.

In summary, this data shows the novel finding of increase MAP1S protein abundance in both *mdx* EDL (Fig. 27) and SOL (Fig. 32) muscles compared to WT muscles, with spermidine supplementation further increasing MAP1S levels compared to non-supplemented *mdx* controls. Furthermore, AMPK phosphorylation was increased in spermidine supplemented *mdx* EDL muscles compared to non-supplemented *mdx* controls (Fig. 28A). Phosphorylated forms of p70^{S6k1} and 4EBP1 were upregulated genotypically in *mdx* EDL (Fig. 29 and 30) and SOL (Fig. 34 and 35) muscles, with spermidine supplementation further increasing the abundance of both p-4EBP1 (Fig. 30A) and total 4EBP1 (Fig. 30B) in *mdx* EDL muscles. Despite these, spermidine supplementation failed to induce changes in the static measures of

LC3B and p62 expression, suggesting no changes to rate of autophagy. A dynamic measure of LC3B and p62 with spermidine supplementation, however, is needed to confirm this conclusion.

16. The effect of spermidine supplementation on autophagy flux in WT and *mdx* skeletal muscle

In an attempt to obtain more 'dynamic' evidence of whether spermidine treatment was able to regulate autophagy *in vivo*, a colchicine-based autophagic flux assay was employed (107). The administration of colchicine leads to the inhibition of tubulin polymerisation and ultimately to the inhibition of autophagosome/lysosome fusion and the formation of autolysosomes (107). As a result, this leads to the build-up of autophagosomes (107). As there are no autolysosomes formed, there is no breakdown of the inner membrane of the autophagosome resulting in the accumulation of both LC3B-II and p62 (107). Because of this, if the autophagy process is upregulated by spermidine supplementation, there would be an exaggerated increase in LC3B-II and p62 in the presence of colchicine compared to non-supplemented controls (107). This allows for a 'dynamic/static' measure of autophagy when probing these markers via Western blotting.

To this end, 8-week-old mice were supplemented with spermidine for 7 days, and received either 0.4mg/kg IP injections colchicine or PBS on days 5 and 6 (Discussed in methods 5.2), after which the EDL and SOL muscles were analysed via Western blotting for differences in LC3B and p62 expression. This is the first study to have compared the 'dynamic/static' expression of LC3B and p62 in fast-twitch (EDL) and slow-twitch (SOL) muscles from WT and *mdx* mice utilising an autophagy flux study.

Importantly, compared to PBS treated controls, colchicine induced an accumulation of p62 in WT EDL muscles (Fig. 37), indicative of arrested autophagy due to decreased autolysosome formation. However, no colchicine effect was observed on p62 build-up in the WT SOL muscles (Fig. 39). These data are suggestive of a colchicine muscle/fibre-type preference for

the fast-twitch EDL muscle (139). Furthermore, there was a strong trend ($p=0.0833$) for colchicine increased p62 accumulation in *mdx* EDL muscles compared to PBS controls (Fig. 37), with no changes within *mdx* SOL muscles (Fig. 39). This indicates that colchicine's inhibitory effect on autolysosome formation is lower in *mdx* skeletal muscle whilst further highlighting colchicine's potential to influence fast-twitch muscle over slow-twitch muscle. Interestingly, despite previously showing a genotypic increase in p62 abundance in *mdx* EDL (Fig.31) and SOL (Fig. 36) muscles from 16-week-old mice, only the *mdx* SOL muscles exhibited this same genotypic p62 increase compared to WT SOL muscles in these 9-week-old mice (Fig. 39). This could indicate that the increase in p62 in the EDL is an age-dependant phenomenon in the *mdx* EDL muscles, perhaps due to the higher susceptibility to damage on the fast-twitch fibres (157). Importantly, there was no effect of spermidine supplementation on p62 accumulation in WT or *mdx* EDL (Fig. 37) and SOL (Fig. 39) muscles, further suggestive of no increased autophagy.

In regard to LC3B, a colchicine effect was observed in WT EDL muscles, with colchicine inducing an increase in LC3B-I and LC3B-II (but no significant increase in the LC3B-II/LC3B-I ratio) compared to muscles from the PBS treated WT control mice (Fig. 38A-C), further confirming the biological activity of the colchicine *in vivo*. Interestingly, despite no change in LC3B-I abundance in WT SOL muscles (Fig. 40A), a colchicine effect was observed with LC3B-II being increased by colchicine in WT SOL muscles compared to WT PBS controls (Fig. 40B), suggesting that WT SOL muscles are not completely unresponsive to the actions of colchicine. The potential for colchicine's inhibitory effect to be lower in *mdx* muscle was reaffirmed with no colchicine effect observed on LC3B-I and LC3B-II expression for both *mdx* EDL (Fig. 38A and 38B) and SOL (Fig. 40A and 40B) muscles. However, despite the lack of colchicine induced *mdx* LC3B expression, *mdx* EDL muscles showed a trend ($p=0.0781$) for colchicine-induced increase of LC3B-II/LC3B-I ratio (Fig. 38C) that *mdx* SOL muscles did not (Fig. 40C), further suggesting that fast-twitch muscles/fibres are more sensitive to colchicine than slow-twitch muscles/fibres, and that *mdx* muscles may be less sensitive to colchicine

than WT muscles. As colchicine binds and inhibits microtubule elongation through its binding to tubulin, disorganized microtubules with the *mdx* model may have the potential to inhibit the colchicine/tubulin formation, corresponding in lower responsiveness to colchicine within the *mdx* model (167). Future studies would be needed to confirm this however.

Interestingly, unlike our findings in 16-week-old mice (Fig. 31A), there was a main genotypic effect of LC3B-I expression, with *mdx* EDL muscles having higher levels than WT EDL muscles (Fig. 37A). This suggests that the relative difference in LC3B-I expression between *mdx* and WT EDL muscles change between 9 and 16 weeks of age (Fig. 31A). Furthermore, similar to the p62 data, no evidence was found that spermidine supplementation led to increased LC3B-I, LC3B-II or the LC3B-II/LC3B-I ratio, further suggesting that spermidine is unable to increase the *in vivo* rate of autophagy in EDL muscles from either WT or *mdx* mice (Fig. 38).

The lack of effect of spermidine supplementation stands in contrast to a recent study that found 3mM of spermidine in drinking water for 30 days increased LC3B-II expression in WT muscle and in muscles from collagen-VI null mice [see Suppl. Fig. 1A in (138)]. One potential reason for spermidine not impacting autophagy markers is the timeframes that both supplementation experiments were conducted in the current study compared to the 30 days of supplementation used in the collagen-VI null mouse study (138), suggesting that spermidine's influence on autophagy may be timepoint specific. As such, 7-day spermidine supplementation used for the autophagy flux assay may not have been long enough for spermidine to induce an upregulation autophagy, while a spermidine-induced activation of autophagy may have diminished after 13-week spermidine supplementation. As such, future studies could incorporate a time course to examine potential spermidine-induced changes to autophagy at multiple time points.

In summary, this data documents colchicine's ability to induce an accumulation of autophagy-related proteins in WT and *mdx* muscles. Colchicine has a more potent effect on WT than *mdx* muscle, and on fast-twitch rather than slow-twitch muscles. Importantly, spermidine

supplementation had no influence on LC3B or p62 abundance within *mdx* EDL and SOL muscles, suggesting no spermidine-induced changes to the rate of autophagy.

17. Limitations

In this study, spermidine supplementation was used as a potential therapeutic compound to improve *mdx* skeletal muscle structure and function. Furthermore, this study also examined genotypic differences in the expression of polyamine pathway enzymes between WT and *mdx* skeletal muscle. Despite identifying several novel findings that advance our understanding of the *mdx* genotype, as well as the potential for spermidine supplementation to effect autophagy in WT and *mdx* muscle, this study has some limitations. One major limitation is that polyamine levels were not quantified in WT or *mdx* EDL and SOL muscles, with and without spermidine supplementation. This measurement would have enabled an analysis of whether the spermidine supplementation model was sufficient to increase steady state intra-muscular spermidine content, and spermidine content to be correlated with key mechanistic changes identified in *mdx* skeletal muscle. We did have discussion with Metabolomics Australia to perform this analysis on the EDL and SOL muscles that were specifically collected for this purpose, however, they could not guarantee that they could detect all required polyamine species and their precursor molecules and degradation products. As such, this metabolomic analysis was postponed until the method can be further refined.

Another limitation of this study is the use of a single age of 16-week-old mice. With the variation of autophagy-related proteins documented at different age groups of *mdx* mice, replicating this experiment in younger and older age groups could help to further define the spermidine-induced mechanistic changes within *mdx* skeletal muscle.

18. Future Directions

Because of the encouraging novel findings from this study, there are different potential studies that can be completed to further elaborate on the genotypic and spermidine-induced changes observed. Some potential future studies include:

- Use of an mTORC1 inhibitor, such as rapamycin, with *mdx* mice to assess whether Amd1 and SpdSyn expression is inhibited to strengthen the hypothesis that expression of Amd1 and SpdSyn are mTORC1-dependant.
- Quantification of polyamine levels in WT and *mdx* muscles to assess whether spermidine-supplementation altered the polyamine levels in WT and/or *mdx* muscle
- Further investigation for mechanistic changes correlating with both spermidine-induced decreases in *mdx* skeletal muscle mass and improved *mdx* EDL tetanic specific forces.
- Investigate spermidine-induced effects on immune cell infiltration, inflammatory cytokine levels and TGB- β expression in *mdx* skeletal muscle which could influence the improved *mdx* EDL morphology.
- Undertake an autophagy flux on *mdx* EDL and SOL muscles after 30-day's of spermidine supplementation at the current and higher doses of spermidine, to assess potential limiting effects on autophagy proteins such as LC3B and p62.
- Examine other muscles, such as the diaphragm, which is more severely affected within DMD pathology, to further define the polyamine pathway enzymes in different age and muscle groups, and the effect of spermidine supplementation.
- Examine different *mdx* hindlimb muscles of both fast-twitch and slow-twitch composition to further define whether differences observed with spermidine supplementation are muscle and/or fibre-type specific.
- Examine the effect of knockdown or overexpressing polyamine enzymes to determine their function in *mdx* muscles. For example, the knockdown of Amd1 and/or SpdSyn using adeno-associated viral (AAV) vectors encoding inhibitory RNAs could help

answer the question of whether the upregulation of the proteins is beneficial or detrimental to the DMD pathology in fast or slow-twitch muscles. Alternatively, increasing the expression of Sat1, which was reduced in *mdx* SOL muscles, will identify the molecular consequence of this genotypic difference.

19. Conclusion

This is the first study to examine differences in the expression of polyamine pathway enzymes between WT and *mdx* EDL and SOL muscles, basally and with spermidine supplementation. Our findings show the novel findings that various polyamine pathway enzyme levels differ between both genotype and muscle fibre-type, however, spermidine supplementation fails to induce further changes in polyamine enzyme abundance. This is also the first study to undergo spermidine-supplementation within the *mdx* mouse, resulting in positive improvements to *mdx* skeletal muscle tetanic specific forces and muscle morphology. Furthermore, we have documented the novel findings that spermidine supplementation induces changes to MAP1S abundance, AMPK phosphorylation and both phosphorylated and total 4EBP1 within *mdx* skeletal muscle. Moreover, these beneficial differences appear unlikely to be due to spermidine-induced changes in rates of autophagy. Overall, these novel data provide further evidence of a dynamic regulation of polyamine metabolism in skeletal muscle, and that exogenous spermidine induces beneficial improvements to *mdx* skeletal muscle highlighting, the potential for spermidine as a non-toxic long-term treatment for those with DMD.

20. References

1. Janssen I, Heymsfield SB, Wang ZM, Ross R. Skeletal muscle mass and distribution in 468 men and women aged 18-88 yr. *J Appl Physiol* (1985). 2000;89(1):81-8.
2. Izumiya Y, Hopkins T, Morris C, Sato K, Zeng L, Viereck J, et al. Fast/Glycolytic muscle fiber growth reduces fat mass and improves metabolic parameters in obese mice. *Cell Metab*. 2008;7(2):159-72.

3. Lynch GS. Tackling Australia's future health problems: developing strategies to combat sarcopenia – age-related muscle wasting and weakness. *Internal Medicine Journal*. 2004;34(5):294-6.
4. Uttley L, Carlton J, Woods HB, Brazier J. A review of quality of life themes in Duchenne muscular dystrophy for patients and carers. *Health Qual Life Outcomes*. 2018;16(1):237.
5. Landfeldt E, Edström J, Buccella F, Kirschner J, Lochmüller H. Duchenne muscular dystrophy and caregiver burden: a systematic review. *Dev Med Child Neurol*. 2018;60(10):987-96.
6. Landfeldt E, Lindgren P, Bell CF, Schmitt C, Guglieri M, Straub V, et al. The burden of Duchenne muscular dystrophy: an international, cross-sectional study. *Neurology*. 2014;83(6):529-36.
7. Thompson LV. Age-related muscle dysfunction. *Exp Gerontol*. 2009;44(1-2):106-11.
8. Jokl P, Konstadt S. The effect of limb immobilization on muscle function and protein composition. *Clin Orthop Relat Res*. 1983(174):222-9.
9. Bianchi L, Volpato S. Muscle dysfunction in type 2 diabetes: a major threat to patient's mobility and independence. *Acta Diabetol*. 2016;53(6):879-89.
10. Straight CR, Toth MJ, Miller MS. Current perspectives on obesity and skeletal muscle contractile function in older adults. *Journal of Applied Physiology*. 2021;130(1):10-6.
11. Robinson-Papp J, Simpson DM. Neuromuscular diseases associated with HIV-1 infection. *Muscle Nerve*. 2009;40(6):1043-53.
12. Loeffler JP, Picchiarelli G, Dupuis L, Gonzalez De Aguilar JL. The Role of Skeletal Muscle in Amyotrophic Lateral Sclerosis. *Brain Pathol*. 2016;26(2):227-36.
13. Duan D, Goemans N, Takeda Si, Mercuri E, Aartsma-Rus A. Duchenne muscular dystrophy. *Nature Reviews Disease Primers*. 2021;7(1):13.
14. Bulfield G, Siller WG, Wight PA, Moore KJ. X chromosome-linked muscular dystrophy (mdx) in the mouse. *Proc Natl Acad Sci U S A*. 1984;81(4):1189-92.
15. McGreevy JW, Hakim CH, McIntosh MA, Duan D. Animal models of Duchenne muscular dystrophy: from basic mechanisms to gene therapy. *Dis Model Mech*. 2015;8(3):195-213.
16. Fairclough RJ, Bareja A, Davies KE. Progress in therapy for Duchenne muscular dystrophy. *Exp Physiol*. 2011;96(11):1101-13.
17. Gao QQ, McNally EM. The Dystrophin Complex: Structure, Function, and Implications for Therapy. *Compr Physiol*. 2015;5(3):1223-39.
18. Nelson DaM, Ervasti JM. Structural Proteins | Dystrophin: A Multifaceted Protein Critical for Muscle Health. In: Jez J, editor. *Encyclopedia of Biological Chemistry III (Third Edition)*. Oxford: Elsevier; 2021. p. 625-38.

19. Koenig M, Monaco AP, Kunkel LM. The complete sequence of dystrophin predicts a rod-shaped cytoskeletal protein. *Cell*. 1988;53(2):219-28.
20. Suzuki A, Yoshida M, Hayashi K, Mizuno Y, Hagiwara Y, Ozawa E. Molecular organization at the glycoprotein-complex-binding site of dystrophin. Three dystrophin-associated proteins bind directly to the carboxy-terminal portion of dystrophin. *Eur J Biochem*. 1994;220(2):283-92.
21. Ibraghimov-Beskrovnaya O, Ervasti JM, Leveille CJ, Slaughter CA, Sernett SW, Campbell KP. Primary structure of dystrophin-associated glycoproteins linking dystrophin to the extracellular matrix. *Nature*. 1992;355(6362):696-702.
22. Zhao J, Kodippili K, Yue Y, Hakim CH, Wasala L, Pan X, et al. Dystrophin contains multiple independent membrane-binding domains. *Hum Mol Genet*. 2016;25(17):3647-53.
23. Blake DJ, Weir A, Newey SE, Davies KE. Function and Genetics of Dystrophin and Dystrophin-Related Proteins in Muscle. *Physiological Reviews*. 2002;82(2):291-329.
24. Straub V, Rafael JA, Chamberlain JS, Campbell KP. Animal models for muscular dystrophy show different patterns of sarcolemmal disruption. *J Cell Biol*. 1997;139(2):375-85.
25. Vilquin JT, Brussee V, Asselin I, Kinoshita I, Gingras M, Tremblay JP. Evidence of mdx mouse skeletal muscle fragility in vivo by eccentric running exercise. *Muscle Nerve*. 1998;21(5):567-76.
26. Lawler JM. Exacerbation of pathology by oxidative stress in respiratory and locomotor muscles with Duchenne muscular dystrophy. *J Physiol*. 2011;589(Pt 9):2161-70.
27. Zhou L, Lu H. Targeting fibrosis in Duchenne muscular dystrophy. *J Neuropathol Exp Neurol*. 2010;69(8):771-6.
28. Li W, Zheng Y, Zhang W, Wang Z, Xiao J, Yuan Y. Progression and variation of fatty infiltration of the thigh muscles in Duchenne muscular dystrophy, a muscle magnetic resonance imaging study. *Neuromuscul Disord*. 2015;25(5):375-80.
29. Lo Mauro A, Aliverti A. Physiology of respiratory disturbances in muscular dystrophies. *Breathe (Sheff)*. 2016;12(4):318-27.
30. Allen J. Pulmonary complications of neuromuscular disease: a respiratory mechanics perspective. *Paediatr Respir Rev*. 2010;11(1):18-23.
31. Passamano L, Taglia A, Palladino A, Viggiano E, D'Ambrosio P, Scutifero M, et al. Improvement of survival in Duchenne Muscular Dystrophy: retrospective analysis of 835 patients. *Acta Myol*. 2012;31(2):121-5.
32. Matthews E, Brassington R, Kuntzer T, Jichi F, Manzur AY. Corticosteroids for the treatment of Duchenne muscular dystrophy. *Cochrane Database of Systematic Reviews*. 2016(5).
33. Manzur AY, Kuntzer T, Pike M, Swan A. Glucocorticoid corticosteroids for Duchenne muscular dystrophy. *Cochrane Database of Systematic Reviews*. 2004(2).

34. Bylo M, Farewell R, Coppentrath VA, Yogaratnam D. A Review of Deflazacort for Patients With Duchenne Muscular Dystrophy. *Ann Pharmacother*. 2020;54(8):788-94.
 35. Beenakker EA, Fock JM, Van Tol MJ, Maurits NM, Koopman HM, Brouwer OF, et al. Intermittent prednisone therapy in Duchenne muscular dystrophy: a randomized controlled trial. *Arch Neurol*. 2005;62(1):128-32.
 36. Dubow J, Meyer J. Corticosteroids in Duchenne Muscular Dystrophy—A Deflazacort Review. *US Neurology*. 2016.
 37. Gloss D, Moxley RT, 3rd, Ashwal S, Oskoui M. Practice guideline update summary: Corticosteroid treatment of Duchenne muscular dystrophy: Report of the Guideline Development Subcommittee of the American Academy of Neurology. *Neurology*. 2016;86(5):465-72.
 38. Le Guiner C, Servais L, Montus M, Larcher T, Fraysse B, Moullec S, et al. Long-term microdystrophin gene therapy is effective in a canine model of Duchenne muscular dystrophy. *Nature Communications*. 2017;8(1):16105.
 39. Duan D. Systemic AAV Micro-dystrophin Gene Therapy for Duchenne Muscular Dystrophy. *Molecular therapy : the journal of the American Society of Gene Therapy*. 2018;26(10):2337-56.
 40. Al-Zaidy S, Rodino-Klapac L, Mendell JR. Gene therapy for muscular dystrophy: moving the field forward. *Pediatr Neurol*. 2014;51(5):607-18.
 41. Wagner KR, Hamed S, Hadley DW, Gropman AL, Burstein AH, Escolar DM, et al. Gentamicin treatment of Duchenne and Becker muscular dystrophy due to nonsense mutations. *Ann Neurol*. 2001;49(6):706-11.
 42. Politano L, Nigro G, Nigro V, Piluso G, Papparella S, Paciello O, et al. Gentamicin administration in Duchenne patients with premature stop codon. Preliminary results. *Acta Myol*. 2003;22(1):15-21.
 43. Flanigan KM, Dunn DM, von Niederhausern A, Soltanzadeh P, Gappmaier E, Howard MT, et al. Mutational spectrum of DMD mutations in dystrophinopathy patients: application of modern diagnostic techniques to a large cohort. *Hum Mutat*. 2009;30(12):1657-66.
 44. Darras BT, Urion DK, Ghosh PS. Dystrophinopathies. In: Adam MP, Ardinger HH, Pagon RA, Wallace SE, Bean LJH, Mirzaa G, et al., editors. *GeneReviews*(®). Seattle (WA): University of Washington, Seattle
- Copyright © 1993-2021, University of Washington, Seattle. GeneReviews is a registered trademark of the University of Washington, Seattle. All rights reserved.; 1993.
45. Lee HL, Dougherty JP. Pharmaceutical therapies to recode nonsense mutations in inherited diseases. *Pharmacology & therapeutics*. 2012;136(2):227-66.

46. Dent KM, Dunn DM, von Niederhausern AC, Aoyagi AT, Kerr L, Bromberg MB, et al. Improved molecular diagnosis of dystrophinopathies in an unselected clinical cohort. *Am J Med Genet A*. 2005;134(3):295-8.
47. Flanigan KM, von Niederhausern A, Dunn DM, Alder J, Mendell JR, Weiss RB. Rapid direct sequence analysis of the dystrophin gene. *Am J Hum Genet*. 2003;72(4):931-9.
48. Mendell JR, Buzin CH, Feng J, Yan J, Serrano C, Sangani DS, et al. Diagnosis of Duchenne dystrophy by enhanced detection of small mutations. *Neurology*. 2001;57(4):645-50.
49. Beartiz A. Cost-effectiveness análisis of microdystrophin: a novel gene therapy for duchenne muscular dystrophy. Barcelona School of Management. 2020.
50. Radley-Crabb HG, Marini JC, Sosa HA, Castillo LI, Grounds MD, Fiorotto ML. Dystropathology increases energy expenditure and protein turnover in the mdx mouse model of duchenne muscular dystrophy. *PLoS One*. 2014;9(2):e89277.
51. Dudley RW, Danelou G, Govindaraju K, Lands L, Eidelman DE, Petrof BJ. Sarcolemmal damage in dystrophin deficiency is modulated by synergistic interactions between mechanical and oxidative/nitrosative stresses. *Am J Pathol*. 2006;168(4):1276-87; quiz 404-5.
52. Petrillo S, Pelosi L, Piemonte F, Travaglini L, Forcina L, Catteruccia M, et al. Oxidative stress in Duchenne muscular dystrophy: focus on the NRF2 redox pathway. *Hum Mol Genet*. 2017;26(14):2781-90.
53. Imbert N, Cognard C, Duport G, Guillou C, Raymond G. Abnormal calcium homeostasis in Duchenne muscular dystrophy myotubes contracting in vitro. *Cell Calcium*. 1995;18(3):177-86.
54. Mosqueira M, Brinkmeier H, Jaimovich E. Editorial: Calcium Homeostasis in Skeletal Muscle Function, Plasticity, and Disease. *Frontiers in Physiology*. 2021;12(369).
55. Vallejo-Illarramendi A, Toral-Ojeda I, Aldanondo G, López de Munain A. Dysregulation of calcium homeostasis in muscular dystrophies. *Expert Rev Mol Med*. 2014;16:e16.
56. Rosenberg AS, Puig M, Nagaraju K, Hoffman EP, Villalta SA, Rao VA, et al. Immune-mediated pathology in Duchenne muscular dystrophy. *Sci Transl Med*. 2015;7(299):299rv4.
57. Abou-Khalil R, Yang F, Mortreux M, Lieu S, Yu YY, Wurmser M, et al. Delayed bone regeneration is linked to chronic inflammation in murine muscular dystrophy. *J Bone Miner Res*. 2014;29(2):304-15.
58. Miyatake S, Shimizu-Motohashi Y, Takeda S, Aoki Y. Anti-inflammatory drugs for Duchenne muscular dystrophy: focus on skeletal muscle-releasing factors. *Drug Des Devel Ther*. 2016;10:2745-58.

59. Nitahara-Kasahara Y, Takeda Si, Okada T. Inflammatory predisposition predicts disease phenotypes in muscular dystrophy. *Inflammation and Regeneration*. 2016;36(1):14.
60. Schieber M, Chandel NS. ROS function in redox signaling and oxidative stress. *Curr Biol*. 2014;24(10):R453-62.
61. Powers SK, Ji LL, Kavazis AN, Jackson MJ. Reactive oxygen species: impact on skeletal muscle. *Compr Physiol*. 2011;1(2):941-69.
62. Steinbacher P, Eckl P. Impact of oxidative stress on exercising skeletal muscle. *Biomolecules*. 2015;5(2):356-77.
63. Terrill JR, Radley-Crabb HG, Iwasaki T, Lemckert FA, Arthur PG, Grounds MD. Oxidative stress and pathology in muscular dystrophies: focus on protein thiol oxidation and dysferlinopathies. *The FEBS Journal*. 2013;280(17):4149-64.
64. Dudley RW, Khairallah M, Mohammed S, Lands L, Des Rosiers C, Petrof BJ. Dynamic responses of the glutathione system to acute oxidative stress in dystrophic mouse (mdx) muscles. *Am J Physiol Regul Integr Comp Physiol*. 2006;291(3):R704-10.
65. Kaczor JJ, Hall JE, Payne E, Tarnopolsky MA. Low intensity training decreases markers of oxidative stress in skeletal muscle of mdx mice. *Free Radic Biol Med*. 2007;43(1):145-54.
66. Renjini R, Gayathri N, Nalini A, Srinivas Bharath MM. Oxidative damage in muscular dystrophy correlates with the severity of the pathology: role of glutathione metabolism. *Neurochem Res*. 2012;37(4):885-98.
67. Rando TA, Disatnik MH, Yu Y, Franco A. Muscle cells from mdx mice have an increased susceptibility to oxidative stress. *Neuromuscul Disord*. 1998;8(1):14-21.
68. Murray BE, Froemming GR, Maguire PB, Ohlendieck K. Excitation-contraction-relaxation cycle: role of Ca²⁺-regulatory membrane proteins in normal, stimulated and pathological skeletal muscle (review). *Int J Mol Med*. 1998;1(4):677-87.
69. Andersson DC, Betzenhauser MJ, Reiken S, Meli AC, Umanskaya A, Xie W, et al. Ryanodine receptor oxidation causes intracellular calcium leak and muscle weakness in aging. *Cell Metab*. 2011;14(2):196-207.
70. Agrawal A, Suryakumar G, Rathor R. Role of defective Ca⁽²⁺⁾ signaling in skeletal muscle weakness: Pharmacological implications. *J Cell Commun Signal*. 2018;12(4):645-59.
71. Petrof BJ, Shrager JB, Stedman HH, Kelly AM, Sweeney HL. Dystrophin protects the sarcolemma from stresses developed during muscle contraction. *Proc Natl Acad Sci U S A*. 1993;90(8):3710-4.
72. Yeung EW, Whitehead NP, Suchyna TM, Gottlieb PA, Sachs F, Allen DG. Effects of stretch-activated channel blockers on [Ca²⁺]_i and muscle damage in the mdx mouse. *J Physiol*. 2005;562(Pt 2):367-80.

73. Ruegg UT, Nicolas-Métral V, Challet C, Bernard-Hélary K, Dorchies OM, Wagner S, et al. Pharmacological control of cellular calcium handling in dystrophic skeletal muscle. *Neuromuscul Disord.* 2002;12 Suppl 1:S155-61.
74. Allen DG, Gervasio OL, Yeung EW, Whitehead NP. Calcium and the damage pathways in muscular dystrophy. *Can J Physiol Pharmacol.* 2010;88(2):83-91.
75. Turner PR, Westwood T, Regen CM, Steinhardt RA. Increased protein degradation results from elevated free calcium levels found in muscle from mdx mice. *Nature.* 1988;335(6192):735-8.
76. Burns DP, Drummond SE, Bolger D, Coiscaud A, Murphy KH, Edge D, et al. N-acetylcysteine Decreases Fibrosis and Increases Force-Generating Capacity of mdx Diaphragm. *Antioxidants (Basel).* 2019;8(12).
77. Burns DP, Drummond SE, Bolger D, Murphy KH, Coiscaud AP, Edge D, et al. N-Acetyl cysteine improves dystrophic (mdx) mouse diaphragm muscle quality and strength. *The FASEB Journal.* 2019;33(S1):843.12-.12.
78. Tidball JG, Spencer MJ. Calpains and muscular dystrophies. *Int J Biochem Cell Biol.* 2000;32(1):1-5.
79. Alderton JM, Steinhardt RA. How calcium influx through calcium leak channels is responsible for the elevated levels of calcium-dependent proteolysis in dystrophic myotubes. *Trends Cardiovasc Med.* 2000;10(6):268-72.
80. Berchtold MW, Brinkmeier H, Müntener M. Calcium ion in skeletal muscle: its crucial role for muscle function, plasticity, and disease. *Physiol Rev.* 2000;80(3):1215-65.
81. Cruz-Guzmán Odel R, Rodríguez-Cruz M, Escobar Cedillo RE. Systemic Inflammation in Duchenne Muscular Dystrophy: Association with Muscle Function and Nutritional Status. *Biomed Res Int.* 2015;2015:891972.
82. De Paepe B, De Bleecker JL. Cytokines and chemokines as regulators of skeletal muscle inflammation: presenting the case of Duchenne muscular dystrophy. *Mediators Inflamm.* 2013;2013:540370.
83. De Pasquale L, D'Amico A, Verardo M, Petrini S, Bertini E, De Benedetti F. Increased muscle expression of interleukin-17 in Duchenne muscular dystrophy. *Neurology.* 2012;78(17):1309-14.
84. Yang W, Hu P. Skeletal muscle regeneration is modulated by inflammation. *J Orthop Translat.* 2018;13:25-32.
85. Deconinck N, Dan B. Pathophysiology of duchenne muscular dystrophy: current hypotheses. *Pediatr Neurol.* 2007;36(1):1-7.
86. Wattin M, Gaweda L, Muller P, Baritaud M, Scholtes C, Lozano C, et al. Modulation of Protein Quality Control and Proteasome to Autophagy Switch in Immortalized Myoblasts from Duchenne Muscular Dystrophy Patients. *Int J Mol Sci.* 2018;19(1).

87. Herczenik E, Gebbink MF. Molecular and cellular aspects of protein misfolding and disease. *Faseb j.* 2008;22(7):2115-33.
88. Sandri M. Autophagy in skeletal muscle. *FEBS Lett.* 2010;584(7):1411-6.
89. De Palma C, Morisi F, Cheli S, Pambianco S, Cappello V, Vezzoli M, et al. Autophagy as a new therapeutic target in Duchenne muscular dystrophy. *Cell Death Dis.* 2012;3(11):e418.
90. Glick D, Barth S, Macleod KF. Autophagy: cellular and molecular mechanisms. *J Pathol.* 2010;221(1):3-12.
91. Tyler JK, Johnson JE. The role of autophagy in the regulation of yeast life span. *Ann N Y Acad Sci.* 2018;1418(1):31-43.
92. Hars ES, Qi H, Ryazanov AG, Jin S, Cai L, Hu C, et al. Autophagy regulates ageing in *C. elegans*. *Autophagy.* 2007;3(2):93-5.
93. Maruzs T, Simon-Vecsei Z, Kiss V, Csizmadia T, Juhász G. On the Fly: Recent Progress on Autophagy and Aging in *Drosophila*. *Frontiers in Cell and Developmental Biology.* 2019;7(140).
94. Pyo JO, Yoo SM, Ahn HH, Nah J, Hong SH, Kam TI, et al. Overexpression of Atg5 in mice activates autophagy and extends lifespan. *Nat Commun.* 2013;4:2300.
95. Bibee KP, Cheng YJ, Ching JK, Marsh JN, Li AJ, Keeling RM, et al. Rapamycin nanoparticles target defective autophagy in muscular dystrophy to enhance both strength and cardiac function. *Faseb j.* 2014;28(5):2047-61.
96. Madeo F, Zimmermann A, Maiuri MC, Kroemer G. Essential role for autophagy in life span extension. *J Clin Invest.* 2015;125(1):85-93.
97. Wang C, Wang H, Zhang D, Luo W, Liu R, Xu D, et al. Phosphorylation of ULK1 affects autophagosome fusion and links chaperone-mediated autophagy to macroautophagy. *Nature Communications.* 2018;9(1):3492.
98. Ganley IG, Lam du H, Wang J, Ding X, Chen S, Jiang X. ULK1.ATG13.FIP200 complex mediates mTOR signaling and is essential for autophagy. *J Biol Chem.* 2009;284(18):12297-305.
99. Kim J, Kundu M, Viollet B, Guan K-L. AMPK and mTOR regulate autophagy through direct phosphorylation of Ulk1. *Nature Cell Biology.* 2011;13(2):132-41.
100. Saxton RA, Sabatini DM. mTOR Signaling in Growth, Metabolism, and Disease. *Cell.* 2017;168(6):960-76.
101. Brier LW, Ge L, Stjepanovic G, Thelen AM, Hurley JH, Schekman R. Regulation of LC3 lipidation by the autophagy-specific class III phosphatidylinositol-3 kinase complex. *Mol Biol Cell.* 2019;30(9):1098-107.

102. Kihara A, Noda T, Ishihara N, Ohsumi Y. Two distinct Vps34 phosphatidylinositol 3-kinase complexes function in autophagy and carboxypeptidase Y sorting in *Saccharomyces cerevisiae*. *J Cell Biol.* 2001;152(3):519-30.
103. Hurley JH, Young LN. Mechanisms of Autophagy Initiation. *Annu Rev Biochem.* 2017;86:225-44.
104. Itakura E, Kishi C, Inoue K, Mizushima N. Beclin 1 forms two distinct phosphatidylinositol 3-kinase complexes with mammalian Atg14 and UVRAG. *Mol Biol Cell.* 2008;19(12):5360-72.
105. Bento CF, Renna M, Ghislat G, Puri C, Ashkenazi A, Vicinanza M, et al. Mammalian Autophagy: How Does It Work? *Annu Rev Biochem.* 2016;85:685-713.
106. Runwal G, Stamatakou E, Siddiqi FH, Puri C, Zhu Y, Rubinsztein DC. LC3-positive structures are prominent in autophagy-deficient cells. *Scientific Reports.* 2019;9(1):10147.
107. Ju JS, Varadhachary AS, Miller SE, Weihl CC. Quantitation of "autophagic flux" in mature skeletal muscle. *Autophagy.* 2010;6(7):929-35.
108. Liu WJ, Ye L, Huang WF, Guo LJ, Xu ZG, Wu HL, et al. p62 links the autophagy pathway and the ubiquitin–proteasome system upon ubiquitinated protein degradation. *Cellular & Molecular Biology Letters.* 2016;21(1):29.
109. Rusten TE, Stenmark H. p62, an autophagy hero or culprit? *Nature Cell Biology.* 2010;12(3):207-9.
110. Jiang P, Nishimura T, Sakamaki Y, Itakura E, Hatta T, Natsume T, et al. The HOPS complex mediates autophagosome-lysosome fusion through interaction with syntaxin 17. *Mol Biol Cell.* 2014;25(8):1327-37.
111. McEwan DG, Popovic D, Gubas A, Terawaki S, Suzuki H, Stadel D, et al. PLEKHM1 regulates autophagosome-lysosome fusion through HOPS complex and LC3/GABARAP proteins. *Mol Cell.* 2015;57(1):39-54.
112. Nam S-E, Cheung YWS, Nguyen TN, Gong M, Chan S, Lazarou M, et al. Insights on autophagosome–lysosome tethering from structural and biochemical characterization of human autophagy factor EPG5. *Communications Biology.* 2021;4(1):291.
113. Spaulding HR, Kelly EM, Quindry JC, Sheffield JB, Hudson MB, Selsby JT. Autophagic dysfunction and autophagosome escape in the mdx *mus musculus* model of Duchenne muscular dystrophy. *Acta Physiol (Oxf).* 2018;222(2).
114. Spaulding HR, Ballmann C, Quindry JC, Hudson MB, Selsby JT. Autophagy in the heart is enhanced and independent of disease progression in *mus musculus* dystrophinopathy models. *JRSM Cardiovasc Dis.* 2019;8:2048004019879581.
115. Kim D-H, Sarbassov DD, Ali SM, Latek RR, Guntur KVP, Erdjument-Bromage H, et al. GβL, a Positive Regulator of the Rapamycin-Sensitive Pathway Required for the Nutrient-Sensitive Interaction between Raptor and mTOR. *Molecular Cell.* 2003;11(4):895-904.

116. Hausch F, Kozany C, Theodoropoulou M, Fabian AK. FKBP_s and the Akt/mTOR pathway. *Cell Cycle*. 2013;12(15):2366-70.
117. Salmon AB. About-face on the metabolic side effects of rapamycin. *Oncotarget*. 2015;6(5):2585-6.
118. Casero RA, Murray Stewart T, Pegg AE. Polyamine metabolism and cancer: treatments, challenges and opportunities. *Nature Reviews Cancer*. 2018;18(11):681-95.
119. Eisenberg T, Knauer H, Schauer A, Büttner S, Ruckenstein C, Carmona-Gutierrez D, et al. Induction of autophagy by spermidine promotes longevity. *Nature Cell Biology*. 2009;11(11):1305-14.
120. Morselli E, Mariño G, Bennetzen MV, Eisenberg T, Megalou E, Schroeder S, et al. Spermidine and resveratrol induce autophagy by distinct pathways converging on the acetylproteome. *J Cell Biol*. 2011;192(4):615-29.
121. Pietrocola F, Lachkar S, Enot DP, Niso-Santano M, Bravo-San Pedro JM, Sica V, et al. Spermidine induces autophagy by inhibiting the acetyltransferase EP300. *Cell Death Differ*. 2015;22(3):509-16.
122. Higaki I, Matsui-Yuasa I, Terakura M, Kinoshita H, Otani S. Increased spermidine or spermine level is essential for hepatocyte growth factor-induced DNA synthesis in cultured rat hepatocytes. *Gastroenterology*. 1994;106(4):1024-31.
123. Eisenberg T, Abdellatif M, Schroeder S, Primessnig U, Stekovic S, Pendl T, et al. Cardioprotection and lifespan extension by the natural polyamine spermidine. *Nature Medicine*. 2016;22(12):1428-38.
124. Mossmann D, Park S, Hall MN. mTOR signalling and cellular metabolism are mutual determinants in cancer. *Nat Rev Cancer*. 2018;18(12):744-57.
125. Zabala-Letona A, Arruabarrena-Aristorena A, Martín-Martín N, Fernandez-Ruiz S, Sutherland JD, Clasquin M, et al. Corrigendum: mTORC1-dependent AMD1 regulation sustains polyamine metabolism in prostate cancer. *Nature*. 2018;554(7693):554.
126. Seidel ER, Ragan VL. Inhibition by rapamycin of ornithine decarboxylase and epithelial cell proliferation in intestinal IEC-6 cells in culture. *Br J Pharmacol*. 1997;120(4):571-4.
127. Bello-Fernandez C, Packham G, Cleveland JL. The ornithine decarboxylase gene is a transcriptional target of c-Myc. *Proc Natl Acad Sci U S A*. 1993;90(16):7804-8.
128. Flynn AT, Hogarty MD. Myc, Oncogenic Protein Translation, and the Role of Polyamines. *Med Sci (Basel)*. 2018;6(2).
129. Forshell TP, Rimpi S, Nilsson JA. Chemoprevention of B-cell lymphomas by inhibition of the Myc target spermidine synthase. *Cancer Prev Res (Phila)*. 2010;3(2):140-7.
130. Tabbaa M, Gomez TR, Campelj DG, Gregorevic P, Hayes A, Goodman CA. The regulation of polyamine pathway proteins in models of skeletal muscle hypertrophy and

- atrophy: a potential role for mTORC1. *American Journal of Physiology-Cell Physiology*. 2021;320(6):C987-C99.
131. Mihaylova MM, Shaw RJ. The AMPK signalling pathway coordinates cell growth, autophagy and metabolism. *Nat Cell Biol*. 2011;13(9):1016-23.
132. Hong-Brown LQ, Brown CR, Navaratnarajah M, Lang CH. FoxO1-AMPK-ULK1 Regulates Ethanol-Induced Autophagy in Muscle by Enhanced ATG14 Association with the BECN1-PIK3C3 Complex. *Alcohol Clin Exp Res*. 2017;41(5):895-910.
133. Fan J, Yang X, Li J, Shu Z, Dai J, Liu X, et al. Spermidine coupled with exercise rescues skeletal muscle atrophy from D-gal-induced aging rats through enhanced autophagy and reduced apoptosis via AMPK-FOXO3a signal pathway. *Oncotarget*. 2017;8(11):17475-90.
134. Xie R, Nguyen S, McKeenan K, Wang F, McKeenan WL, Liu L. Microtubule-associated protein 1S (MAP1S) bridges autophagic components with microtubules and mitochondria to affect autophagosomal biogenesis and degradation. *J Biol Chem*. 2011;286(12):10367-77.
135. Yue F, Li W, Zou J, Jiang X, Xu G, Huang H, et al. Spermidine Prolongs Lifespan and Prevents Liver Fibrosis and Hepatocellular Carcinoma by Activating MAP1S-Mediated Autophagy. *Cancer Res*. 2017;77(11):2938-51.
136. Liu P, de la Vega MR, Dodson M, Yue F, Shi B, Fang D, et al. Spermidine Confers Liver Protection by Enhancing NRF2 Signaling Through a MAP1S-Mediated Noncanonical Mechanism. *Hepatology*. 2019;70(1):372-88.
137. Atlas THP. MAP1S Skeletal Muscle expression The Human Protein Atlas2021 [Available from: <https://www.proteinatlas.org/ENSG00000130479-MAP1S/tissue/skeletal+muscle>.
138. Chrisam M, Pirozzi M, Castagnaro S, Blaauw B, Polishchuck R, Cecconi F, et al. Reactivation of autophagy by spermidine ameliorates the myopathic defects of collagen VI-null mice. *Autophagy*. 2015;11(12):2142-52.
139. Brooks SV, Faulkner JA. Contractile properties of skeletal muscles from young, adult and aged mice. *J Physiol*. 1988;404:71-82.
140. Close RI. Dynamic properties of mammalian skeletal muscles. *Physiol Rev*. 1972;52(1):129-97.
141. Orbán-Németh Z, Simader H, Badurek S, Trančíková A, Propst F. Microtubule-associated Protein 1S, a Short and Ubiquitously Expressed Member of the Microtubule-associated Protein 1 Family*. *Journal of Biological Chemistry*. 2005;280(3):2257-65.
142. Kaminska AM, Stern LZ, Russell DH. Altered muscle polyamine levels in human neuromuscular diseases. *Ann Neurol*. 1981;9(6):605-7.

143. Frederick DW, McDougal AV, Semenas M, Vappiani J, Nuzzo A, Ulrich JC, et al. Complementary NAD⁺ replacement strategies fail to functionally protect dystrophin-deficient muscle. *Skeletal Muscle*. 2020;10(1):30.
144. Pal R, Palmieri M, Loehr JA, Li S, Abo-Zahrah R, Monroe TO, et al. Src-dependent impairment of autophagy by oxidative stress in a mouse model of Duchenne muscular dystrophy. *Nat Commun*. 2014;5:4425.
145. Kauppinen L. Regulation of the human spermidine synthase mRNA translation by its 5'-untranslated region. *FEBS Lett*. 1995;365(1):61-5.
146. Wahlfors J, Alhonen L, Kauppinen L, Hyvönen T, Jänne J, Eloranta TO. Human spermidine synthase: cloning and primary structure. *DNA Cell Biol*. 1990;9(2):103-10.
147. Manzella JM, Rychlik W, Rhoads RE, Hershey JW, Blackshear PJ. Insulin induction of ornithine decarboxylase. Importance of mRNA secondary structure and phosphorylation of eucaryotic initiation factors eIF-4B and eIF-4E. *J Biol Chem*. 1991;266(4):2383-9.
148. Csibi A, Lee G, Yoon SO, Tong H, Ilter D, Elia I, et al. The mTORC1/S6K1 pathway regulates glutamine metabolism through the eIF4B-dependent control of c-Myc translation. *Curr Biol*. 2014;24(19):2274-80.
149. Dever TE, Gutierrez E, Shin BS. The hypusine-containing translation factor eIF5A. *Crit Rev Biochem Mol Biol*. 2014;49(5):413-25.
150. de Proença ARG, Pereira KD, Meneguello L, Tamborlin L, Luchessi AD. Insulin action on protein synthesis and its association with eIF5A expression and hypusination. *Mol Biol Rep*. 2019;46(1):587-96.
151. MacLennan PA, Edwards RH. Protein turnover is elevated in muscle of mdx mice in vivo. *Biochem J*. 1990;268(3):795-7.
152. Pegg AE. Spermidine/spermine-N(1)-acetyltransferase: a key metabolic regulator. *Am J Physiol Endocrinol Metab*. 2008;294(6):E995-1010.
153. Law GL, Raney A, Heusner C, Morris DR. Polyamine regulation of ribosome pausing at the upstream open reading frame of S-adenosylmethionine decarboxylase. *J Biol Chem*. 2001;276(41):38036-43.
154. Pearce GW, Pearce JM, Walton JN. The Duchenne type muscular dystrophy: histopathological studies of the carrier state. *Brain*. 1966;89(1):109-20.
155. Jeong JW, Cha HJ, Han MH, Hwang SJ, Lee DS, Yoo JS, et al. Spermidine Protects against Oxidative Stress in Inflammation Models Using Macrophages and Zebrafish. *Biomol Ther (Seoul)*. 2018;26(2):146-56.
156. Seo SY, Kim YJ, Park KY. Increasing Polyamine Contents Enhances the Stress Tolerance via Reinforcement of Antioxidative Properties. *Frontiers in Plant Science*. 2019;10(1331).

157. Webster C, Silberstein L, Hays AP, Blau HM. Fast muscle fibers are preferentially affected in Duchenne muscular dystrophy. *Cell*. 1988;52(4):503-13.
158. Hibaoui Y, Reutenauer-Patte J, Patthey-Vuadens O, Ruegg UT, Dorchies OM. Melatonin improves muscle function of the dystrophic mdx5Cv mouse, a model for Duchenne muscular dystrophy. *Journal of Pineal Research*. 2011;51(2):163-71.
159. Duddy W, Duguez S, Johnston H, Cohen TV, Phadke A, Gordish-Dressman H, et al. Muscular dystrophy in the mdx mouse is a severe myopathy compounded by hypotrophy, hypertrophy and hyperplasia. *Skelet Muscle*. 2015;5:16.
160. Chae HS, Park HJ, Hwang HR, Kwon A, Lim WH, Yi WJ, et al. The effect of antioxidants on the production of pro-inflammatory cytokines and orthodontic tooth movement. *Mol Cells*. 2011;32(2):189-96.
161. Meng X-m, Nikolic-Paterson DJ, Lan HY. TGF- β : the master regulator of fibrosis. *Nature Reviews Nephrology*. 2016;12(6):325-38.
162. Rao JN, Li L, Bass BL, Wang JY. Expression of the TGF-beta receptor gene and sensitivity to growth inhibition following polyamine depletion. *Am J Physiol Cell Physiol*. 2000;279(4):C1034-44.
163. Pauly M, Daussin F, Burelle Y, Li T, Godin R, Fauconnier J, et al. AMPK activation stimulates autophagy and ameliorates muscular dystrophy in the mdx mouse diaphragm. *Am J Pathol*. 2012;181(2):583-92.
164. Radley-Crabb HG, Grounds MD, Fiorotto ML. P1.26 A comparison of metabolism and protein synthesis rates in young and adult dystrophic mdx and control C57Bl/10 mice. *Neuromuscular Disorders*. 2011;21(9):649.
165. Zhang Y, Zheng XF. mTOR-independent 4E-BP1 phosphorylation is associated with cancer resistance to mTOR kinase inhibitors. *Cell Cycle*. 2012;11(3):594-603.
166. Spitali P, Grumati P, Hiller M, Chrisam M, Aartsma-Rus A, Bonaldo P. Autophagy is Impaired in the Tibialis Anterior of Dystrophin Null Mice. *PLoS Curr*. 2013;5.
167. Hastie SB. Interactions of colchicine with tubulin. *Pharmacology & therapeutics*. 1991;51(3):377-401.